



BRNO UNIVERSITY OF TECHNOLOGY

VYSOKÉ UČENÍ TECHNICKÉ V BRNĚ

FACULTY OF ELECTRICAL ENGINEERING AND COMMUNICATION

FAKULTA ELEKTROTECHNIKY
A KOMUNIKAČNÍCH TECHNOLOGIÍ

DEPARTMENT OF TELECOMMUNICATIONS

ÚSTAV TELEKOMUNIKACÍ

DESIGN OF A SECURE DATA TRANSMISSION SYSTEM IN NB-IOT ENVIRONMENT

NÁVRH ZABEZPEČENÉHO SYSTÉMU PŘENOSU DAT V NB-IOT PROSTŘEDÍ

MASTER'S THESIS

DIPLOMOVÁ PRÁCE

AUTHOR

AUTOR PRÁCE

Bc. Daniel Kluka

SUPERVISOR

VEDOUCÍ PRÁCE

Ing. et Ing. Petr Musil

BRNO 2025

Master's Thesis

Master's study program **Information Security**

Department of Telecommunications

Student: Bc. Daniel Kluka

ID: 203251

**Year of
study:** 2

Academic year: 2024/25

TITLE OF THESIS:

Design of a secure data transmission system in NB-IoT environment

INSTRUCTION:

The aim of this thesis is to design and implement a robust data transmission system in an NB-IoT environment with the resilience against cyber threats. The work will focus on designing a hardware and software platform for the secure transmission of data using NB-IoT technology.

The thesis will include the design of a secure communication solution based on NB-IoT technology, ensuring the integrity and confidentiality of transmitted data. Emphasis will be placed on implementing security measures, for example, in the Node-RED platform, which will be used for device management and data processing. The work will also cover the design and implementation of security for the selected broker and the use of TLS for encrypting communication.

Additionally, a hardware solution will be designed to integrate selected sensors and enable data collection and transmission. The measured values, including diagnostic data about the transmission, will subsequently be stored in a suitable database, with clear visualization provided. The thesis will also include a comprehensive analysis of the security levels of individual components, describing potential vulnerabilities. The communication efficiency within the NB-IoT network will also be evaluated, including an analysis of the energy consumption during operation.

The output of the diploma thesis will be a functional device and an assessment of its resilience to security threats in the NB-IoT environment.

RECOMMENDED LITERATURE:

According to the instructions of the thesis supervisor.

**Date of project
specification:** 10.2.2025

**Deadline for
submission:** 27.5.2025

Supervisor: Ing. et Ing. Petr Musil

prof. Ing. Jan Hajný, Ph.D.
Chair of study program board

ABSTRACT

This thesis presents the design and implementation of a modern weather station utilizing Narrowband IoT (NB-IoT) technology for secure and reliable transmission of measured meteorological data. The station monitors temperature, light intensity, air quality, pressure, humidity, and precipitation, with a focus on low power consumption and long-term autonomous operation in demanding outdoor environments. The device is powered by a solar panel and integrates the ESP32-S3 controller with the Quectel BC660K-GL communication module.

Data is transmitted using the MQTT protocol over a TLS-encrypted connection, processed through the Node-RED platform, stored in an InfluxDB time-series database, and visualized in real time using Grafana. The thesis also addresses system security aspects in detail, including protection against *man-in-the-middle* attacks, data encryption, and device authentication. Compared to commercial solutions, the system offers a significantly more affordable yet fully functional alternative suitable for scientific, environmental, or industrial deployments. The results confirm reliable operation in real-world conditions, contributing to the development of sustainable and secure IoT-based systems.

KEYWORDS

Internet of Things, NB-IoT, Weather Station, Data Transmission, Secure Communication, MQTT Protocol, TLS Encryption, Power Consumption, Remote Monitoring, Node-RED, InfluxDB, ESP32-S3, Quectel BC660K-GL, Environmental Sensors, Autonomous Operation, Environmental Monitoring, Solar Power Supply, IoT Security, Data Visualization

ABSTRAKT

Táto práca predstavuje návrh a realizáciu modernej meteorologickej stanice, ktorá prostredníctvom technológie NB-IoT (Narrowband Internet of Things) umožňuje spoľahlivý a bezpečný prenos nameraných meteorologických údajov. Stanica monitoruje teplotu, intenzitu osvetlenia, kvalitu ovzdušia, tlak, vlhkosť a zrážky, pričom kladie dôraz na nízku spotrebu energie a dlhodobú autonómnú prevádzku v náročných podmienkach. Zariadenie je napájané zo solárneho panelu a využíva riadiacu jednotku ESP32-S3 spolu s komunikačným modulom Quectel BC660K-GL.

Prenos dát prebieha pomocou protokolu MQTT cez šifrované spojenie TLS, pričom údaje sú spracovávané v systéme Node-RED, ukladané do časovej databázy InfluxDB a vizualizované v reálnom čase prostredníctvom platformy Grafana. Práca sa podrobne zaoberá aj bezpečnostnými aspektmi systému vrátane ochrany pred útokmi typu *man-in-the-middle*, šifrovania komunikácie a autentifikácie zariadení. V porovnaní s komerčnými riešeniami ide o výrazne lacnejšiu, no plne funkčnú alternatívu vhodnú pre vedecké, environmentálne či priemyselné nasadenie. Výsledky potvrdzujú spoľahlivú prevádzku v reálnych podmienkach, čím práca prispieva k rozvoju udržateľných a bezpečných IoT riešení.

KĽÚČOVÉ SLOVÁ

Internet vecí, NB-IoT, Meteorologická stanica, Prenos dát, Zabezpečená komunikácia, MQTT protokol, TLS šifrovanie, Spotreba energie, Diaľkové monitorovanie, Node-RED, InfluxDB, ESP32-S3, Quectel BC660K-GL, Sensory prostredia, Autonómna prevádzka, Environmentálne merania, Solárne napájanie, Bezpečnosť IoT, Vizualizácia dát

EXTENDED ABSTRACT

Internet vecí (IoT) sa stáva neoddeliteľnou súčasťou každodenného života ľudí. Táto technológia je čoraz viac prítomná nielen v priemysle či medicíne, ale aj v bežných domácnostiach, nositeľných zariadeniach a inteligentných bezpečnostných systémoch. Vďaka možnostiam vzdialenej komunikácie umožňuje IoT komplexné monitorovanie prostredia, pričom jednou z jeho najvýznamnejších aplikácií je zber presných meteorologických údajov. Tieto údaje sú nevyhnutné pre spoľahlivú predikciu počasia, klimatologický výskum, ako aj pre environmentálnu ochranu a správu územia.

S narastajúcim využitím IoT zariadení rastie aj potreba spoľahlivého a bezpečného prenosu dát. Prenášané údaje musia byť chránené pred neoprávneným prístupom a manipuláciou, čo vyžaduje zavádzanie moderných bezpečnostných mechanizmov. V tomto kontexte zohráva dôležitú úlohu technológia *Narrowband IoT* NB-IoT, ktorá je špeciálne navrhnutá pre zariadenia s nízkou spotrebou energie, umiestnené vo vzdialených oblastiach bez prístupu k tradičnej sieťovej infraštruktúre. NB-IoT ponúka spoľahlivú komunikáciu na veľké vzdialenosti pri minimálnej energetickej náročnosti, čím sa stáva vhodnou voľbou pre autonómne senzory a zariadenia.

Táto diplomová práca sa zameriava na návrh, realizáciu a zabezpečenie systému určeného na zber meteorologických a diagnostických údajov s využitím NB-IoT. Ústredným prvkom systému je navrhnutá meteostanica pozostávajúca z riadiacej jednotky ESP32-S3, komunikačného modulu Quectel BC660K-GL a vybraných senzorov pre meranie teploty, svetelnej intenzity, kvality ovzdušia a zložitejších meteorologických premenných. Systém je navrhnutý tak, aby bol energeticky úsporný, robustný a schopný dlhodobej autonómnej prevádzky v náročných vonkajších podmienkach.

Hardvérový návrh meteostanice zahŕňa nielen výber senzorov, ale aj vývoj prototypovej dosky a následne návrh finálnej dosky plošných spojov (PCB), ktorá umožňuje kompaktné a spoľahlivé osadenie všetkých komponentov. Napájanie je riešené pomocou solárneho panelu, nabíjacieho modulu TP4056 s ochranou, a stabilizácie napätia pomocou DC-DC meničov (TPS63020, SX1308). Súčasťou návrhu je aj tranzistorový obvod, ktorý umožňuje selektívne vypínať jednotlivé časti zariadenia pre minimalizáciu odberu v režime spánku.

Na softvérovej úrovni je systém navrhnutý tak, aby efektívne spracovával merania, optimalizoval spotrebu energie a zabezpečoval šifrovaný prenos údajov. Prenos prebieha pomocou protokolu MQTT cez NB-IoT sieť a broker Mosquitto. Prenesené dáta sú následne spracovávané prostredníctvom platformy Node-RED a ukladané do časovej databázy InfluxDB. Vizualizácia nameraných údajov prebieha v reálnom čase pomocou platformy Grafana, ktorá poskytuje prehľadné grafy a analýzy nameraných hodnôt.

Dôraz je kladený na etablovanie komunikácie šifrovanej pomocou TLS medzi me-

teostanicou a MQTT brokerom, ktorý bol implementovaný prostredníctvom služby **Mosquitto** nasadenej na platforme založenej na systéme Debian. Broker vystupuje ako server, zatiaľ čo klientské zariadenia, ako platforma **Node-RED** a NB-IoT modul **Quectel BC660K-GL**, predstavujú autentifikovaných klientov. Systém používa certifikáty vo formáte **PEM**, ktoré sú do komunikačného modulu nahrávané prostredníctvom špeciálnych AT príkazov.

Na automatizáciu tohto procesu boli vyvinuté vlastné firmvérové funkcie mikrokontroléra, ktoré zabezpečujú nahrávanie certifikátov, konfiguráciu TLS parametrov a naviazanie na MQTT spojenie. Tieto funkcie zabezpečujú vzájomnú autentifikáciu a šifrovaný prenos dát. **Mosquitto** broker bol zabezpečený vypnutím anonymného prístupu, zapnutím autentifikácie používateľským menom a heslom, a aktiváciou TLS šifrovania na porte 8883. Certifikáty pre root CA, server a klienta boli vygenerované pomocou nástrojov **OpenSSL**, nakonfigurované v súboroch brokera a slúžia na overenie identity klientov.

Node-RED, ktorý vystupuje ako ďalší klient MQTT, používa rovnaké TLS certifikáty na bezpečné pripojenie k brokeru. Kombinácia týchto opatrení zaručuje, že údaje prenášané z meteostanice do cloudových služieb zostávajú dôverné, autentifikované a odolné voči zachyteniu alebo modifikácii. Kapitola je ukončená detailným prehľadom implementovaných funkcií, procesu generovania certifikátov a konfigurácií zabezpečenia, čím poskytuje opakovateľný model pre zabezpečenie MQTT komunikácie aj v iných IoT systémoch.

Významná časť práce je venovaná bezpečnostným aspektom celého systému. IoT zariadenia vrátane NB-IoT modulov čelia mnohým hrozbám, ako sú útoky typu *man-in-the-middle* (MITM), fyzické kompromitovanie zariadenia, softvérové zraniteľnosti či neoprávnený prístup k prenášaným údajom. V práci je vykonaná komplexná bezpečnostná analýza, ktorá identifikuje najvýznamnejšie riziká, hodnotí odolnosť jednotlivých komponentov systému a navrhuje konkrétne opatrenia na zvýšenie bezpečnosti. Medzi implementované opatrenia patrí šifrovanie komunikácie pomocou *Transport Layer Security* (TLS), autentifikácia klienta, ochrana pred *replay* útokmi, a takisto obmedzenie zdrojovej náročnosti pre zachovanie nízkej spotreby.

Výsledný systém bol navrhnutý tak, aby poskytoval porovnateľnú funkcionálnosť ako profesionálne meteostanice, avšak s výrazne nižšími nákladmi. Profesionálne riešenia môžu stať až 2 000 000 CZK, pričom údržba a servis zvyšujú túto cenu ešte výraznejšie. Navrhovaná meteostanica dokáže tieto náklady zredukovať na približne 7 500 CZK, pričom stále poskytuje vysokú presnosť meraní, možnosť rozšírenia o ďalšie senzory a robustné zabezpečenie dát. Vďaka svojej modularite, energetickej efektívnosti a spoľahlivosti sa navrhované zariadenie stáva vhodným riešením pre vzdialené monitorovanie prostredia napríklad v mestách, priemyselných zónach, poľnohospodárstve či lesníctve.

Okrem samotného návrhu a vývoja meteostanice sa práca venuje aj hodnoteniu dlhodobej prevádzky zariadenia. Analyzovaný bol vplyv napájania z batérie, efektívnosť nabíjania zo solárneho panelu, presnosť časového značkovania meraní a celková odolnosť systému voči nepriaznivým vplyvom vonkajšieho prostredia. Výsledky potvrdzujú, že zariadenie je schopné stabilnej prevádzky aj v náročných klimatických podmienkach a je odolné voči výpadkom siete, fyzickým manipuláciám a softvérovým útokom.

Záverečné časti práce sa zameriavajú na analýzu bezpečnostných rizík a návrh odporúčaní do budúcnosti. Získané poznatky zároveň poukazujú na potrebu dôsledného zohľadnenia bezpečnosti už pri návrhu IoT systémov. V kontexte narastajúcej hrozby kybernetických útokov a zraniteľností v inteligentných zariadeniach sa potvrdzuje, že kombinácia moderných šifrovacích techník, dôslednej autentifikácie a segmentácie systému sú kľúčové pre zabezpečenie dát a spoľahlivý chod celého riešenia.

Výsledky tejto práce môžu slúžiť ako základ pre ďalší výskum a rozšírenie systému o nové prvky, ako aj referenčný model pre návrh zabezpečených IoT riešení v praxi. V budúcnosti môže podobný koncept prispieť k efektívnejšiemu monitorovaniu životného prostredia, smart city projektom alebo vývoju bezpečných a autonómnych senzorických sietí. Výskum preukazuje, že dôsledné plánovanie, bezpečnostná analýza a praktické overenie v reálnych podmienkach sú kľúčom k úspešnej implementácii moderných technológií do bežného života.

Okrem technologických aspektov práca tiež reflektuje ekonomické a praktické hľadiská. Návrh meteostanice sa zameriava na dostupnosť použitých komponentov, jednoduchosť montáže a možnosť replikácie riešenia aj v iných prostrediach. Vďaka otvorenému prístupu k zdrojovým kódom, dokumentácii a technickým výkresom je systém vhodný ako výučbový nástroj pre technické školy, univerzity alebo nezávislé výskumné tímy. Práca zároveň ukazuje, ako možno v praxi aplikovať princípy *secure-by-design* už v počiatočných fázach vývoja IoT zariadení.

Na záver možno konštatovať, že práca poukazuje na praktické využitie technológie NB-IoT v kombinácii so zabezpečeným prenosom dát a energetickou efektívnosťou. V dobe rozmachu digitálnych technológií je zber a ochrana údajov čoraz dôležitejšou súčasťou dizajnu akéhokoľvek distribuovaného systému. Riešenie predstavené v tejto práci je konkrétnym príkladom toho, ako možno prepojiť elektronický návrh, softvérovú architektúru, bezpečnostné princípy a praktické nasadenie do funkčného a udržateľného celku.

KLUKA, Daniel. *Design of a secure data transmission system in NB-IoT environment*. Master's Thesis. Brno: Brno University of Technology, Faculty of Electrical Engineering and Communication, Department of Telecommunications, 2025. Advised by Ing. et Ing. Petr Musil

Author's Declaration

Author:	Bc. Daniel Kluka
Author's ID:	203251
Paper type:	Master's Thesis
Academic year:	2024/25
Topic:	Design of a secure data transmission system in NB-IoT environment

I declare that I have written this paper independently, under the guidance of the advisor and using exclusively the technical references and other sources of information cited in the paper and listed in the comprehensive bibliography at the end of the paper.

As the author, I furthermore declare that, with respect to the creation of this paper, I have not infringed any copyright or violated anyone's personal and/or ownership rights. In this context, I am fully aware of the consequences of breaking Regulation § 11 of the Copyright Act No. 121/2000 Coll. of the Czech Republic, as amended, and of any breach of rights related to intellectual property or introduced within amendments to relevant Acts such as the Intellectual Property Act or the Criminal Code, Act No. 40/2009 Coll. of the Czech Republic, Section 2, Head VI, Part 4.

Brno
author's signature*

*The author signs only in the printed version.

ACKNOWLEDGEMENT

I would like to thank the supervisor of this diploma thesis, Mr. Ing. et Ing. Petr Musil, for his professional guidance, consultations, patience, and valuable suggestions for the work. Furthermore, I would like to thank my family, partner, and friends for their support during the writing of this thesis.

Contents

Introduction	27
1 Theoretical Introduction	29
1.1 Atmospheric Precipitation	29
1.2 Categorisation of Atmospheric Precipitation	29
1.3 Measurement of Atmospheric Precipitation	30
1.3.1 Stationary Rain Gauge	31
1.3.2 Float and Mass Ombrograph	31
1.3.3 Radar and Satellite Measurements	33
1.3.4 Microwave Links	34
1.4 Air Temperature	35
1.5 Air Temperature Measurement	35
1.5.1 Stationary Thermometer	35
1.5.2 Electronic Thermometers	36
1.6 Atmospheric Pressure	36
1.7 Atmospheric Pressure Measurement	37
1.7.1 Mercury Barometer	37
1.7.2 Aneroid Barometer	37
1.7.3 Digital Barometer	38
1.8 Modern Weather Stations	39
1.9 Internet of Things	39
1.9.1 Types of IoT Networks	40
1.9.2 Standards for Low-Power, Short-Range Networks	40
1.9.3 Standards for Low-Power, Wide-Area Networks	42
1.9.4 IoT Protocols	45
2 Practical Solution	49
2.1 Hardware Platform	50
2.1.1 Hardware Architecture	50
2.1.2 Professional Weather Station	51
2.1.3 Radiation Shield	52
2.1.4 Hardware Casing	53
2.1.5 Data Correlation	54
2.1.6 Measured Meteorological Quantities	55
2.1.7 Measuring ranges of the weather station	56
2.2 Prototype Device Development	56
2.2.1 Solar Panel	57

2.2.2	Battery Charging Module TP4056 with Protection	58
2.2.3	Micro Voltage Regulator Module AMS1117 3.3 V	59
2.2.4	Automatic Buck-Boost TPS63020 Converter (1.8–5.5 V, 2 A)	59
2.2.5	Step-Up Boost Converter with SX1308 (2 A)	60
2.2.6	Line Driver and Receiver MAX3232 Multichannel RS-232	61
2.2.7	Transistor	62
2.2.8	Batteries	63
2.3	Developed Prototype Device	64
2.3.1	Selected Modules	65
2.3.2	Prototype Device Layout	65
2.3.3	Advantages and Disadvantages	66
2.4	Developed Final PCB Device	67
2.4.1	Final Device Layout	67
2.4.2	Improvements over Prototype Device	68
2.4.3	Power Management	69
2.4.4	Device Testing	70
2.5	Device Documentation	70
2.6	System Software Design and Implementation	70
2.6.1	Main Algorithm	71
2.6.2	Node-RED, InfluxDB, and Grafana	72
2.6.3	Data Timestamping	73
2.6.4	Power Optimization	76
2.6.5	Power Consumption Evaluation	79
2.6.6	Network Consumption Evaluation	81
2.6.7	Doxygen Documentation	82
2.7	System Security	82
2.7.1	System Security Design	83
2.7.2	System Security Level Analysis	90
Conclusion		95
Bibliography		99
Symbols and Abbreviations		107
List of Appendices		111
A Technical Documentation of Weather Station Components		113
A.1	ESP32-S3-WROOM-1 N16R8	114
A.2	Quectel BC660K-GL	115

A.3	Sensors	116
A.3.1	Temperature Sensor UMW DS18B20	116
A.3.2	Light Intensity Sensor Vishay VEML7700	117
A.3.3	Air Quality Sensor Nova PM SDS011	118
A.3.4	Weather Transmitter Vaisala WXT536	119
B	Main Algorithm Flow Chart	123
C	Doxygen Documentation	125
D	Radiation Shield Visualisation	127
E	DKWS PCB Schematic Documentation	131

List of Figures

1.1	Example of stationary rain gauge	31
1.2	Float ombrograph principle	32
1.3	Weight ombrograph principle	32
1.4	Radar located in Brdy u Prahy	33
1.5	METEOSAT satellite pictures	34
1.6	Microwave links meteorological measurement principle	35
1.7	Thermocouple principle	36
1.8	Mercury barometer principle	37
1.9	Digital barometer principle	38
2.1	Weatherstation created for this project	49
2.2	Weather station block scheme	50
2.3	Professional weather station on the roof of the Faculty of Electrical Engineering and Communication at BUT	51
2.4	Developed radiation shield	52
2.5	Developed casing	53
2.6	Differences in measurement between DS18B20 and WXT536	54
2.7	Meteo visualisation	55
2.8	Solar panel 6 V/1 W used for prototype testing	57
2.9	Battery charger with protection TP4056	58
2.10	Micro voltage regulator module AMS1117 3.3 V	59
2.11	Automatic Buck-Boost TPS63020 power converter 1.8–5.5 V, 2 A . . .	60
2.12	Step-up boost converter with SX1308 2 A	61
2.13	Line Driver and Receiver MAX3232 Multichannel RS-232	61
2.14	Transistor NPN STMicroelectronics TIP132	62
2.15	UART driver and receiver CH9102	63
2.16	Battery GeB LiPo1 503035 500mAh 3.7 V JST-PH 2.0	64
2.17	Used batteries in the weather station	64
2.18	Developed prototype board top	65
2.19	Developed prototype board bottom	66
2.20	DKWS PCB (89x81mm) designed by the prototype board	67
2.21	Manufactured DKWS PCB	68
2.22	Detail DKWS PCB	71
2.23	Created flow on the Node-RED server, which processes the data and stores them in the InfluxDB database	72
2.24	Grafana dashboard created to visualise measured data	73
2.25	Implemented logic of light power saving mode	78

2.26	Battery charging efficiency during cloudy days (Jan 15 to Jan 23, 2025) and sunny days (Jan 23 to Feb 23, 2025), based on time series with a sending frequency of 24 messages per day	80
2.27	Charging efficiency during April 6, 2025, as observed from 12:00 AM to 11:59 PM	81
2.28	Example of function documentation, file Sensors.cpp	83
2.29	Demonstration of a logger used to monitor the traffic of the proposed secure system	87
2.30	Used Node-RED certificates	89
A.1	Microcontroller ESP32-S3 DevKitC-1 WROOM-1 N16R8	114
A.2	NB-IoT module Quectel BC660K-GL-TE-B KIT	115
A.3	Temperature sensor UMW DS18B20	117
A.4	Temperature sensor UMW Dallas DS18B20	117
A.5	Light intensity sensor Vishay VEML7700	118
A.6	Air quality sensor Nova PM SDS011	119
A.7	Multiparameter weather sensor Vaisala WXT536	120
C.1	Automatically generated Doxygen documentation, file Sensors.cpp .	125
D.1	Front side of the proposed radiation shield	127
D.2	Back side of the proposed radiation shield	128
D.3	Cross section side of the proposed radiation shield	129

List of Tables

1.1	Standards for Low-power, Short-range IoT Networks	41
1.2	Standards for Low-power, Wide-area IoT Networks (LPWAN)	43
1.3	IoT Protocols Categorized by OSI Model Layer	45
2.1	Technical specifications of the selected sensors	56
2.2	Technical parameters of power management components used in the prototype board	57
2.3	Power management components and parameters	69
2.4	Overview of data sent by the weather station via MQTT	75
2.5	Phases of MQTT message transmission in an NB-IoT network	81
A.1	Overview of main DKWS hardware components	113

Listings

2.1	Part of the function generating the message	76
2.2	Macros defined at the beginning of the code	76
2.3	Calculation of the message buffer size	77
2.4	Charging current estimation	79
2.5	Function writePemTLS	84
2.6	Function configTLS.	85
2.7	Function openMQTTSecure	85
2.8	Installing required Debian packages	87
2.9	Starting and enabling the Mosquitto service	87
2.10	Authentication-related configuration options	88
2.11	Installing OpenSSL tools	88
2.12	Generating CA certificate	88
2.13	Creating server certificates	88
2.14	Creating client certificates	88
2.15	TLS-related broker configuration	89

Introduction

The Internet of Things (IoT) is becoming an integral part of people's lives. In recent years, this technology has been so widespread that it can be found in industry, in medicine, but also in ordinary people's homes and in wearable devices. IoT devices are referred to as smart devices that can comprehensively monitor not only the environment but also secure homes using security systems. This is achieved through comprehensive remote communication. One of the most significant applications of IoT is the collection of accurate meteorological data, which is required for comprehensive environmental analysis and accurate weather forecasting. This data is also used in climatological research or environmental protection.

Nowadays, there is an increasing emphasis on the need for reliable data transmission and secure communication ensuring the integrity and confidentiality of the transmitted data. This is achieved by advanced communication technologies suitable for remote communication. It is important that the equipment has sufficient computing power to implement these technologies and sufficient energy. As it turns out, these factors can be limiting and because of this, the use of advanced communication technologies can be very limiting. IoT devices do not need to use Wi-Fi or a traditional cellular network. Narrowband Internet of Things (NB-IoT) technology has been developed to meet the requirements for low power consumption and reliable data transmission over a wide area.

NB-IoT technology also carries security risks like any other. For this reason, devices using NB-IoT technology require a comprehensive analysis that focuses on the individual parts of not only the devices, but also all the systems that the devices use during their operation. Whether it is physical attacks or software attacks, it is important to be aware of them and design devices to be secure and resilient to potential threats.

A system enabling the collection of accurate meteorological and diagnostic data must be designed with security risks in mind and must implement safeguards to prevent potential attacks. In an NB-IoT environment, emphasis is placed on optimizing power consumption, transmission reliability, and the use of advanced security measures in the form of communication encryption, authentication, and analysis of potential threats. Hence, the thesis comprehensively analyzes the development and final design of a weather station that integrates selected environment sensing sensors, the power management of the weather station and the software structure.

Thanks to their functions, weather stations are becoming an integral part of households, where they can comprehensively analyse the home environment and predict the weather in the location in which they are located. Accurate professional stations are, however, too expensive, and for this reason, ordinary users cannot get them

for their homes. Depending on the configuration, professional weather stations can cost up to 2,000,000 Czech Koruna (CZK) and their servicing another 100,000 CZK. Robustness is also important, which in the case of professional weather stations is at a very high level.

Therefore, the main objectives of the work include the design and implementation of a system using NB-IoT technology that enables secure data transmission. This requires market analysis and selection of suitable sensors that can comprehensively monitor the environment with high accuracy. Also important are the electronic components that enable the robustness and reliability of the weather station in challenging meteorological conditions. As a next step, the implementation of a software design for the device and the server is necessary. Within the software, optimization of energy and data consumption is necessary. Finally, identification of security risks of the designed weather station, design of countermeasures, evaluation of energy and data consumption, reliability, and security of the whole system is necessary.

The diploma thesis introduces the reader in the introduction to the problem of sensing meteorological variables and presents the available methods that have been improved over the centuries. In addition to proven methods, opportunistic sensing methods are presented, which are for example carried out at the Faculty of Electrical Engineering and Communication by the Meteo Telcorain team via microwave links. The design of the weather station consists of the design of the radiation shield, the hardware and software architecture, and the implementation of the entire proposed system. The hardware part deals with sensor selection and implementation, prototype board and printed circuit board development. The software part consists of the use of available platforms, namely Node-RED, InfluxDB and Grafana for data transfer, storage and visualization. Finally, the entire system is secured by Transport Layer Security (TLS) encryption, which ensures the integrity and trustworthiness of the transmitted data.

Chapters **Theoretical Introduction** and **Practical Solution** provide the necessary theoretical and practical background for meteorological measurements and IoT technologies. The theoretical part covers topics such as **Atmospheric Precipitation**, **Air Temperature**, **Atmospheric Pressure**, modern **Weather Stations**, and the **IoT**, including types of IoT networks and communication protocols. The second chapter, **Practical Solution**, focuses on the hardware and software implementation of a custom weather station. It includes the design of a prototype and final printed circuit board (PCB), detailed documentation of hardware modules, as well as the development of the main algorithm, data logging, and communication with external platforms Node-RED, InfluxDB, and Grafana. The final section, **System Security**, addresses cybersecurity aspects by introducing system security design and providing a detailed **System Security Level Analysis**.

1 Theoretical Introduction

The *Theoretical Introduction* chapter begins by presenting meteorological variables that can be measured using the principles described below. These measurement principles have evolved over centuries and represent established techniques for determining precipitation, atmospheric pressure, and air temperature. Their application is subject to specific rules that ensure accurate measurements, particularly in professional-grade weather stations.

These professional stations serve as a benchmark for this thesis, which aims to achieve a similar level of quality and accuracy at a significantly lower cost. To support this objective, the proposed weather station includes the professional-grade Vaisala WXT536 multiparameter sensor, known for its high precision and robustness. This sensor is used to correlate and verify the accuracy of the data collected by the other components of the station.

The chapter also introduces the concept of the **Internet of Things (IoT)**, which is utilized in this thesis through **NB-IoT** technology. A comparison is made with other available communication technologies to highlight the advantages of **NB-IoT**, such as low power consumption, low data usage, and wide coverage availability not only in the Czech Republic but globally. In the proposed weather station, this technology is used to transmit both meteorological and diagnostic data securely. **Transport Layer Security (TLS)** encryption ensures the confidentiality and integrity of transmitted data, which is a key requirement in the secure design of modern IoT systems.

1.1 Atmospheric Precipitation

The condensation or desublimation of water vapour produces water particles, which are called atmospheric precipitation. When the air temperature drops to the dew point, they are found in the air or fall to the Earth's surface. In some cases, they can form on the Earth's surface, and they can also form on objects. Precipitation is water in a liquid or solid state and falls from various types of clouds or fog and belongs to hydrometeors.[1]

1.2 Categorisation of Atmospheric Precipitation

Precipitation is observed by meteorological stations, which determine the type of precipitation, its duration, intensity and precipitation total, or the amount of snow cover and its water value. Precipitation intensity represents the amount of precipitation that has fallen over a certain period of time, and precipitation total represents

the amount of precipitation indicating the height of the water column in millimetres. 1 millimetre of precipitation corresponds to 1 litre of water over an area of 1 square metre.[1]

Atmospheric precipitation is divided into several categories. One of these is falling precipitation, which includes all forms of water falling from the atmosphere to the Earth's surface. These are, for example, rain, hail or snow. Other categories of atmospheric precipitation are divided according to [1]:

- **state** – liquid (rain, drizzle and dew) and solid (snow, freezing rain and hail) precipitation
- **origin** – falling (rain, drizzle, snow, sleet, snowflakes, hail and ice needles) and settled precipitation
- **conditions under which condensation occurs** – liquid (dew and wetting) and solid (grey frost, initate, frost and ice) precipitation
- **duration of occurrence** – persistent and intermittent precipitation and showers
- **conditions of occurrence** – frontal, orographic, local and regional precipitation

Since falling precipitation is all forms of falling water, it is important to measure the amount of this falling water. Vertically falling atmospheric precipitation is divided into [1]:

- **rain** – liquid precipitation, with drop sizes of 0.5 millimetres (mm) and a fall speed of 9 metres per second (m/s), divided into **weak** (1 millimetre per hour (mm/h)), **mild** (1.1–5 mm/h), **heavy** (5.1–10 mm/h), **rainstorm** (15.1–23 mm/h), **torrential rain** (23.1–58 mm/h) and **cloudburst** (more than 58 mm/h)
- **drizzle** – liquid precipitation, with droplets of small size greater than 0.5 mm
- **snow** – precipitation in solid state, it is formed by ice crystals in the form of snowflakes
- **clusters** – solid precipitation, it is pieces of ice or snow with several layers of frozen water

1.3 Measurement of Atmospheric Precipitation

In hydrological situations or meteorological forecasts it is very important to have accurately measured rainfall data. Accurate knowledge of rainfall activity is critical for a number of industries, for example, agriculture, aviation, energy, transport and logistics, insurance, and the large variability of rainfall over time and space makes obtaining reliable meteorological data challenging. The three most basic ways of measuring precipitation activity are rainfall gauges, radars and satellites.[3][4]

1.3.1 Stationary Rain Gauge

Vertical precipitation is captured in a funnel and from there it flows into a jug in a rain gauge, in which the amount of water is measured by a measuring cup with segments representing millimetres of the water column. The measurement is always taken at 7 a.m. and summarises the rainfall over the previous 24 hours, i.e. the previous day. In winter, this rain gauge is modified and a reserve container is added. The snow is collected in a container without a funnel and kettle, melted, and the amount of dissolved water is measured with a measuring spoon.[5]

Totalizers are found in secluded places, for example on mountain peaks, and the measurement is only carried out once every 6 months. In a totalizer, it is necessary that the captured water from precipitation does not evaporate and remains in the totalizer for a long period of time. Evaporation is prevented by the oil that floats to the surface of the water, thus forming a blanket to prevent evaporation. The example of this rain gauge can be found in Figure 1.1.[5]



Fig. 1.1: Example of stationary rain gauge.[5]

1.3.2 Float and Mass Ombrograph

An ombrograph in Figure 1.2 is a device that provides a more complete record of precipitation compared to stationary rain gauges. Compared to the latter, the float ombrograph is characterised by the fact that the captured precipitation flows through a funnel into a float chamber, where an arm, float and recording pen record the progress of the precipitation on a tape. This tape is wound on a drum which is rotated by means of a clockwork movement. The float ombrograph cannot be used in winter. [5][6]

The weight ombrograph in Figure 1.3 measures weight differences in real time, making it possible to achieve highly accurate records of actual rainfall totals com-

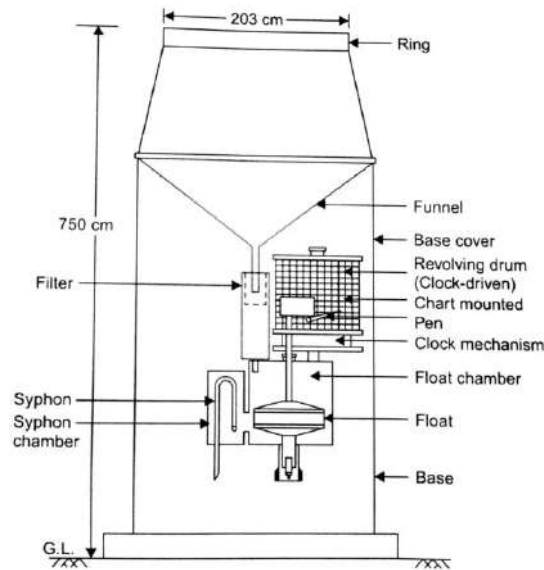


Fig. 1.2: Float ombrograph principle.[6]

bined with fast data recording. The weight of the collection vessel is measured by weight sensors such as strain gauges. This type of rain gauge is the most commonly used by meteorological companies due to its high cost and frequent maintenance requirements. When not maintained properly, mass ombrographs produce measurement errors because impurities on the rain gauge weights contribute to the measured weight of the water from the precipitation. Water evaporation also occurs, which is solved by oil on the water surface, similar to a totalizer. With this type of ombrograph it is possible to measure both liquid and solid precipitation as well as its intensity and duration.[5][6][7]

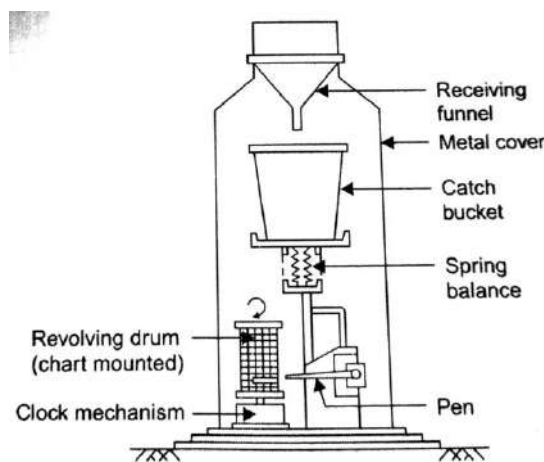


Fig. 1.3: Weight ombrograph principle.[6]

1.3.3 Radar and Satellite Measurements

Radar measurements are not just localised over one small area, but over a larger area. Radar estimates are made using the transmitted signal. This signal is reflected from the precipitation and then picked up by the radar that sent the signal, which measures the power of the reflected signal. From the power it is possible to mathematically estimate the type of precipitation and its distance from the radar. The intensity of the precipitation is determined by the signal reflectivity and intensity. Radar shown in Figure 1.4 is located in Brdy u Prahy in Czech Republic.[3][7][8]



Fig. 1.4: Radar located in Brdy u Prahy.[9]

Satellite measurements are used for weather forecasting, which can determine, for example, wind speed, cloud development and occurrence, and other meteorological data. The development and occurrence of clouds as measured by satellites helps to estimate emerging precipitation activity.[3][7][8]

The Czech Republic uses two radars emitting electromagnetic radiation using a parabolic antenna directed into a narrow beam of the atmosphere with a range of 260 km. The radars are part of the Czech Radar Network (CZRAD) and are located in Brdy u Prahy and in Skalka u Boskovic.[9] The satellites measuring precipitation in the Czech Republic belong to the intergovernmental European Organisation for the Exploitation of Meteorological Satellites (EUMETSAT) and the National Oceanic and Atmospheric Administration (NOAA). The satellite named METEOSAT (belonging to EUMETSAT) is placed in Earth orbit at an altitude of 37 000 kilometres and orbits the Earth once every 24 hours. It senses not only precipitation in the Czech Republic, but the whole area of Europe, Africa, a small area of Asia

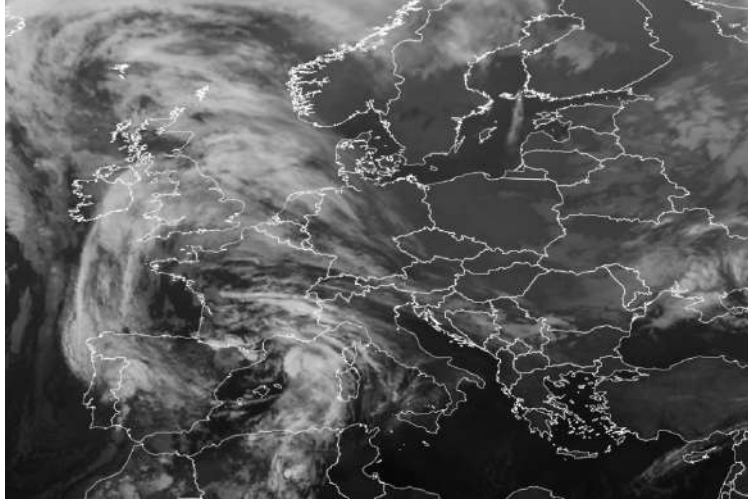


Fig. 1.5: METEOSAT satellite pictures.[10]

and South America as well. The NOAA satellite is located in the Earth's polar orbit at an altitude of 810 to 870 kilometres and orbits the Earth once every 100 minutes. Satellite images made by METEOSAT are shown in Figure 1.5.[3][7][8][9]

1.3.4 Microwave Links

Measuring precipitation using microwave links in Figure 1.6 is one of the opportunistic measurements of meteorological data. Microwave links transmit digital data from point to point via antennas emitting electromagnetic radiation. In telecommunication networks, they are used by mobile operators to distribute 4G and 5G networks and operate in the frequency range of 5 to 80 gigahertz (GHz). The advantage of these links is their fast installation, low cost coupled with low planning costs and high flexibility. To calculate the rainfall, the equation $k = a * R^2$ is used, where the parameter k represents the signal attenuation of the electromagnetic radiation and the parameter R represents the rainfall in mm/h. The parameter a is dependent on the frequency of the microwave link.[3][11]

The measurement of meteorological data consists in measuring the signal decay of electromagnetic radiation. A reference level of the received signal is determined from the dry season and this is compared with the actual value of the received signal during rainfall. The average rainfall intensity is best measured at signal frequencies above 15 GHz, as the magnitude of the attenuation along the path of the link increases significantly then. Using the decay of the received signal, the microwave links can also be used to measure the actual temperature, which is also compared with the dry season temperature reference. The measurement depends

on the hardware (HW) link used, the frequency and the polarization of the microwave unit. A higher Pearson's coefficient is typical for dry periods and a lower one for wet periods, and in statistics it expresses the strength of the relationship between the two variables, in this case between the microwave couplers.[3][11]

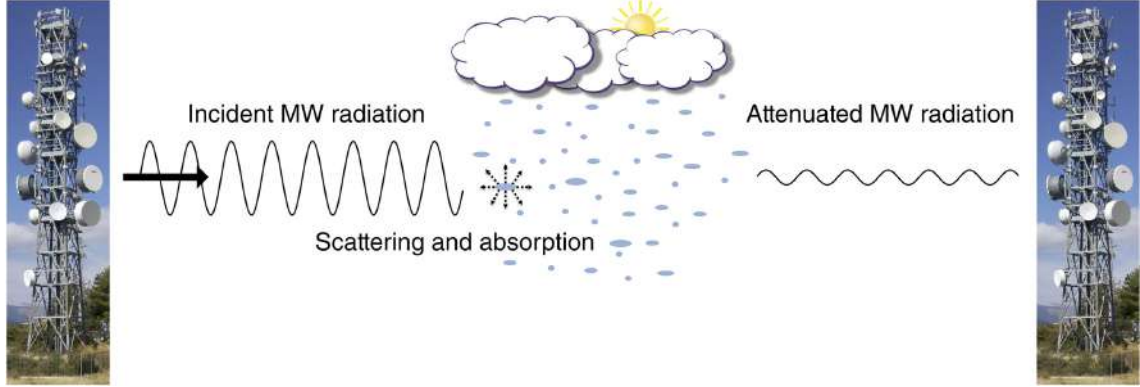


Fig. 1.6: Microwave links meteorological measurement principle.[11]

1.4 Air Temperature

Air temperature is a basic and important meteorological variable indicating the thermal state of the air, i.e. the ability of air to transfer or receive heat energy. A special case of measured temperature is also the ground minimum air temperature, which is measured by a meteorological station just above the Earth's surface, and which is useful in arable farming.[12][13]

1.5 Air Temperature Measurement

Weather stations that measure air temperature are subject to 2 conditions. The first condition is that **the thermometer must be shielded from radiation effects** and the second is that **the thermometer vessel must be in constant contact with as much air as possible**. Meteorological stations are equipped with psychrometric (louvre) booths or various enclosures which fulfil these two basic conditions.[13][14][15]

1.5.1 Stationary Thermometer

The basic thermometer for measuring air temperature is a stationary thermometer that uses mercury, a liquid substance. However, at -39°C , mercury solidifies

and therefore there is a larger deviation of the measured value from the actual value around this temperature. The category of liquid thermometers also includes alcohol thermometers, which have a low freezing point. In meteorological stations, the stationary thermometer is placed up to a height of 2 metres above the ground surface.[13]

1.5.2 Electronic Thermometers

Compared to liquid thermometers, electronic thermometers offer several advantages that are appreciated both in meteorology and hydrology. They are divided into [13][15]:

- **resistive** – they use the properties of metals to change their electrical resistance depending on the measured ambient temperature
- **thermoelectric** – thermocouple connected from two different metals creating thermoelectric voltage at the point of their connection (the need to apply different temperatures to the thermocouple to create thermoelectric voltage in the measuring circuit); principle shown in Figure 1.7.

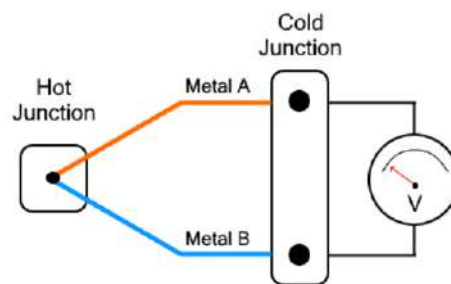


Fig. 1.7: Thermocouple principle.[15]

Electronic thermometers are easy to operate and maintain, small in size and have negligible thermal inertia. In weather stations it is important that thermometers are protected from radiation and these electronic thermometers are almost insensitive to radiation.[13][15]

1.6 Atmospheric Pressure

Atmospheric air exerts pressure on the Earth's surface due to the force of gravity. The highest pressure is found at the Earth's surface and the pressure decreases with increasing altitude. The unit of hectopascal [hPa] is used to express atmospheric pressure, and under normal conditions it is normally 1013.25 hPa. However,

the measured air pressure is converted to sea level for comparison, when the measured absolute value of air pressure is converted to comparable values.[12][18]

1.7 Atmospheric Pressure Measurement

A barometer, whose measuring medium is a liquid or gas, is used to measure atmospheric pressure. The principle of measurement consists in the change of the mass and density of the medium by the action of atmospheric pressure on the medium to be measured.[16]

1.7.1 Mercury Barometer

The measuring medium in this type of barometer is mercury. In the instrument there is a glass vacuum tube which has one end immersed in a container of mercury. The tube is exposed to external atmospheric pressure and the level of mercury in it varies according to atmospheric conditions. The higher the pressure, the lower the mercury level. There is a gauge on the glass tube used to read the height of the mercury level and therefore to measure the actual atmospheric pressure. This is an accurate and reliable measurement shown in Figure 1.8.[16][17][18]

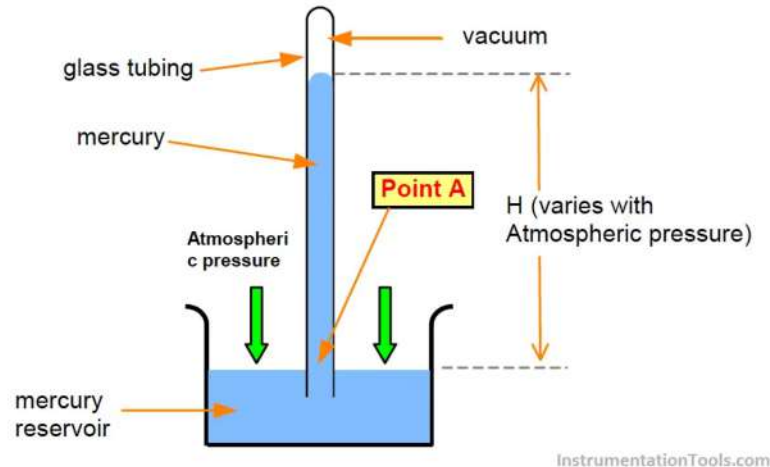


Fig. 1.8: Mercury barometer principle.[17]

1.7.2 Aneroid Barometer

It is a rarely used barometer whose measuring medium is not mercury, but flexible metal walls that change according to the actual external atmospheric pressure.

When it is applied to the metal walls, it causes deformation of the walls, which is measured by an attached needle pointer. The greater the atmospheric pressure, the greater the deformation of the metal walls, which is easily read from the scale of the barometer by the measuring pointer.[16][18]

1.7.3 Digital Barometer

It is the most widely used device for measuring atmospheric pressure using electronics and a micro-electromechanical (MEMS) sensor. Integrated circuits use electronic and mechanical parts to measure atmospheric pressure using a capacitive or piezoelectric sensor. Capacitive sensors in Figure 1.9 are placed around the membrane deformed by atmospheric pressure and measure the changing capacitance.[16][18][19]

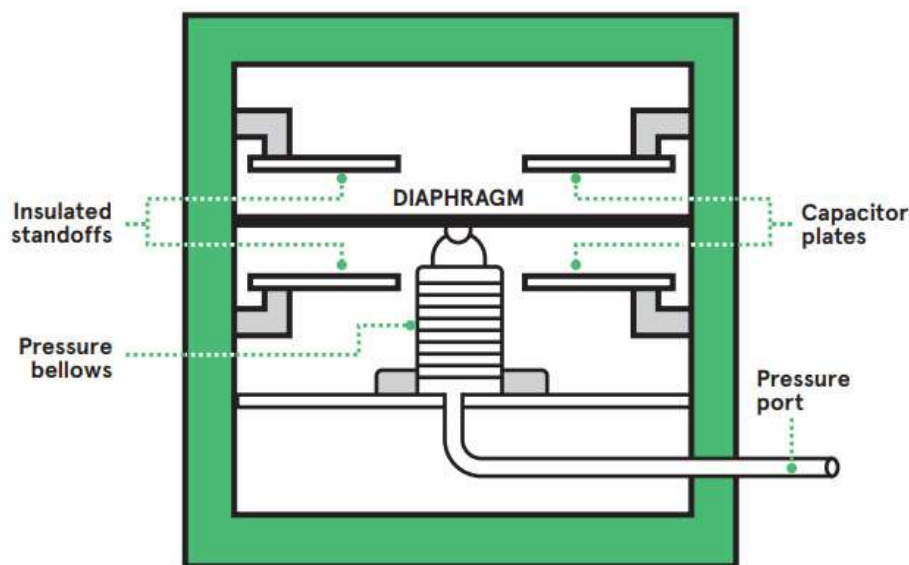


Fig. 1.9: Digital barometer principle.[19]

The principle in Figure of using a piezoelectric sensor is to place the sensor directly into the membrane, which changes its resistivity by deformation when atmospheric pressure is applied. The resistivity can be measured using, for example, a Wheatstone bridge.[18]

Their main advantages are small size, high accuracy and constructional robustness. Digital barometers are used in weather stations for weather forecasting, as a low pressure reading predicts impending bad weather and a higher pressure reading predicts good weather. Digital barometers are used in IoT devices, but also in aviation and marine applications for navigation and traffic planning.[18]

1.8 Modern Weather Stations

The meteorological quantities mentioned above represent basic data that mankind has been trying to measure for centuries. With the passage of time, a number of measuring instruments have been developed and their measurement principles have been improved. However, in modern times it is necessary to look at the measurement of meteorological quantities in a more comprehensive way. With rapidly changing and less predictable meteorological conditions, there are increasing demands for accurate and on-time measurements that can predict changes.

This requires the search for new principles that are more accurate and the measurement of more quantities than has been necessary in the past. Professional meteorological stations are able to measure more variables and provide information on the current weather forecast or air quality.

In forecasting clouds and precipitation, they work with, among other factors, measurements of the humidity of the outside air and provide information on wind speed and direction. Weather stations are also good helpers in the field of health, as they can measure noise levels, detect CO₂ levels in the air and thus help to prevent health complications caused by these elements.

Professional weather stations are becoming more and more accessible to ordinary users, who receive early warnings of weather changes and, at the same time, care about the quality of the environment in which they live and thus protect their health.

1.9 Internet of Things

All physical addressable devices that are connected to a network and that communicate with each other are part of a working concept called the **Internet of Things**. These are, for example, devices in the smart home, industry, medicine or transport, and can be connected using central units and intelligent control systems. The **Internet of Things** connects physical devices called 'objects' with objects in the virtual world, which form a virtual code describing the state of the device and is based on communication technologies.[20]

Another important requirement for these devices is that they must have low energy consumption and be constructably robust. Smart devices are able to use multiple communication protocols to connect to the **Internet** and to communicate with each other (e.g. 4G, 5G, Bluetooth, ...), and the **Internet** can send information to these devices and control them.[20]

The processor of the device processes the data and the received commands and, after processing, sends them to a communication module, which, for example, transfers them from one communication network to another, or the data is received

and processed by a server.[20]

1.9.1 Types of IoT Networks

There are several ways to connect to IoT networks and it depends on the specific device and its purpose. Data must travel a short distance or a long distance to reach the Internet. Therefore, IoT networks are divided into [21]:

- **Low-power, short-range networks** – this includes smart homes, offices or small environments, where the device can run on batteries and is low-maintenance and easy to operate.
- **Low-power, wide-area networks (LPWAN)** – devices supporting LPWAN are able to send data over a minimum distance of 500 meters before connecting to the Internet, and require minimal power consumption.

Low-power, short-range networks support connections over distances of a few centimetres. Typical connectivity options are Bluetooth, Near Field Communication (NFC), Wireless Fidelity (Wi-Fi/802.11), Z-Wave and ZigBee. The latter supports high-level protocol communication and creates a personal network with low-power digital radios. Compared to Wi-Fi, Wi-Fi has a limited connection range, high power consumption, and is the standard for connecting devices in homes and offices that have higher power consumption, such as televisions, washing machines, computers, printers, etc.[21][22]

Low-power, wide-area networks support connecting to the network even from longer distances and at higher data rates. To do this, they use, for example, 4G Long-Term Evolution (LTE) IoT, 5G IoT, Cat-0, Cat-1, Long Range Wide Area Network (LoRaWAN), LTE Cat-M1, Narrowband/NB-IoT/Cat-M2, Sigfox and many others. Other advantageous features are the low performance of the equipment, guaranteeing low energy consumption. This enables the devices to operate for a long time with an almost lifetime battery life.[21][22]

1.9.2 Standards for Low-Power, Short-Range Networks

Standards in Table 1.1 form the basis of communication between devices in indoor environments such as smart homes, offices, or industry. These technologies are designed to minimize power consumption while maintaining reliable and secure connectivity over short distances. Typical applications include automation systems, health monitoring, and portable electronics.[23]

When selecting the appropriate technology, it is important to consider the requirements of the environment and the supported topologies. Devices often operate

on batteries and must ensure low maintenance and long service life. Most technologies in this group use unlicensed frequency bands and support mesh or star network topologies.[23]

The guiding parameters when selecting a short-range wireless standard include:

- Operating frequency and channel bandwidth
- Network topology and device capacity
- Data rate and connection latency
- Interference resistance and communication security

Table 1.1: Standards for Low-power, Short-range IoT Networks

Technology	Frequency	Data Rate	Range	Notes
Bluetooth LE	2.4–2.4835 GHz	1.4 Mbps	10–30 m	Up to 20 devices, 3 s connection time, low power use
Wi-Fi HaLow	750–950 MHz	Up to 600 Mbps	Up to 1 km	Star topology, up to 8191 devices, energy-saving versions
Z-Wave	868 MHz (EU), 915 MHz (USA)	100 Kbps	10–30 m	Mesh topology, up to 200 devices, encrypted
Zigbee	868 MHz (EU), 915 MHz (USA)	250 Kbps	Up to 70 m	Mesh topology, up to 100 devices, fast connection (30 ms)

Bluetooth Low Energy

This relatively widespread technology uses low power at maximum load and in stand-by mode. It is a wireless technology used to transmit small amounts of data over a short distance, and devices with this technology are characterized by low battery power consumption without the need for frequent charging. It is used in a variety of industries, for example for monitoring meteorological variables and in hydrology. It can connect a maximum of 20 devices in a star or point-to-point topology with a range of 10 to 30 m. The bandwidth is from 2.4 to 2.4835 GHz. The transmission rate is 1.4 megabits per second (Mbps). Connecting to the network takes approximately 3 seconds.[23]

Wi-Fi/802.11

Wi-Fi serves as a basic communication standard, but was initially developed to secure high-speed wireless data transmission. However, this makes it an energy-intensive solution that does not meet the low power consumption standards imposed by the IoT concept. Therefore, several versions of Wi-Fi communication have been developed, such as Wi-Fi HaLow, operating in the frequency range of less than 1 GHz. Devices supporting this technology consume less power, for example through hibernation, a target wake-up time or a designated working window. It supports the connection of up to 8191 devices in a star network topology or point-to-point, with a range of up to approximately 1 km. Bandwidth ranges from 750 to 950

megahertz (MHz), with transmission speeds of up to 600 megabits per second (Mbps). However, the frequencies vary: 863 to 868 MHz for Europe and 902 to 928 MHz for the US.[23]

Z-Wave

It is a patented communication protocol based on radio frequency. It is used for automation in smart homes and offices, and only rarely in small industrial environments. It offers a high level of security through encrypted communication and is resistant to noise. Up to approximately 200 devices can be connected to this communication standard in a mesh-like topology with a range of 10 to 30 m. The bandwidth is 1 gigahertz (GHz). The data rate is 100 kilobits per second (Kbps), with different frequencies allocated for Europe and the USA. The frequency for Europe is 868 megahertz (MHz), and for the USA it is 915 MHz.[23]

Zigbee

Zigbee is a wireless communication protocol designed for home and industrial automation, also known as a smart home solution, with a low data rate. It operates in the same frequency range as **Bluetooth**, but connects to the network at a speed of 30 milliseconds, which helps reduce battery consumption. **Zigbee** provides a high level of immunity to interference and ensures secure communication. Between 35 and 100 devices can be connected to this communication standard in a mesh-like topology with a range of up to 70 m. The operating frequency varies: 868 megahertz (MHz) for Europe and 915 MHz for the USA. The data rate is 250 kilobits per second (Kbps).[23]

1.9.3 Standards for Low-Power, Wide-Area Networks

LPWAN is a group of low-energy broadband networking technologies in Table 1.2 in various forms. When choosing the right solution, it is important to consider several factors that play an important role in the desired application. These technologies are divided into licensed (e.g. **Cat-1**, **LTE Cat-M1** and **NB-IoT**) and unlicensed (e.g. **Sigfox** and **LoRa-WAN**).

The guiding parameters in choosing the right solution can be, for example:[24]

- Transmission channel bandwidth
- Transmission duplexity
- Peak downlink and uplink speed
- Latency range

- User Equipment (UE) bandwidth
- Maximum transmission power

Table 1.2: Standards for Low-power, Wide-area IoT Networks (LPWAN)

Tech.	BW	Data Rate	Latency	Power	Notes
Cat-1	1.4 MHz	DL: 10 Mbps, UL: 5 Mbps	10–15 ms	23 dBm	Licensed, full duplex, for video and commercial use
Cat-M1	1.08 MHz	DL/UL: 1 Mbps	50–100 ms	20–23 dBm	Licensed, half/full duplex, low energy
NB-IoT	200 kHz	DL: 26 Kbps, UL: 66 Kbps	1600–10000 ms	23–33 dBm	Licensed, high latency, for stationary/periodic apps
LoRaWAN	125 kHz	DL: 300 bps, UL: 50 Kbps	> 20 s	22 dBm	Unlicensed, 10–15 km, user-maintained infra
Sigfox	0.1 kHz	DL: 100 bps, UL: 600 bps	1–100 ms	22 dBm	Unlicensed, 30–50 km, 140 msg/-day, 12 B/msg

LPWAN technologies are primarily used in scenarios where devices need to operate over long periods without frequent battery replacement and must transmit small amounts of data over long distances. Their robustness and low cost make them suitable for a wide range of IoT applications, including:

- Smart metering (water, gas, electricity)
- Agricultural monitoring (soil moisture, crop status)
- Smart cities (waste management, parking sensors, public lighting)
- Industrial automation and predictive maintenance
- Asset tracking and logistics
- Environmental and weather monitoring

Cat-1

Long Term Evolution (LTE) was the first standard to provide IoT solutions using 4G connectivity. Later, a revised version was released with Cat-1 BIS antenna. Among the selected parameters, Cat-1 has a bandwidth of 1.4 MHz with full duplex transmission. The peak downlink speed is 10 Mbps and uplink speed is 5 Mbps with a latency range of approximately 10 to 15 milliseconds (ms). The UE bandwidth is 20 MHz with a maximum transmission power of 23 decibel-milliwatts (dBm). This licensed standard is suitable for several IoT applications such as video streaming and various thoughtful, commercial, and consumer projects.[24]

LTE Cat-M1

Cat-M1 is a licensed LPWA technology used for the transmission of small to medium amounts of data. It has a bandwidth of 1.08 MHz with half or full duplex transmission. Peak downlink and uplink speeds are the same – 1 Mbps with a latency

range of 50 to 100 ms. The UE bandwidth is 1.4 MHz with a maximum transmission power of 20 to 23 dBm. This standard helps to minimize data cost and improves the efficiency of the equipment based on it in the form of low power consumption.[24]

NB-IoT

The technology is used for cellular network devices and services with indoor coverage, long battery life, and high-density connectivity. It has a narrow bandwidth of 200 kilohertz (kHz) with half-duplex transmission. Peak downlink and uplink speeds are 26 Kbps and 66 Kbps, respectively, with a latency range of 1600 to 10 000 ms. The UE bandwidth is 200 kHz with a maximum transmission power of 23 to 33 dBm. Due to the high latency range, it may not be an ideal choice for applications where high emphasis is placed on response and suits stationary applications with occasional data sending and low transmission speed. There is a high level of noise in the transmitted signal and therefore it transmits small data and not large data streams.[23][24]

LoRaWAN

LoRaWAN is one of the unlicensed technologies that does not rely on mobile infrastructure, but uses independently running infrastructure to run. Its providers are few and it is usually up to the application creators to build their own infrastructure. It has a bandwidth of 125 kHz with half-duplex transmission. Peak downlink speed is 300 bits per second (bps) and uplink is 50 Kbps with a latency range of more than 20 seconds. The UE bandwidth is 200 kHz with a maximum transmission power of 22 dBm. This alternative technology is suitable for applications where mobile LPWAN is not supported. Its range is usually 10 to 15 km and is used to connect a large number of industrial devices with low power and sending a low amount of data.[23][24]

SigFox

SigFox is again an alternative technology with the same limitations as LoRaWAN, but it is a more robust technology than LPWAN. It has a bandwidth of 0.1 kHz with half-duplex transmission. Peak downlink speed is 100 bps and uplink 600 bps with a latency range of 1 to 100 ms. The UE bandwidth is 125 kHz with a maximum transmission power of 22 dBm. It is a low-speed communication technology that overcomes distances from 30 to 50 km in open space and up to 10 km in cities. The number of messages sent from the station to the end device is also limited, which is set at 140 per day with a maximum information size of 12 B.[23][24]

1.9.4 IoT Protocols

IoT devices communicate via IoT protocols in Table 1.3, which are used to transport data from one device to another. The device receiving data has to understand the received information and, for example, perform another service. However, IoT protocols are meant to control how data reaches the Internet.

Table 1.3: IoT Protocols Categorized by OSI Model Layer

OSI Layer	IoT Protocols
Application	AMQP, CoAP, DDS, MQTT
Transport	TCP, UDP
Network	IPv4, IPv6, 6LoWPAN
Data Link	IEEE 802.15.4, LPWAN
Physical	BLE, Ethernet, LTE, NFC, PLC, RFID, Wi-Fi, Z-Wave, Zigbee

The structure and purposes of the IoT may differ in several cases and place different demands on themselves; for those reasons, the ways of connecting to the Internet are also variable, the communication protocols are different, and categorized into layers of the Open Systems Interconnection (OSI) model:[21][25]

- **Application layer** – serves to connect the user to the device using protocols Advanced Message Queuing Protocol (AMQP), Constrained Application Protocol (CoAP), Data Distribution Service (DDS), Message Queuing Telemetry Transport (MQTT).
- **Transport layer** – activates and protects data communication in traveling between layers using protocols Transmission Control Protocol (TCP), User Datagram Protocol (UDP).
- **Network layer** – provides communication between devices and router using Internet Protocols IPv4, IPv6, and IPv6 over Low power Wireless Personal Area Networks (6LoWPAN).
- **Data link layer** – transmits data within the internal system architecture and corrects errors found in the physical layer using protocols IEEE 802.15.4, LPWAN.
- **Physical layer** – provides a communication channel between devices within the environment using protocols Bluetooth Low Energy (BLE), Ethernet, Long-Term Evolution (LTE), Near Field Communication (NFC), Power Line Communication (PLC), Radio Frequency Identification (RFID), Wi-Fi/802.11, Z-Wave, Zigbee.

AMQP

The Advanced Message Queuing Protocol belongs to the group of protocols used for communication between IoT devices. AMQP is primarily designed for reliable data

transfer. Similar to other protocols, it consists of several parts: exchanges, channels, queues, bindings, and virtual hosts. Due to its reliability, interoperability, and scalability, it is mainly used in the financial sector, industries, and internet services. Specific uses are in payment processing, fast exchange of coordination messages on production lines in automated systems, and in real-time analytics in monitoring systems.[25][26]

CoAP

The Constrained Application Protocol (**CoAP**) belongs to the group of protocols used in the IoT. Due to its design requirements, **CoAP** is suitable for devices limited in memory, power, and processing capabilities. This server-client protocol is based on request-response messages. **CoAP** is particularly advantageous for resource-constrained environments; however, it has some disadvantages such as latency issues and unreliability in certain conditions. These conditions include low signal strength, high latency, and environments with high levels of interference from other frequencies. **CoAP** shares several features with **Hypertext Transfer Protocol (HTTP)**, such as methods **DELETE**, **POST**, **GET**, and **PUT**. [25][27]

DDS

DDS, also known as Data Distribution Service, is a database shared across multiple communication points (sites), that are accessible to a large amount of users. The main advantage of the **DDS** is global access for users. [25][28]

MQTT

MQTT, also known as Message Queuing Telemetry Transport, is an IoT protocol. Communication with **MQTT** is established between devices using **TCP**. The two main components of **MQTT** are the **MQTT Broker** (central server) and the **MQTT Client** (publisher). The client is the one who sends (publishes) messages to the broker. The received data from the client to the broker are then sent to subscribed clients. Due to its reliability and ability to handle high latency, it is recommended for a large number of clients. **MQTT** is mainly used in automation, smart homes, the automotive industry, and in the health service. [25][29]

TCP and UDP

The **TCP** and **UDP** are the main protocols used on the Internet. The **TCP** provides reliable communication established with a handshake, in contrast to **UDP**. **UDP** provides unreliable but fast communication. **TCP** ensures that every packet is received

in the same order as when it was sent and without errors, making it suitable for applications where data integrity is crucial, such as web browsing and email. On the other hand, UDP does not guarantee delivery or order, making it ideal for real-time applications like online gaming and video streaming, where speed is more critical than reliability. Both protocols operate at the transport layer of the OSI model, with TCP prioritizing connection-oriented communication and UDP focusing on connectionless communication.[25][30]

2 Practical Solution

Accurate meteorological data are essential for environmental monitoring and weather forecasting. Traditional weather stations rely on wired communication or high-power wireless networks, which are not optimal for remote, battery-powered deployments. This work focuses on designing a secure, energy-efficient weather station using NB-IoT, a low-power wide-area network (LPWAN) technology, to enable long-range data transmission with minimal energy consumption. The system incorporates robust sensors and security mechanisms to ensure reliable data collection and transmission. The collected data are processed, analyzed, and visualized using suitable platforms to provide actionable insights and demonstrate the system's capabilities.

The primary objectives of this project are:

- Development of a low-power, autonomous weather station for remote deployment.
- Integration of multiple sensors for comprehensive environmental monitoring.
- Secure data transmission using MQTT and TLS encryption over NB-IoT.
- Optimization of energy consumption to extend battery life.
- Optimization of network consumption.



Fig. 2.1: Weatherstation created for this project.

2.1 Hardware Platform

Many electronic components and sensors were tested during the development of the weather station prototype. Not all of them worked reliably, and therefore it was necessary to find replacements that would be reliable and meet the desired purpose and requirements. These include, for example, the **TPS63020** 3.3 Volts (V) power supply with automatic buck-boost function, which supports input voltages from 1.8 to 5.5 V. In the context of a weather station, this is the most reliable method of power transfer with fluctuating battery and solar panel input voltages.

2.1.1 Hardware Architecture

The weather station in Figure 2.1 consists of the following key components:

- **ESP32-S3-WROOM-1** - microcontroller responsible for sensor data acquisition and communication.
- **Quectel BC660K-GL** - NB-IoT module enabling long-range data transmission.
- **Sensors** - DS18B20 (temperature), VEML7700 (light intensity), SDS011 (air quality), Vaisala WXT536 (multi-parameter weather sensor).
- **Power Management** - solar panel with a TP4056 battery management system and TPS63020 voltage regulator.

As part of the semester project, a number of components on the market that could be part of a prototype device were investigated to meet the requirements for low cost and robust processing. Support for low power modes and broad feature support is important. Complete block scheme of the weather station is in Figure 2.2.

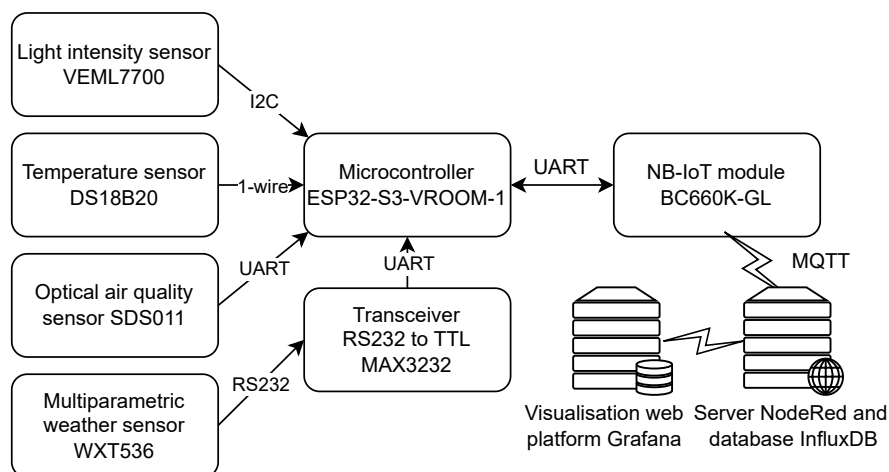


Fig. 2.2: Weather station block scheme.

Design of a prototype board serves as a template for the PCB circuit board of the weather station. The prototype board along with the PCB is designed with an emphasis on robustness and low cost. A radiation shield is designed for the weather station to measure the temperature and shield the temperature sensor from sunlight. The modular design of the weather station is convenient for testing individual components and handling.

2.1.2 Professional Weather Station

A professional weather station consists of a number of advanced sensors, which significantly increase the overall cost. These are sensors with very high accuracy and robustness, commonly used not only in various industries but also in remote or harsh environments around the world. Such regions are characterised by extreme meteorological conditions that often push technology to the limits of its functionality. These sensors include, for example, the PWD (Present Weather Detector), disdrometer, ultrasonic wind meter, acoustic rain sensor, and others.



Fig. 2.3: Professional weather station on the roof of the Faculty of Electrical Engineering and Communication at BUT.

Servicing a professional weather station in Figure 2.3 is also expensive, and refurbishment can cost more than 100,000 CZK. Regular servicing eliminates the risk of possible malfunctions and replaces components that have been worn out in harsh meteorological conditions. It also guarantees the highest accuracy of measured data, which is essential for comprehensive environmental monitoring.

The weather station designed in this thesis emphasizes meeting the requirements of professional weather stations in terms of high accuracy of measured data and robustness. Equally important is the resulting price tag, which is intended to be several times lower than that of professional systems.

2.1.3 Radiation Shield

The radiation shield is an integral part of the weather station. It serves to position the temperature sensor and protect it from parasitic solar radiation, which heats the sensor and artificially increases its temperature. It is essential that a minimum amount of solar radiation penetrates the shield. This is achieved by a white outer coating that reflects sunlight and a black inner coating that absorbs any penetrating radiation. A complete visualization of the radiation shield can be found in the appendices.



Fig. 2.4: Developed radiation shield.

For deployment on the faculty roof, the radiation shield in Figure 2.4 is designed to withstand strong, swirling winds and rain. At the contact points with the 11 cm diameter pole, aluminium profile reinforcement was chosen. The remaining sections are bonded with a strong structural adhesive, and the critical structure of the shield

is reinforced with plastic strips and thin steel cable. In case the plastic fails, the entire structure is secured with a thin steel bow to prevent the shield from being torn off and falling from the roof onto a person.

The entire shield has two points of contact with the pole and is attached using a 4-inch U-shaped steel profile and M12 thread size. A 30 mm diameter aluminium rod can be mounted to this structure, which, together with the base of the weather station, provides up to three connection points for the steel strips. The WXT536 is mounted on this rod.

The top of the radiation shield houses the wiring management and supports the sensor section with a more powerful solar panel, which is also securely bonded and protected against detachment. The protector with all necessary cabling to the solar panel, the VEML7700 light intensity sensor, and the DS18B20 temperature sensor enters this section. Another protector carrying the wiring for the WXT536 exits from this section.

2.1.4 Hardware Casing

There were also high demands on the case in Figure 2.5 in terms of waterproofness, dimensions, and mechanical robustness. The box houses the remaining hardware, namely the printed circuit board with the ESP32-S3 microcontroller, the communication module Quectel BC660K-GL, the DS18B20 temperature sensor, and the SDS011 air quality sensor.



Fig. 2.5: Developed casing.

For the air quality sensor, air tubes were created that are shielded to reduce

the amount of light entering the dust particle measurement chamber. The inlet tube consists of an outer, thicker tube that shields the sensor entrance, and an inner tube that draws in air from outside the enclosure. The thin inner tube increases airflow into the sensor based on the Pitot tube principle, thereby shortening the duration of the air quality measurement.

The entrance to the box is protected by a shield that prevents direct precipitation from reaching the openings and also blocks liquids from entering the SDS011 sensor. An antenna is routed from inside the box, as it no longer fits within the enclosure. The antenna is waterproofed, since it does not meet ingress protection (IP) certification against water and dust. A replacement antenna with proper protection is planned for future deployment.

2.1.5 Data Correlation

The weather station includes a professional multiparametric weather sensor Vaisala WXT536, the price of which is approximately 67,000 CZK. This robust and highly accurate sensor is used to correlate the data with the designed weather station. From the measured data shown in Figure 2.6, it is evident that the proposed station meets the requirements of professional weather stations, and the measured sensor curves align with the curves obtained from the WXT536 sensors.

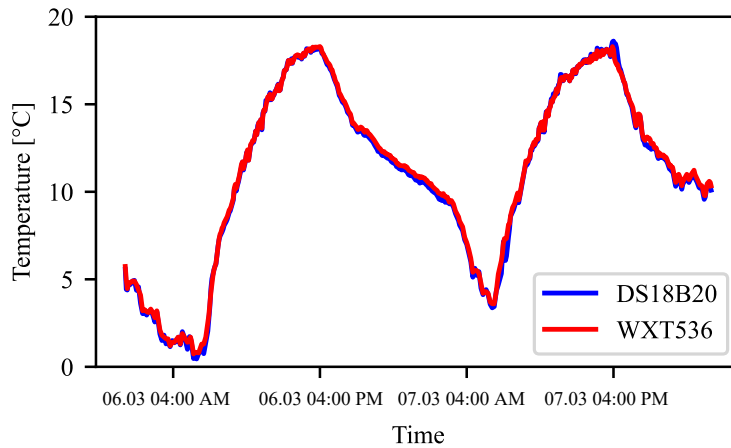


Fig. 2.6: Differences in measurement between DS18B20 and WXT536.

The WXT536 extends the capabilities of the weather station by adding high-precision measurements. These include an acoustic rain sensor, an ultrasonic sensor for measuring wind direction and speed, a humidity sensor, and a barometric pressure sensor. These advanced features enhance the station's ability for comprehensive environmental sensing and, in combination with the air quality sensor and sunlight

measurement, surpass conventional solutions. These are measurements that are not commonly performed by other systems.

The weather station is used within the Meteo Telcorain team, which specializes in opportunistic temperature sensing via microwave links. The measured data in Figure 2.7 demonstrates high accuracy and is also used to correlate results with the proposed weather station, further improving the calibration and accuracy of its sensors. This represents a unique approach to meteorological monitoring not commonly implemented elsewhere.

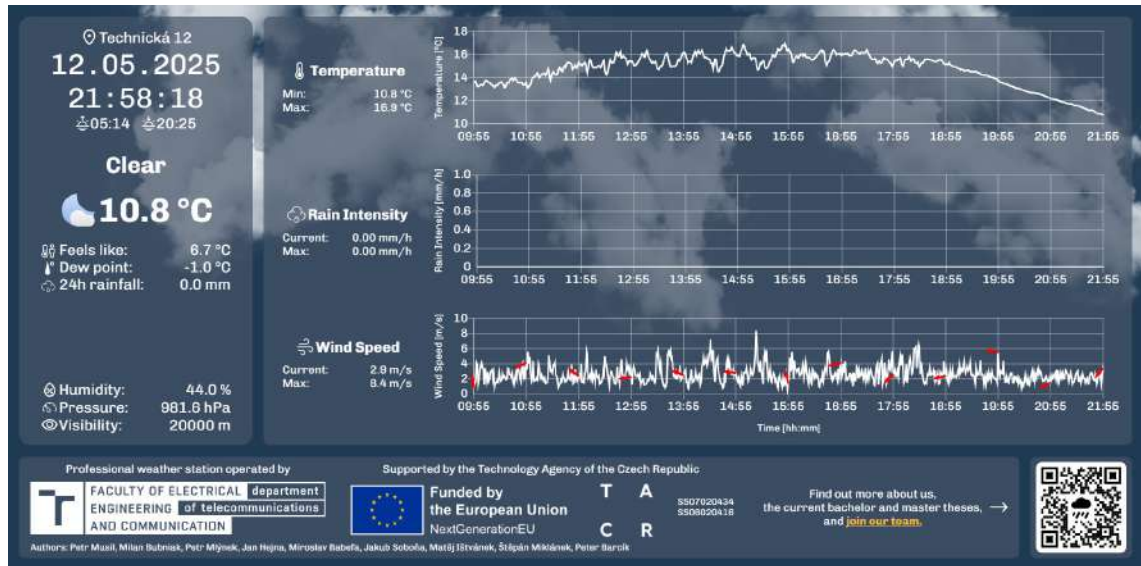


Fig. 2.7: Meteo visualisation.

2.1.6 Measured Meteorological Quantities

The proposed weather station measures the following meteorological variables:

- Temperature – sensor UMW DS18B20
- Sunshine – sensor Vishay VEML7700
- **Air quality** – sensor Nova PM SDS011
- Temperature, humidity, pressure, wind speed and direction (ultrasonic sensor), and precipitation (acoustic sensor) – **professional multiparametric weather sensor Vaisala WXT536, priced at 67,000 CZK**

A complete description of the hardware design is provided in the following chapters. These chapters focus on the development process of the weather station and the challenges addressed during its implementation. A prototype board

was designed and later implemented on a printed circuit board (PCB). The chapters also include specifications of the sensors used, a detailed description of the software solution, and an explanation of the optimization strategies for energy and data consumption.

All measured data are transmitted via the communication module to a remote server, where they are processed and visualized. In addition, software documentation has been prepared, describing the hardware and software solutions in greater detail.

2.1.7 Measuring ranges of the weather station

The technical parameters of the weather station consist of two essential parts. The first are the technical parameters of the sensors and their accuracy in Table 2.1, the second are the technical parameters of the power supply in Table 2.2.

Table 2.1: Technical specifications of the selected sensors

Sensor	Quantity	Accuracy	Interface
UMW DS18B20	Temperature	−55 to +125 °C, ± 0.4 °C (from −10 to +70 °C), resolution 9–12 bits	OneWire, 2.5–5.5 V, pull-up 4.7 k Ω
Vishay VEML7700	Light intensity	0–120,000 lx, resolution 0.0036 lx	I2C, 3.3/5 V
Nova PM SDS011	PM2.5, PM10 [$\mu\text{g}/\text{m}^3$]	0–999.9 $\mu\text{g}/\text{m}^3$, acc. from 0.3 μm	UART / PWM, 4.7–5.3 V, <4 mA (sleep)
Vaisala WXT536	Temp., RH, pressure, wind, rainfall, hail	<ul style="list-style-type: none"> Temp: −52 to +60 °C, ± 0.6 °C RH: 0–100 %, ± 3 % Pressure: 500–1100 hPa, ± 1 hPa Wind: 0–60 m/s, ± 3 % Rain: 0–200 mm/h, res. 0.1 mm/h Hail: 0.1 hits/cm²/h 	RS-232, RS-485, RS-422, SDI-12; 6–24 V, typ. 3.5 mA (12 V), heating up to 1.2 A @ 24 VDC

The complete technical documentation of the ESP32-S3 microcontroller and the BC660K-GL communication module can be found in the appendices together with the technical documentation of the used sensors in the chapter *Technical Documentation of the Weather Station Components*. There is also a complete technical documentation of the weather station in Table A.1.

2.2 Prototype Device Development

During the development process, a number of electronic components were tested and only some of them met the high demands placed on an NB-IoT device. The components listed in Table 2.2 were selected as the most reliable.

Table 2.2: Technical parameters of power management components used in the prototype board

Component	Technical Parameters and Description
Solar Panel	6 V/4.5 W polycrystalline panel, max current 520 mA, replaces 6 V/1 W testing panel (167 mA), used for outdoor autonomous charging.
TP4056	Lithium-ion charging module with integrated protection (DW01A + FS8205A), input 4.5–5.5 V, charging current 1 A (adjustable), overcharge protection at 4.2 V, undervoltage protection at 2.4 V, microUSB input, operating temp. -40 to $+85$ °C.
TPS63020	Buck-boost converter, input 1.8–5.5 V, output selectable (2.5 V, 3.3 V, 4.2 V, 5 V), max output current 3 A, switching frequency 2.4 MHz, high efficiency, stable output even with variable input, operating temp. -40 to $+85$ °C.
SX1308	Boost converter, input 2–24 V, output 3–28 V, max current 2 A, efficiency up to 98 %, frequency 1.2 MHz, quiescent current 1.5 mA, undervoltage shutdown, output adjustable via trimmer. Used for 5 V and 12 V outputs.
IRLZ44N	Logic-level N-MOSFET, gate threshold 2–4 V, low $R_{DS(on)}$, low heat losses, ideal for switching on GND side, used in final version (horizontal mount IRLZ44NSTRR).
Battery 18650	Two parallel 18650 Li-Ion batteries, 3.7 V, 3500 mAh each, total capacity 7000 mAh, rechargeable via solar panel, replaceable/testable via dual battery connectors.

2.2.1 Solar Panel

The solar panel in Figure 2.8 with parameters 6 V and 1 W is a simple solar panel that is 3 mm thick and provides waterproof protection from rainfall. It is suitable for battery charging in combination with the TP4056 charging circuit and has been used as an “entry-level” solar panel to test the functionality of the TP4056 charging module.

On a cloudy day, it provided an output charging voltage of 4.2 V and was fitted with the same charging module in a prototype weather station. Demands are placed on high performance and it is questionable how this panel would be able to recharge the battery during the winter period (short and cloudy days with a lack of sunlight). On the face of it, it is a robust solar panel and this is a very important parameter in the project.[48]

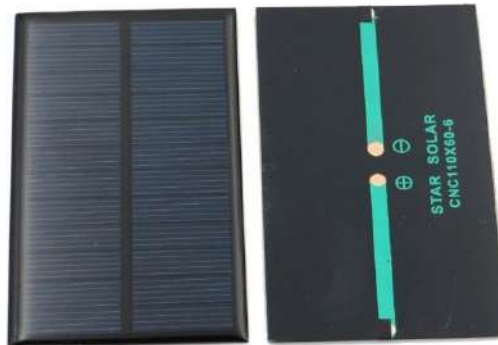


Fig. 2.8: Solar panel 6 V/1 W used for prototype testing.[48]

It is a polycrystalline solar panel with an output voltage of 6 V and an output current of up to 167 mA.[48] However, the output power is not sufficient and for this reason, the final design of the weather station was equipped with a photovoltaic solar panel with an output power of 6 V/4.5 W and a maximum output current of 520 mA.

2.2.2 Battery Charging Module TP4056 with Protection

The lithium-ion cell charging module TP4056 with integrated protection and microUSB connector, shown in Figure 2.9, is a practical solution for efficient and safe charging of lithium-ion batteries. This charger uses the TP4056's integrated circuitry to precisely control the charging process while ensuring the battery is protected from adverse effects such as overcharging, over-discharging, or overloading. The project initially used a USB-C variant, which was damaged during battery discharge. The module experienced significant overheating when connected to a computer and eventually failed. After replacement, charging via a computer power source was no longer tested.

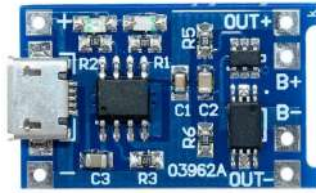


Fig. 2.9: Battery charger with protection TP4056.[49]

The device operates with input voltages ranging from 4.5 to 5.5 V, allowing for easy power supply via USB ports or adapters. The default charging current is set to 1 A, and can be adjusted by changing the resistor R3 on the board, providing flexibility for different battery types and applications.[49]

One of the main advantages of this module is the presence of integrated protection circuits. Over-discharge protection is activated when the voltage drops below 2.4 V, while overcharge protection is triggered when the voltage reaches $4.2 \text{ V} \pm 1\%$. In addition, the module incorporates short-circuit and overload protection to minimize the risk of damage to the battery and the device itself. The operating temperature range is from -40 to $+85$ °C.[49]

The charger features LED indicators that show the charging status. A red LED indicates that charging is in progress, while a blue LED signals a fully charged battery. A microUSB connector is used for power input, and the battery is connected via solder pads on the board.

Thanks to its compact dimensions, the module is easy to integrate into a wide range of applications. Its use is particularly suitable for projects requiring reliable and safe charging of lithium-ion batteries, such as portable devices, battery-powered systems, or DIY electronics. The combination of ease of use, built-in protection, and configurability makes the TP4056 a versatile solution for modern electronic applications. This module is used in the prototype board.

2.2.3 Micro Voltage Regulator Module AMS1117 3.3 V

The AMS1117 module in Figure 2.10 was intended to be used within the project to regulate and stabilize the output voltage from the TP4056 module. A fully charged battery can have a voltage of 4.2 V, which is not an acceptable value for powering a microcontroller. To address this issue, the AMS1117 module was chosen and initially functioned properly, until the battery voltage dropped to approximately 3.5 V. At that point, it was no longer possible to supply the microcontroller with the required 3.3 V, because the AMS1117 requires a higher input voltage to maintain regulation — this dropout voltage was too high for the needs of this project. It was therefore replaced during development with a more advanced regulator with a low dropout, capable of maintaining the output voltage even when the input voltage is close to or below the target output.



Fig. 2.10: Micro voltage regulator module AMS1117 3.3 V.[50]

The input voltage for this module should be in the range of 4.8 to 15 V, and the output voltage is 3.3 V. The maximum output current is 800 mA and the operating temperature range is from -40 to $+125$ °C.[50]

2.2.4 Automatic Buck-Boost TPS63020 Converter (1.8–5.5 V, 2 A)

This is a replacement module for the AMS1117 that provides a 3.3 V output voltage with minimal output signal ripple. The TPS63020, manufactured by Texas Instruments in Figure 2.11, is an automatic buck-boost voltage converter that can regulate the 3.3 V output voltage regardless of whether the input voltage is lower or higher. It can produce a stable output voltage even with a variable input voltage. Such

a high-quality and stable output signal provides a reliable power supply to the remaining components within the weather station, which is used in variable conditions.



Fig. 2.11: Automatic Buck-Boost TPS63020 power converter 1.8–5.5 V, 2 A.[51]

The required input voltage ranges from 1.8 to 5.5 V, with a recommended minimum of 2 V. The output voltage is selected by a solder jumper and can be set to 2.5 V, 3.3 V, 4.2 V, or 5 V. The maximum output current is 3 A and the switching frequency is 2.4 MHz. The module also provides additional pins and modes, such as external enable signal switching, power-saving (PS) modes, or PS output status indication. All these features are optional, and the module can operate as a standalone element without them. The operating temperature range of the control module is from -40 to $+85$ °C, and it is commonly used in data terminals, barcode scanners, electronic IP cameras, security locks, and similar devices. This module is used in the prototype board.[51]

2.2.5 Step-Up Boost Converter with SX1308 (2 A)

The basic power supply of the prototype weather station is 3.3 V, but components such as the Quectel BC660K-GL, Nova PM SDS011, or Vaisala WXT536 require higher voltages to operate. To achieve these, a simple SX1308 boost converter with a resistive trimmer in Figure 2.12 is used to regulate the input voltage up to output levels such as 5 V. The desired voltage is set by adjusting the trimmer while continuously monitoring the output until 5 V or 12 V is reached.



Fig. 2.12: Step-up boost converter with SX1308 2 A.[52]

A more advanced alternative to this converter is the buck-boost TPS63020 automatic converter, which offers a stable output voltage with minimal ripple. The SX1308 inverter accepts input voltages from 2 to 24 V and provides output voltages from 3 to 28 V with a maximum current of up to 2 A. Its efficiency can reach up to 98 %, and the switching frequency is 1.2 MHz. Quiescent current consumption is 1.5 mA, and the converter includes undervoltage shutdown protection. The operating temperature range is from -40 to $+85$ °C. This module is used twice in the prototype board — for the air quality sensor SDS011 and transceiver MAX3232 (5 V), and for the multiparametric weather sensor WXT536 (12 V).[52]

2.2.6 Line Driver and Receiver MAX3232 Multichannel RS-232

For communication with the Vaisala WXT536 sensor, the RS-232 bus was chosen. A cable is used for this purpose, featuring a female 8-pin M12 power connector on one end and an RS-232 connector on the other, which was purchased and manually soldered. The MAX3232 3 V to 5.5 V multichannel RS-232 line driver and receiver in Figure 2.13, which supports TTL/UART logic levels, was selected for communication with the microcontroller. The specified operating temperature is 0 to $+70$ °C for the MAX3232C variant and -40 to $+85$ °C for the MAX3232I variant.[53][54]



Fig. 2.13: Line Driver and Receiver MAX3232 Multichannel RS-232.[54]

Based on inconsistent labeling and unclear documentation, it was determined that the module carries the designation MAX3232ESE. According to the datasheet, converters with the MAX32_E_ designation fall within the extended operating temperature range from -40 to $+85$ °C. This converter is commonly used for firmware updates of routers, mobile phones, GPS devices, NXP chips, and other electronic equipment. This module is used in the prototype board.[53][54]

2.2.7 Transistor

The project aims to minimize the current consumption of individual components. This can be achieved using sleep modes or by completely disconnecting power from the devices. The Nova PM SDS011 air quality sensor supports sleep mode, but its power consumption is still relatively high. A simple solution is to cut off the supply voltage using a transistor without the need to solder additional wires directly to the sensor. The Quectel BC660K-GL module supports extremely low power modes, but every time it is restarted, it needs to re-register to the NB-IoT network, which temporarily increases consumption. The ESP32-S3 microcontroller supports and uses deep sleep mode effectively.

The NPN STMicroelectronics TIP132 transistor in Figure 2.14 was used in early development. It was controlled by the microcontroller and was activated during its working window to enable power to connected sensors. All sensors had sufficient time to initialize and take valid measurements. The microcontroller entered deep sleep for 1 minute, while the measurement window was precisely timed. Proper estimation of active time and transmission is crucial for battery savings.



Fig. 2.14: Transistor NPN STMicroelectronics TIP132.[55]

Sleep modes can also be used as an efficient alternative, eliminating the need to cut power using a transistor. The BC660K-GL module does not require *PSM_INT* pin for wake-up. In deep sleep mode, it disconnects the UART bus, but if any signal appears on the UART input, the module wakes up and establishes communication. Therefore, it is recommended to send the AT0 command multiple times to ensure wake-up.

Initially, the TIP132 transistor appeared functional, but issues later emerged with power delivery to the BC660K-GL module, which failed to communicate with ESP32-S3 and struggled with network registration.

The BC660K-GL development kit uses a test SIM card from Vodafone CZ, and some prototype testing took place in Slovakia. The module was unable to connect to the network despite roaming support, likely due to incorrect configuration or unstable input voltage.

To diagnose this, a test circuit was assembled to monitor communication between the ESP32-S3 and BC660K-GL using a CH9102 UART converter in Figure 2.15. Voltage levels were measured, revealing a ground fault. After correction, the module functioned correctly and communication was restored. The TIP132 transistor was also confirmed to be functional and did not require replacement. The issue only manifested under load, when the sensor components were powered.



Fig. 2.15: UART driver and receiver CH9102.[56]

However, the TIP132 transistor has low efficiency, with significant power losses at the base and collector. Under higher current, it tends to overheat and requires cooling. It is not ideal for digital circuits and was therefore replaced by the IRLZ44N logic-level MOSFET. This transistor fully opens at a gate voltage of approximately 4–5 V and starts conducting at around 2 V. Its low drain-source resistance ensures minimal thermal losses. The N-channel MOSFET is well suited for low-voltage switching on the ground side in digital and microcontroller applications.

This transistor is used in the prototype board, and in the final PCB it is used in the IRLZ44NSTRR version with horizontal mounting. The prototype board continuously disconnects the BC660K-GL module from the power supply. In the PCB version, the *PSM_INT* line is used to reduce data and power consumption even further.

2.2.8 Batteries

The battery GeB LiPo1 503035 500 milliampere-hour (mAh) 3.7 V JST-PH 2.0 in Figure 2.16 was used as a test battery for the power circuit during the initial

stages of weather station development. However, it was not selected for outdoor use, as these batteries are known to have a short lifespan and may suffer damage under extreme temperature conditions.



Fig. 2.16: Battery GeB LiPoL 503035 500mAh 3.7 V JST-PH 2.0.[57]

As a replacement, a higher-capacity 18650-type battery was chosen, suitable for more demanding conditions. This battery is charged via a solar panel and can be disconnected from the circuit. The prototype board includes two battery connectors with different pin sizes, allowing connection of both a test battery and an 18650 battery independently.



Fig. 2.17: Used batteries in the weather station.

Initially, the Tenpower INR18650-32HE battery with a capacity of 3100mAh and a maximum discharge current of 10 A in Figure 2.17 was used. Later, two KEEPPower 18650 3500mAh 3.7 V batteries were connected in parallel, which increased the overall capacity and prolonged the operating time of the weather station during periods of limited sunlight.

2.3 Developed Prototype Device

The development is carried out on a soldering board, on which small electronic components could also be attached. In the image 2.18 on the left side of the prototype board, the power supply pins of the sensors are mounted, for which the cable terminals were also specially adapted. The ESP32-S3 development board is located near the power supply pins along with the main board switch.

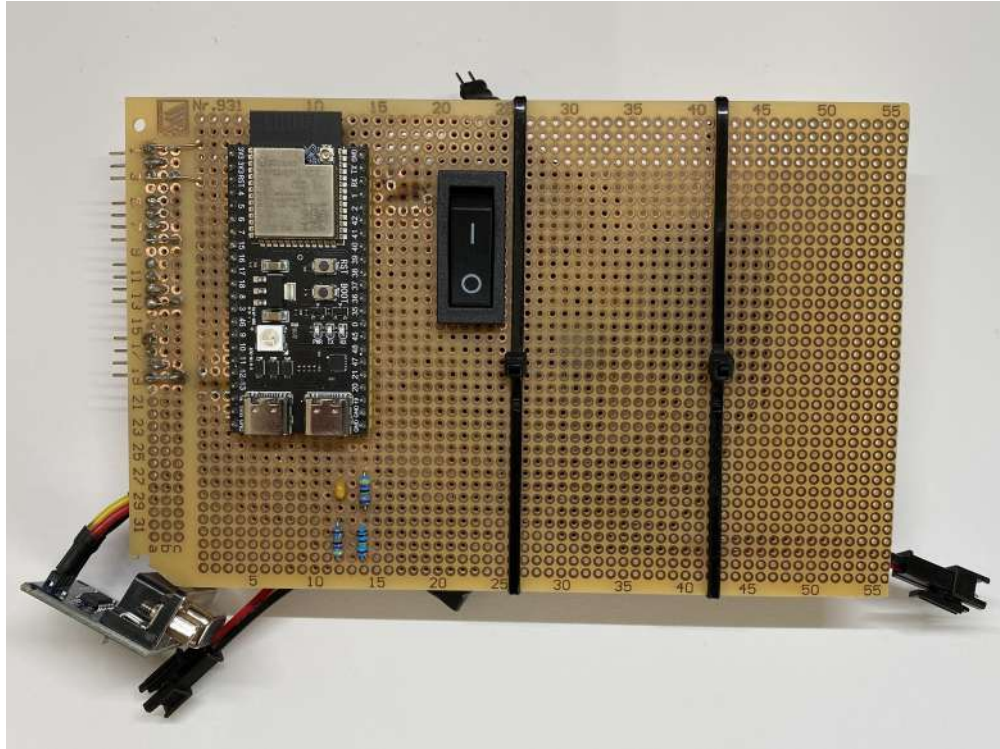


Fig. 2.18: Developed prototype board top.

2.3.1 Selected Modules

The prototype board consists of selected modules that were tested and found to be the most suitable for the design of the weather station control board. The design of the board is modular and easy to manipulate. Using soldering, it was possible to change some modules for others in case a given module did not meet the requirements of the weather station design. Selected modules that were implemented in the prototype board include:

- Microcontroller ESP32-S3-DevKitC-1
- Battery charging module TP4056 with protection
- Automatic Buck-Boost TPS63020 power converter 1.8-5.5V 2A
- Two Step-up boost converters with SX1308 2A
- Line Driver and Receiver MAX3232 Multichannel RS-232
- Transistor N-MOSFET IRLZ44N 55V / 47A - THT

2.3.2 Prototype Device Layout

The individual modules can be seen in 2.18 and 2.19. The NB-IoT module is connected to the microcontroller via wires and is not located on the prototype board. The *PSM_INT* channel is not used and this increases the number of registration

procedures to the network, data consumption, and current consumption. Thus, the module does not rely on sleep modes, but on a power supply that is controlled via a transistor together with the sensor power supply.

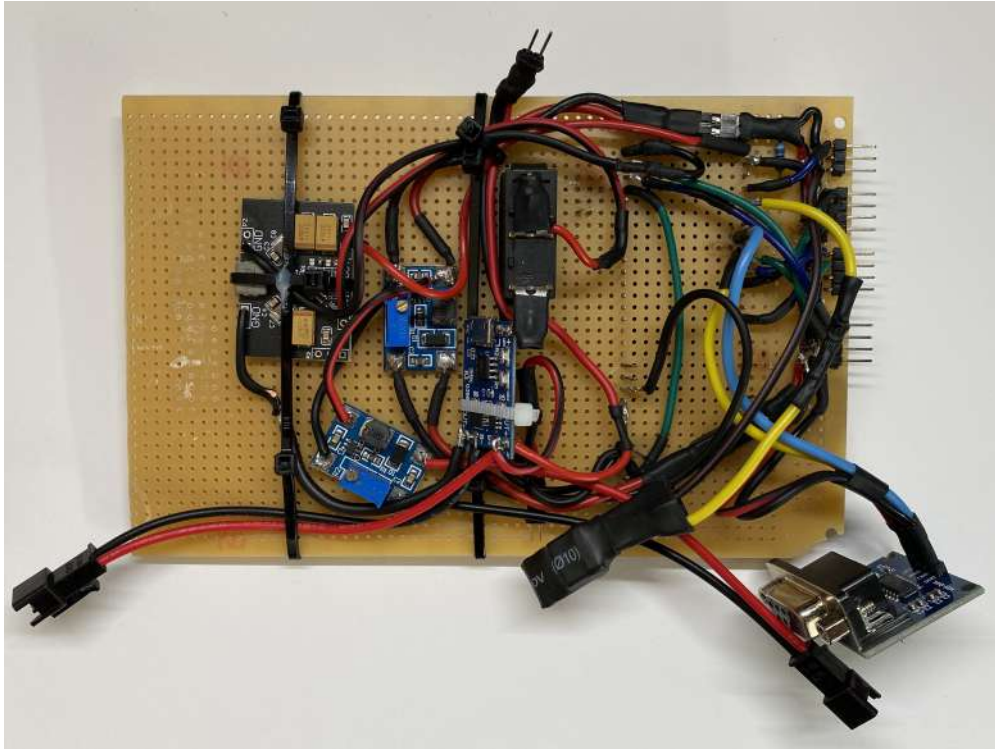


Fig. 2.19: Developed prototype board bottom.

2.3.3 Advantages and Disadvantages

The board is fully functional and can be used as a backup board in case of PCB failure or as a full-fledged control of another weather station. The design, however, is not completely reliable and carries several risks, such as the risk of oxidation, breakage or complete detachment of the wires, disconnection or damage to the module due to vibration or inexpert handling. The design also increases the risk of short-circuiting wires and the biggest minus is the size of the board, which is not compact at all and takes up unnecessary space in the weather station box.

The main switch connects the TP4056 module to the TPS63020 buck-boost converter - battery charging is not affected by the main switch and charges the batteries continuously. It is suitable to connect one 18650 battery or two batteries in parallel to the charging module.

All LEDs on this board can be lit and consume current; disconnecting them is not possible, only unsoldering them. On the PCB it is possible to disconnect these diodes using jumpers and thus save power. During the development of the prototype board, an algorithm that measures the data from the sensors, processes it and sends it to the server was developed at the same time and is implemented on the PCB.

2.4 Developed Final PCB Device

The printed circuit board in Figure 2.20 implements components that are also found in the individual modules in the prototype board. All component wiring diagrams were designed according to the recommendations of the component manufacturers, and the board is divided into multiple areas. All components are fitted on the front side, which facilitates soldering and reduces manufacturing costs.

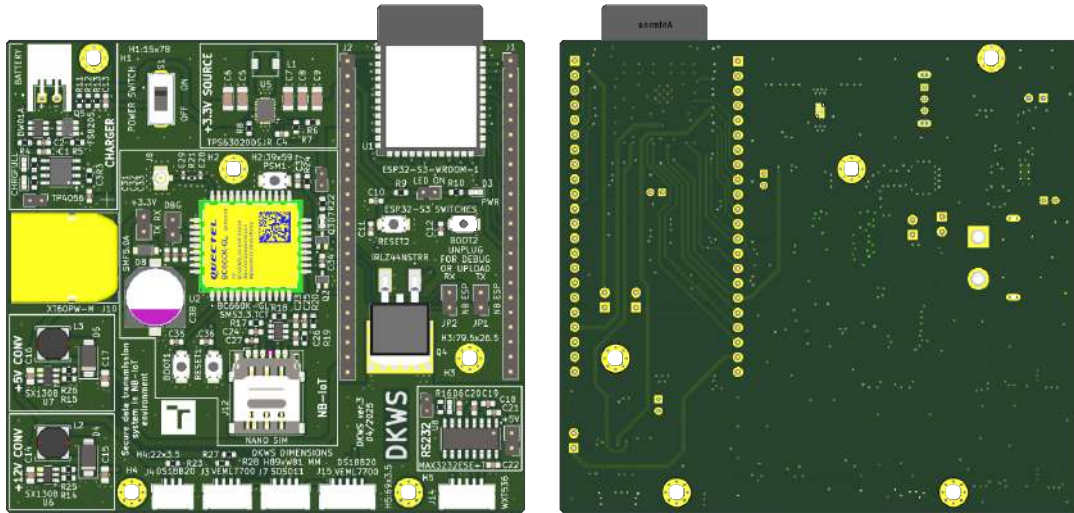


Fig. 2.20: DKWS PCB (89x81mm) designed by the prototype board.

2.4.1 Final Device Layout

The board is divided into 7 areas:

- **Charger** - protected battery charger
- **+3.3V SOURCE** - main voltage source for ESP32-S3 and BC660K-GL
- **+5V CONV** - voltage converter for SDS011 and MAX3232
- **+12V CONV** - voltage converter for WXT536
- **NB-IoT** - module BC660K-GL with antenna connector and NANO SIM card holder
- **ESP32-3-WROOM-1** - microcontroller with transistor controlling sensor power supply

- **RS232** - transceiver MAX3232 for communication with WXT536

The board is a 4-layer design, with the top layer containing most of the signal paths, where conductor widths range from 0.25 mm to 1 mm. A minimum clearance of 0.5 mm is maintained between poured copper areas and signal traces. The first layer also contains poured ground copper zones for the 3.3 V supply, the sensors, and the charging circuit.

The second layer includes additional ground copper areas, which serve to reduce signal interference between layers and improve power distribution to ground. Each grounded component is connected through 3 or 4 vias with a diameter of 0.3 mm, enhancing the electrical stability and ground connection of the component. None of the vias are covered with solder mask (text paint) and fully comply with the manufacturing requirements of JLCPCB, the board manufacturer.



Fig. 2.21: Manufactured DKWS PCB.

2.4.2 Improvements over Prototype Device

All LEDs can be disconnected to reduce battery current consumption. Compared to the prototype board, this is a significant advantage that contributes to the overall stability of the system. The board also includes additional pins connected to the ESP32-S3 microcontroller in the same configuration as on its official development board.

The design anticipates the possibility of connecting additional sensors in the future, which are not currently defined, but could extend the functionality of the DKWS.

The board in Figure 2.21 can be mounted using five holes located on its surface, which are designed to avoid short-circuiting any nearby copper planes. The holes situated within the grounded 3.3 V copper areas are electrically connected to those areas, whereas the remaining holes are isolated from any copper surface.

All holes are plated, which increases their mechanical strength and reduces wear during further development or handling of the weather station. The connectors used for attaching sensors and the battery are equipped with mechanical fuses or locks that prevent accidental disconnection, thus increasing the durability and reliability of the board.

2.4.3 Power Management

Other important advantages of this board include integrated power management in Table 2.3. The power supply parameters relate both to the prototype board of the weather station and to the final printed circuit board, which is based on the prototype design intended to control the entire weather station.

Table 2.3: Power management components and parameters

Component	Description
TP4056	Li-Ion charging module with protection circuit (DW01A) and MOSFET FS8205A
Battery protection	Undervoltage protection under 2.4 V, reconnection at 2.9 V / 130 mA
Charging limits	Safe charging up to 4.2 V with overcurrent and short-circuit protection
Charging method	Constant current or constant voltage charging supported
Input parameters	4.5–6 V input voltage, max. input current 3 A
Battery configuration	2 × Li-Ion 18650 (3.7 V, 3500 mAh) in parallel
Solar panel	6 V / 4.5 W / max. 750 mA
Voltage converters	TPS63020 buck-boost converter and two SX1308 boost converters
Switching components	N-MOSFETs for power control: FS8205A and IRLZ44N

Because all UART lines are used on the board, it is not possible to have a free UART0 line for debugging or serial output. This limitation is solved by dedicated debug pins and jumpers, which can disconnect the connection between the microcontroller and the NB-IoT module.

These pins can be used to upload code either to the microcontroller or to the NB-IoT module, and enable the debug mode implemented in the firmware, which outputs necessary diagnostic information to the serial monitor. The jumpers also serve to disconnect selected modules from the power supply when needed, particularly during debugging, especially the BC660K-GL and MAX3232 modules. Dedicated pushbuttons are used to control the ESP32-S3 and BC660K-GL modules easily.

2.4.4 Device Testing

During testing, several problems were found in the designed board. The schematic design followed the recommendations of the individual module manufacturers; however, the TP4056 module can be found on the market in a variety of wiring designs. Cheap versions of the complete modules of this charger connect the PAD area to the positive pole of the solar panel, but a connection to GND is more appropriate. On the circuit board, a variant with connection to the positive pole of the solar panel was tested, but the new version of the schematic, available in the appendices, implements a grounded PAD.

A problem was also found in the grounding of the voltage divider measuring the battery voltage, where the grounding must be connected to the 3.3 V reference instead of GND for correct operation.

The last issue was identified in the circuitry between the BC660K-GL communication module and the SIM card holder, where a short circuit occurred between the CLK signal and the VCC power supply line of the SIM card. This issue has also been addressed in the new version of the board. The documentation of the latest version of the board can be found in the appendices of the thesis.

2.5 Device Documentation

The board was designed in the KiCad 9.0 development environment, and all PCB documentation can be found in the appendices. All the necessary component designations are printed on the board, and the job title is printed on the board as well, along with the board dimensions and coordinates of all holes to facilitate future design of the board holder.

5 PCB boards have been produced and it is planned to deploy them in several weather stations that will be distributed around the city of Brno. The board is marked DKWS, which stands for “Daniel Kluka Weather Station”. Compared to the prototype board, PCB in Figure 2.22 has much smaller dimensions - only 89 mm in height and 81 mm in width.

2.6 System Software Design and Implementation

The system is programmed using Arduino IDE, with sensor data processed locally before being transmitted via MQTT over NB-IoT. Data integrity and confidentiality are ensured using TLS encryption. The data is sent to a remote server for storage and visualization using Node-RED, InfluxDB, and Grafana.



Fig. 2.22: Detail DKWS PCB.

2.6.1 Main Algorithm

The main measurement algorithm is able to initialize all sensors and continuously measure the actual values from the sensors. A function is also available to measure the average values of the four measurements, which are later sent via the NB-IoT module Quectel BC660K-GL to the Node-Red server via the MQTT broker Mosquitto. The project also tested the implementation of the HiveMQ MQTT broker HiveMQ. Due to its complexity and excessive scope, the complete flow chart describing the control of the weather station can be found in the appendices of the thesis.

Battery Management

Within the source code, several functions are created that work with the batteries and optimize the operation of the weather station so that it does not consume too much power. The algorithm checks several parameters at runtime and adjusts the measurement frequency accordingly, which is advantageous when saving batteries on cloudy days or when using the batteries fully on sunny days. The algorithm is also capable of estimating the actual charging current based on the solar panel parameters and light intensity.

Operating Modes

At the beginning of the source code, several macros are created, and they can be set at will by the user, to start individual modes of operation or to virtually disconnect the HW modules used by the weather station. If a sensor fails to initialize, the algorithm automatically continues without the particular sensor. This principle accounts for the possibility that a sensor has been disconnected or damaged.

Due to the use of all 3 UART buses, communication via the serial monitor is not available and therefore several microcontroller test modes are created to allow this possibility, but in this case, manual reconfiguration of the pins is required.

Measurement Logic

In the prototype board, measurements can be taken every minute, and between measurements, the sensors and BC660K-GL are completely disconnected from the power supply, and the ESP32-S3 microcontroller is in deep sleep mode. When the measurement is switched on, the microcontroller is first initialized, and it is checked that the battery is charged to at least 3.3 V. If the battery is charged, the measurement is performed, and the data are sent. If not, the microcontroller is put into sleep mode again. Data are sent every 6 minutes and are stored in a buffer in the RTC memory of ESP32-S3. In the PCB, module BC660K-GL uses *PSM_EINT* to wake up.

2.6.2 Node-RED, InfluxDB, and Grafana

The Quectel BC660K-GL is used to send data through the MQTT Mosquitto server to Node-RED in Figure 2.23.

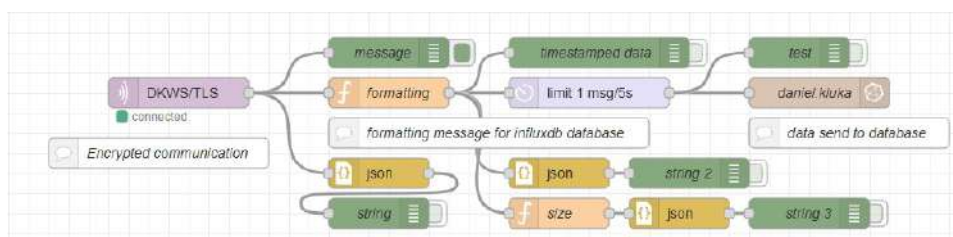


Fig. 2.23: Created flow on the Node-RED server, which processes the data and stores them in the InfluxDB database.

Data Transferring

An MQTT message containing 6 measurements is sent to the server. The server processes these measurements into the form in which they will be entered into the In-

fluxDB time series database. Since all operating time data is measured in the weather station, it is possible to calculate the exact time in milliseconds when each measurement was taken.

Data Visualisation

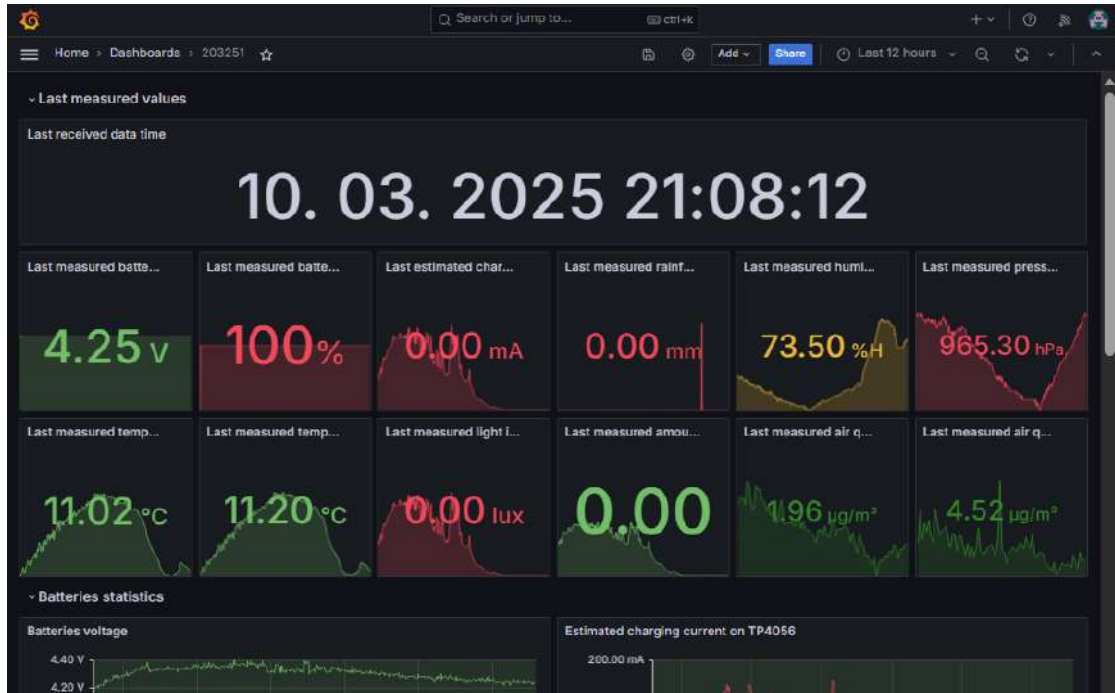


Fig. 2.24: Grafana dashboard created to visualise measured data.

The data entered into the database are further visualized via the Grafana platform in Figure 2.24, where all the necessary graphs of meteorological variables as well as diagnostic operational data are created. Grafana highlights the last measured (current) values, but also graphs in which data in any time interval are visualized with color thresholds.

2.6.3 Data Timestamping

Initially, the timestamps were computed by sending the data from the weather station to Node-RED, which computed when the measurements were taken from the default sleep length, initialization length, and measurement length. It needed the time the data was received by the server to do this, but this caused a time offset against reality. For example, the length of time the BC660K-GL device registered to the network was not included, nor was the time in milliseconds when the ESP32-S3 goes to sleep measured.

Weather Station Diagnostics

Later, new device diagnostic data was added - the first is the total cycle length, which is stored in the RTC memory, and the next time the ESP32-S3 is powered up, it is stored in the buffer at the corresponding previous index. In the last measurement, this value is stored 1 index higher, so this data was missed in the calculation of timestamps. The second diagnostic is the amount of time the BC660K-GL module took to register to the network during the last measurement cycle of the device. After registering to the network, the microcontroller measures the time length of the current ESP32-S3 cycle and retrieves the time from the network when generating the MQTT message. A new function is created to convert this time into UNIX format. This function is used by another function generating the MQTT message to send. After conversion to UNIX format, another function is used to calculate the time offset:

$$offset = espDuration - measureDuration - initDuration \quad (2.1)$$

This time offset indicates how long the measurement has been completed. For the last measurement it includes, for example, the initialization duration of the BC660K-GL and the registration duration to the network, or the total execution duration of the remaining code after the measurement. This is converted from milliseconds to seconds and subtracted from the obtained UNIX stamp, and thus the time of the last measurement is accurately determined. The function further detects how many measurements have been made based on the BUFFER_SIZE variable - the size of the buffer stored in the RTC memory with all the measured data in Table 2.4 - and calculates the stamp for each data measurement.

Sleep Cycling

For the remaining measurements, however, the remaining diagnostic data is also used, not just the aforementioned offset of the current cycle. This includes, for example, the current sleep duration (the sleep duration changes itself after a new update according to the current state of charge), the measurement duration of the previous cycle, and also the initialization duration of the previous cycle.

- offset of the current cycle
- UNIX timestamp for 6th measurement
- measureDuration
- initDuration
- *sleep*
- offset of the current cycle
- UNIX timestamp for 5th measurement

- measureDuration
- initDuration
- *sleep*
- offset of the current cycle
- UNIX timestamp for 4th measurement
- measureDuration
- initDuration
- *sleep*
- offset of the current cycle
- UNIX timestamp for 3rd measurement
- measureDuration
- initDuration
- *sleep*
- offset of the current cycle
- UNIX timestamp for 2nd measurement
- measureDuration
- initDuration
- *sleep*
- offset of the current cycle
- UNIX timestamp for 1st measurement
- measureDuration
- initDuration
- *sleep*
- *device startup*

Table 2.4: Overview of data sent by the weather station via MQTT

Key	Description	Unit
Ts	UNIX timestamp of measurement (computed via BC660K-GL)	s
Vb	Battery voltage at time of measurement	V
Sc	State of charge of the battery	%
Re	Indicates if the battery was recharged	–
Id	Duration of sensor initialization	ms
Md	Duration of measurement	ms
Ed	Duration from wakeup to end of measurement (ESP time)	ms
Rd	Duration of NB-IoT module registration to the network	ms
Td	Air temperature from DS18B20 sensor	°C
Lu	Illuminance from VEML7700 sensor	lx
Wh	White light value from VEML7700 sensor	–
Cc	Estimated charging current from solar panel	mA
PM25	Particulate matter concentration $\leq 2.5 \mu\text{m}$ (SDS011)	$\mu\text{g}/\text{m}^3$
PM10	Particulate matter concentration $\leq 10 \mu\text{m}$ (SDS011)	$\mu\text{g}/\text{m}^3$
Tw	Air temperature from WXT536 sensor	°C
Hu	Relative humidity (WXT536)	%RH
Pr	Atmospheric pressure (WXT536)	hPa
Ra	Precipitation total (WXT536)	mm

Data Processing

All this data is processed by the function shown in Listing 2.1, and the generated timestamps are stored in a buffer located in the RTC memory. The function responsible for generating the MQTT message then retrieves the data from this buffer. Previously, the timestamps were calculated by the Node-RED server; currently, this task is handled directly by the weather station, which determines how long it has been in sleep mode.

Listing 2.1: Part of the function generating the message

```
String generateMQTTMessage() { 1
    #ifdef TIMESTAMP 2
        dataBuffer[bufferIndex-1].espDuration = millis(); 3
    #endif 4
    5
    #ifdef BC660K 6
        dataSendTime = quectel.getDateAndTime(); 7
        int64_t ts = convertCclkToUnix(dataSendTime.c_str()); 8
        computeAllTimestamps(ts, sleepCyclesLimit, dataBuffer); 9
    #endif 10
```

2.6.4 Power Optimization

To extend battery life, the following strategies were implemented:

- Duty cycling to put the ESP32-S3 into deep sleep between measurements.
- Selective power control of sensors using a transistor.
- Adaptive transmission frequency based on environmental conditions.

Sleep Parameters

Initially, the weather station was controlled using macros in Listing 2.2 defined at the beginning of the code, which were used to control the sleep mode:

Listing 2.2: Macros defined at the beginning of the code

```
// ESP32-S3 uses sleep logic to measure samples every 5 or 30 minutes, recharge 1
    ↪ battery for 2 hours and send data every hour
#define ESP_SLEEP 1 // basic measurements - air temperature 2
    ↪ (DS18B20), light intensity (VEML7700), weather parameters (WXT536)
#define SDS_SLEEP 6 // air quality measurement (SDS011) 3
#define RECHARGE 120 // if battery drops below 3300 mV, weather 4
    ↪ station stops measuring for 2 h to recharge
#define DATA_SEND 6 // measured and stored data in data buffer 5
    ↪ sent every hour via BC660K and MQTT to Node-Red server
```

<code>#define SAMPLES 5</code>	<code>// number of sensor data samples to be</code>	6
<code>↪ measured</code>		
<code>// ESP_SLEEP, DATA_SEND and BUFFER_SIZE are connected -> 60 / 10 = 6, alternate</code>		7
<code>↪ version if not evenly divisible used in declaration space</code>		

This sleep management principle has been updated. Initially, it was defined in the `ESP_SLEEP` macro that the weather station should sleep for 10 minutes, in `DATA_SEND` that data should be sent every 60 minutes, and on the basis of this data `BUFFER_SIZE` was defined indicating the number of measurements taken during the hour in Listing 2.3.

Listing 2.3: Calculation of the message buffer size

<code>// buffer storing data in RTC memory while ESP32-S3 is sleeping - buffer sent</code>	1
<code>↪ every hour</code>	
 	2
<code>// automatically calculated buffer size, data measured every 5 minutes - 12</code>	3
<code>↪ times / hour</code>	
<code>// #define BUFFER_SIZE (DATA_SEND / ESP_SLEEP)</code>	4
	5
<code>// alternate version, round up if not evenly divisible</code>	6
<code>#define BUFFER_SIZE ((DATA_SEND + ESP_SLEEP - 1) / ESP_SLEEP)</code>	7

Light Power Saving Mode

The values of macros were originally passed to the corresponding variables before the `setup()` function, which executes the entire weather station program. Currently, they are assigned only within the `setup()` function.

A new logic has been implemented that measures the battery charge level as a percentage. If the battery level is above 80%, the weather station performs standard meteorological measurements (temperature, humidity, pressure, light intensity) and diagnostic readings every minute. These diagnostics include battery voltage (in mV), battery charge (in %), initialization duration, measurement duration, total ESP cycle time, network registration duration, estimated recharge current, and the recharge cycle counter. Air quality is measured every 15 minutes.

However, if the battery charge drops below 80% (4020 mV), the `ESP_SLEEP` and `DATA_SEND` intervals are multiplied by *10, and the `SDS_SLEEP` duration is increased from 15 minutes to 30 minutes. This control logic introduces a light power-saving mode in the weather station.

The logic in Figure 2.25 that determines the sleep duration gets the data from the macros and stores it in the variables `sleepCyclesLimit` and `dataSendCyclesLimit`. The `sleepCyclesLimit` variable is also used by the function counting all timestamps, so it currently knows whether the weather station slept for 1 minute or 10.

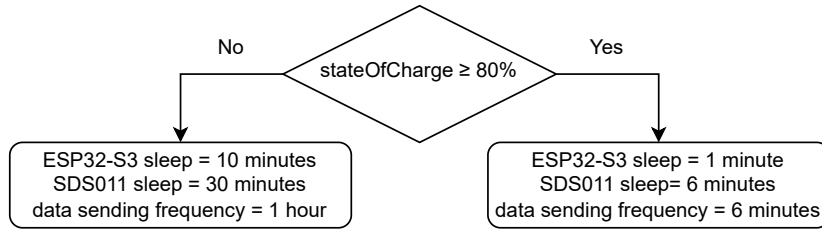


Fig. 2.25: Implemented logic of light power saving mode.

The server does not know this information and therefore it is important that the time stamps are read by the weather station and not by the Node-RED server. The server sometimes had a problem writing the data into the Influx DB, causing measurement dropouts that could be anywhere from 1 to 3 hours, which was very bad. A more frequent measurement period ensures that in the event of a measurement outage, there will only be a window of a few minutes rather than a few hours, and most importantly, the correct time format should completely eliminate these outages. Enough of all critical data is already sent to the server and sending the sleep length is unnecessary for the server to finish calculating.

Another advantage is the partially relieved server and simple flow. The last important advantage is the elimination of dynamic buffer allocation in RTC memory. `BUFFER_SIZE` is currently set to calculate its value from `DATA_SEND` and `ESP_SLEEP`, but if these were changed incorrectly during program execution, the buffer size would change.

The C++ standard does not support such a change at runtime and a solution could have been implemented via dynamic array allocation and subsequent ESP32-S3 memory freeing, but this was too complicated. Multiplying the variables `ESP_SLEEP` and `DATA_SEND * 10` guarantees to extend these cycles, saving battery and, most importantly, preserving the buffer size, thus not changing the `BUFFER_SIZE` variable, which remains constant.

Strong Power Saving Mode

The strong save mode has already been implemented, but it is clear from the measured diagnostic data that it has not been triggered even once. The weather station has been on the roof since mid-January 2025 and has not been completely discharged even once due to the gentle battery operation. The TP4056 charging module works exceedingly well, but lacks the MPPT function that allows the full power of the solar panels to be used. With a 6 V/4.5 W solar panel, this function is ineffective and the higher effect is only noticeable with 12 V solar panels.

Accuracy Improvement

However, the weather station lacked more frequent, more accurate measurements of actual meteorological variables. The TP4056 module in particular was taken into account and a scenario of complete battery discharge in poor conditions was assumed. After a thorough analysis, a light power saving mode was developed, which uses the current power saving treatment and also measures more frequently.

Light power saving mode easily works with scenarios of nice sunny weather days, but also with cloudy or rainy days when there is not enough light outside to charge the batteries. This solution is also more cost friendly, as the TP4056 is cheaper than MPPT rechargeable modules.

2.6.5 Power Consumption Evaluation

Traditional weather stations rely on wired communication or high-power wireless networks, which are not optimal for remote, battery-powered deployments. This work focuses on designing an energy-efficient weather station with minimal energy consumption.

In order to verify the functionality of the weather station and to optimize the energy consumption, the prototype was deployed during development in real conditions, in winter at the turn of 2024 and 2025, on the roof of the Faculty of Electrical Engineering and Communication at BUT.

Charging Current Estimation

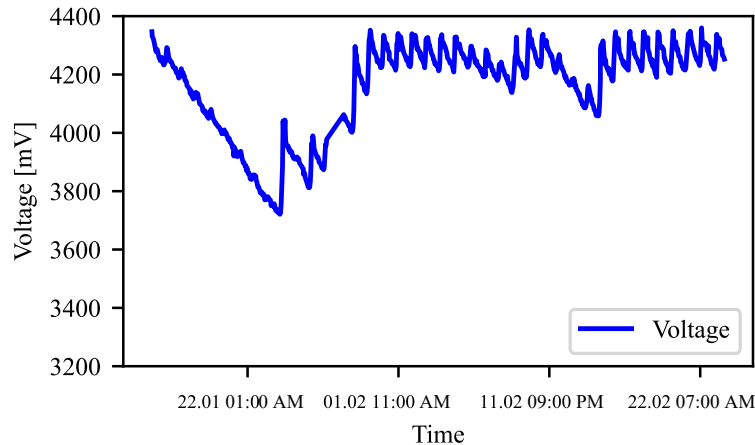
Energy consumption was mainly monitored along with the charging efficiency of the solar panel. The developed function in Listing 2.4 estimating the magnitude of the charging current depending on the light intensity is one of the most important diagnostic functions of the weather station.

Listing 2.4: Charging current estimation

```
float calculateChargingCurrent(float lux) { 1
    float panelPower; 2
    3
    panelPower = (lux / 100000.0) * maxPanelPower; 4
    if (panelPower > maxPanelPower) { 5
        panelPower = maxPanelPower; 6
    } 7
    8
    float chargingCurrent = (panelPower / panelVoltage) * 1000.0; 9
    return chargingCurrent; 10
} 11
```

Long-Term Operation

In poor light conditions during January, the battery voltage dropped to 3.72 V, but it took up to 9 days for the weather station to discharge to this level. As shown in Figure 2.26, bright and sunny weather from 29 January onwards recharged the batteries and maintained a satisfactory charge level.



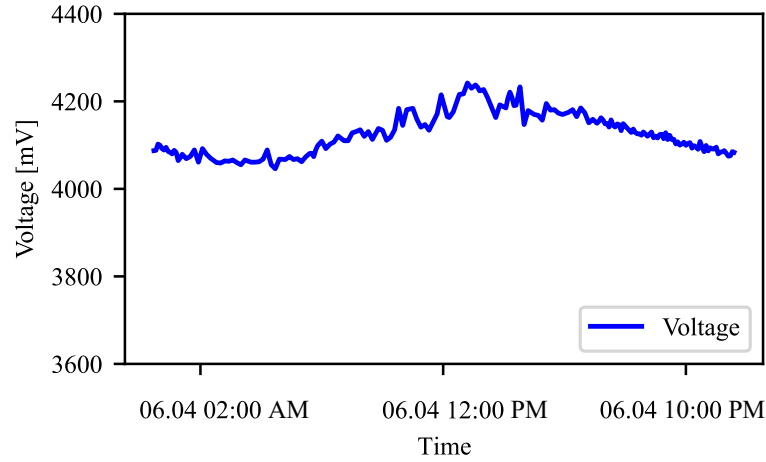


Fig. 2.27: Charging efficiency during April 6, 2025, as observed from 12:00 AM to 11:59 PM.

This is a light power saving mode that takes into account the performance of the solar panel, the current meteorological conditions, and the efficiency of the TP4056.

2.6.6 Network Consumption Evaluation

In the prototype board, the Quectel BC660K-GL module is fully powered off and restarted in each measurement cycle, which requires a complete signalling procedure for registration in the NB-IoT network. It then establishes a TCP connection and sends an **MQTT message of size 182 B** with all measured data using the User Plane (not the Control Plane CIoT), meaning that the IP and TCP layers are included. For example, with a sending frequency of 24 messages per day, a total of 720 transmissions are performed per month.

Table 2.5: Phases of MQTT message transmission in an NB-IoT network

<i>Phase</i>	<i>Size</i>	<i>Source</i>
Random Access + RRC Setup	200–300 B	3GPP TS 36.331, TS 36.321
NAS Attach (Request/Accept)	300–400 B	3GPP TS 24.301, TS 23.401
PDCP + RLC + MAC headers	50–150 B	3GPP TS 36.323, TS 36.322, TS 36.321
IP + TCP headers	40–60 B	RFC 791, RFC 793
TCP handshake + teardown	200–300 B	GSM IoT Guide
MQTT CONNECT + CONNACK	30–100 B	MQTT 3.1.1 (OASIS)
MQTT PUBLISH + PUBACK	202–232 B	MQTT 3.1.1, RFC 793
MQTT DISCONNECT (vol.)	10–20 B	MQTT 3.1.1
RRC Release (vol.)	~500 B	3GPP TS 36.331
MQTT message (payload)	182 B	–
Total (typical)	1000–1500 B	–

As a result, the monthly data consumption ranges from **0.47 MB**, through **0.81 MB**, up to **1.15 MB** when retransmissions or higher protocol overhead are present. The sending frequency is set to 1 hour — 720 transmissions per month:

- **0.47 MB** – under optimal conditions
- **0.81 MB** – in a typical scenario
- **1.15 MB** – in bad conditions, with retransmissions or higher protocol overhead

According to Table 2.5, a key factor is the signalling and protocol overhead, which often significantly exceeds the payload size. When messages are sent every 6 minutes, the monthly usage can increase to **8.12 MB** (or **3.31 MB** if the module remains registered in the network).

The DKWS PCB has a modified BC660K-GL module power supply, and the data consumption drops to **3.31 MB** per month due to the reduction in the number of signalling routines.

2.6.7 Doxygen Documentation

The development of the measurement and communication algorithm was initially carried out using the **Arduino IDE**. Later, it was extended in **Visual Studio**, where libraries for sensor initialization and measurement were created in the **C++** language. Each function contains fully automated documentation generated by the **Doxygen** tool (Figure C.1), highlighting all input and output parameters.

For example, for the air-quality sensor it explains what $\text{PM}_{2.5}$ and PM_{10} dust particles represent, describes the function's purpose, lists the input parameters, the returned values, and their types. The entire documentation set is exported as *index.html*.

Sensors Library Function Documentation

Each function in the **Sensors** library carries detailed Doxygen comments (Figure 2.28). Again, the tool emphasises input/output parameters, describes the meaning of $\text{PM}_{2.5}$ / PM_{10} , and clarifies value ranges or data types. Equivalent documentation is also generated for the main microcontroller algorithm.

2.7 System Security

The following section outlines the implementation of a system for measuring meteorological and diagnostic data. Because the measured values are transmitted to a remote server, the communication channel must be secured by **TLS**. The design

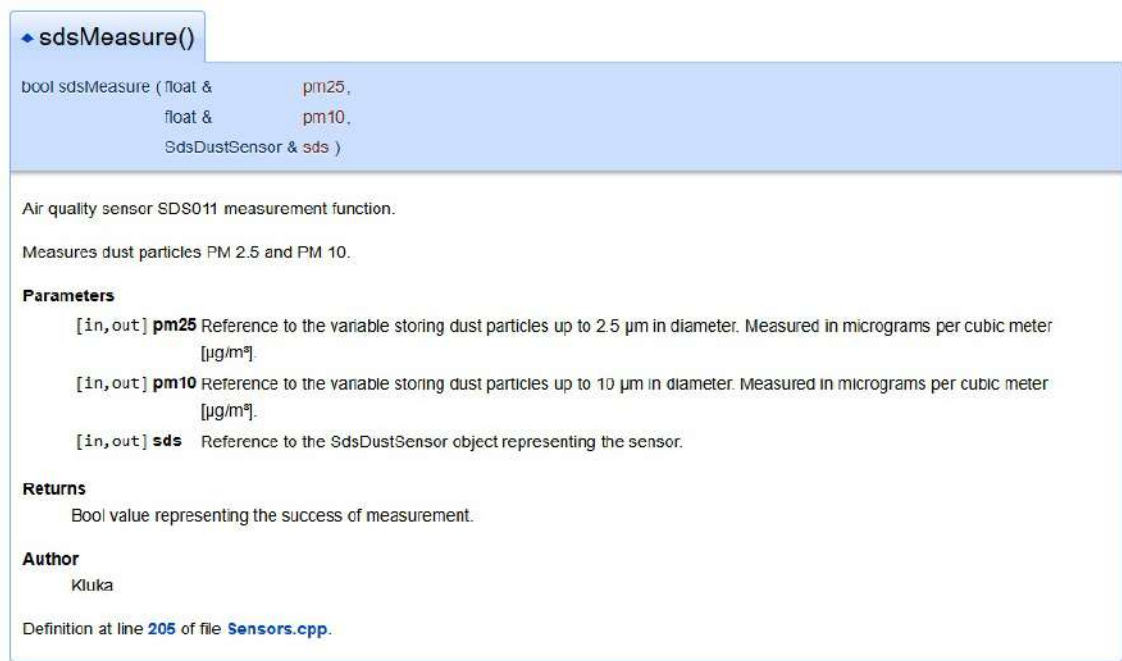


Fig. 2.28: Example of function-level documentation in the file `Sensors.cpp`.

and configuration of this secure link are detailed in subsequent parts of the thesis. After the encrypted channel has been successfully established, a comprehensive analysis of the entire system is performed.

2.7.1 System Security Design

The security design of the system focuses on the `Mosquitto MQTT` broker, which—within a TLS-encrypted channel—acts as the server, whereas all devices (including the `Node-RED` instance) behave as clients connecting to this server. For a proper connection between the weather station and the network, the `BC660K-GL` communication module must be configured with valid certificates. Dedicated firmware functions therefore issue specialised `AT` commands that upload certificates and establish an `MQTT` session, enabling the station to transmit sensor data as encrypted messages.

NB-IoT Technology

The weather station uses certificates that are stored in the microcontroller memory and provided to the `BC660K-GL` communication module as a string. However, the correct configuration is important, which is available in the latest command manuals for this module. For this reason, new functions are created that configure

TLS/SSL communication via PEM certificates and set the communication security level.

Secure Data Transfer According to the documentation for the Quectel BC660K-GL, TLS/SSL certification in PEM format needs to be uploaded directly to the communication module via the `AT+QSSLCFG=0,0,"<tag>"` command. The "<tag>" parameter specifies the certificate strings, namely "cacert", "clientcert" or "client-key" – CA certificate, client certificate or private key. Upon successful receipt of the command, the module prompts with the > character to enter the contents of the certificates.

Upon successful receipt of the command, the module responds with a > prompt, signaling readiness to receive multi-line input. The contents of the PEM file are then transmitted line-by-line over UART. The transmission is terminated using the ASCII character 26 (CTRL+Z), which signals the end of the input. This method supports full PEM formatting including line breaks and special characters.

Listing 2.5: Function writePemTLS

```
bool QuectelBC660::writePemTLS(const char* tag, const char* pem, uint32_t
    ↪ timeout)
{
    if (_debug) { Serial.print(F("[TLS]␣Uploading:␣")); Serial.println(tag); }

    sprintf(_buffer, "AT+QSSLCFG=0,0,\"%s\"", tag);
    wakeUp();
    if (!sendAndCheckReply(_buffer, ">", 2000)) return false;

    const char* p = pem;
    while (*p) {
        const char* e = strchr(p, '\n');
        if (!e) e = p + strlen(p);
        const char* lineEnd = (e > p && *(e - 1) == '\r') ? e - 1 : e;
        _uart->write((const uint8_t*)p, lineEnd - p);
        _uart->write("\r\n");
        p = (*e) ? e + 1 : e;
    }
    _uart->flush();
    _uart->write(0x1A);

    if (!readReply(timeout, 2)) return false;
    return strstr(_buffer, "+QSSLCFG") != nullptr;
}
```

TLS parameters are configured using the `configTLS` function. It first sets the TLS security level using the `AT+QSSLCFG=0,0,"seclevel",<level>` command,

where:

- 1 – one-way authentication (server only)
- 2 – mutual authentication (both client and server)

Then it uploads the necessary certificates by calling `writePemTLS` three times with tags "cacert", "clientcert", and "clientkey" respectively. Each upload uses a timeout of 300 000 ms to accommodate multi-line content.

Listing 2.6: Function `configTLS`.

```
bool QuectelBC660::configTLS(const char* ca, const char* cli, const char* key, 1
    ↪ uint8_t lvl)
{ 2
    sprintf(_buffer, "AT+QSSLCFG=0,0,\"seclvl\",%d", lvl); 3
    if (!sendAndCheckReply(_buffer, _OK)) return false; 4
    if (ca && !writePemTLS("cacert", ca, 300000)) return false; 5
    if (cli && !writePemTLS("clientcert", cli, 300000)) return false; 6
    if (key && !writePemTLS("clientkey", key, 300000)) return false; 7
    return true; 8
} 9
```

Establishing a Secure MQTT Connection After setting up TLS parameters and uploading the certificates, a secure connection with the MQTT broker can be established. The `openMQTTSecure` function performs this setup. It first binds the TLS configuration to the desired MQTT connection using:

- `AT+QMTCFG="ssl",<id>,1,<sslCtxId>,0` – binds TLS context to MQTT session
- `AT+QMTCFG="version",<id>,1` – sets MQTT protocol version 3.1.1

Then, the MQTT connection is opened using the `AT+QMTOPEN` command with the provided host and port. The function waits for a response containing `+QMTOPEN: <id>, <status>`, where `status = 0` confirms a successful connection.

Listing 2.7: Function `openMQTTSecure`

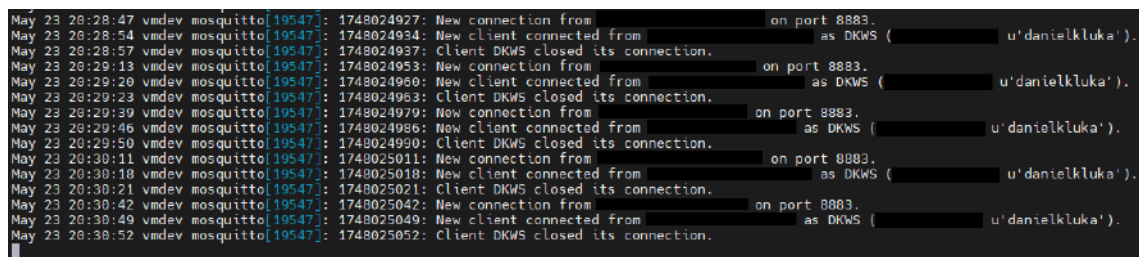
```
bool QuectelBC660::openMQTTSecure(const char* host, uint16_t port, uint8_t 1
    ↪ TCPconnectID, uint8_t sslCtxId)
{ 2
    _TCPconnectID = TCPconnectID; 3
    4
    sprintf(_buffer, "AT+QMTCFG=\"ssl\",%d,1,%d,0", _TCPconnectID, sslCtxId); 5
    wakeUp(); 6
    if (!sendAndCheckReply(_buffer, _OK)) { 7
        if (_debug) Serial.println(F("[ERROR] Failed to configure QMTCFG ssl")); 8
        return false; 9
    } 10
} 11
```

sprintf(_buffer, "AT+QMTCFG=\"version\",%d,1", _TCPconnectID);	12
wakeUp();	13
if (!sendAndCheckReply(_buffer, _OK)) {	14
if (_debug) Serial.println(F("[ERROR]_Failed_to_configure_MQTT_	15
↪ version"));	
return false;	16
}	17
	18
sprintf(_buffer, "AT+QMTOPEN=%d,\"%s\",%d", _TCPconnectID, host, port);	19
wakeUp();	20
if (!sendAndCheckReply(_buffer, _OK)) {	21
if (_debug) Serial.println(F("[ERROR]_QMTOPEN_cmd"));	22
return false;	23
}	24
	25
unsigned long t0 = millis();	26
size_t len = 0;	27
while (millis() - t0 < 30000UL) {	28
if (_uart->available()) {	29
char c = _uart->read();	30
if (_debug) Serial.write(c);	31
if (len < sizeof(_buffer) - 1) _buffer[len++] = c;	32
if (c == '\n') {	33
_buffer[len] = 0;	34
len = 0;	35
if (strstr(_buffer, "+QMTOPEN:")) {	36
char* p = strchr(_buffer, ',');	37
if (p) {	38
uint8_t stat = atoi(p + 1);	39
if (_debug) {	40
Serial.print(F("[MQTT]_QMTOPEN_stat="));	41
Serial.println(stat);	42
}	43
return stat == 0;	44
}	45
}	46
}	47
}	48
	49
if (_debug) Serial.println(F("[ERROR]_QMTOPEN_URC_timeout"));	50
return false;	51
}	52

Broker Mosquitto

The MQTT broker **Mosquitto** was deployed and secured on a Debian-based system using terminal access via **SSH**. The initial step involved updating system repositories and installing the required **Mosquitto** packages. Due to the large number of services available in the system, it is possible to use various advanced cybersecurity methods to prevent cyber-attacks and increase the trustworthiness of communications.

These include, for example, comprehensive logging of all traffic entering the system via the network in Figure 2.29. In this case, this involves linking the weather station via **NB-IoT** technology to the public IP address of the faculty and the local IP address of the server located at the faculty. By comprehensively monitoring traffic and controlling access, it is possible to determine who was connected to the server, at what time, and what actions they performed.



```
May 23 20:28:47 vmdev mosquitto[19547]: 1748024927: New connection from [REDACTED] on port 8883.
May 23 20:28:54 vmdev mosquitto[19547]: 1748024934: New client connected from [REDACTED] as DKWS (u'danielkluka').
May 23 20:28:57 vmdev mosquitto[19547]: 1748024937: Client DKWS closed its connection.
May 23 20:29:13 vmdev mosquitto[19547]: 1748024953: New connection from [REDACTED] on port 8883.
May 23 20:29:20 vmdev mosquitto[19547]: 1748024960: New client connected from [REDACTED] as DKWS (u'danielkluka').
May 23 20:29:23 vmdev mosquitto[19547]: 1748024963: Client DKWS closed its connection.
May 23 20:29:39 vmdev mosquitto[19547]: 1748024979: New connection from [REDACTED] on port 8883.
May 23 20:29:46 vmdev mosquitto[19547]: 1748024986: New client connected from [REDACTED] as DKWS (u'danielkluka').
May 23 20:29:50 vmdev mosquitto[19547]: 1748024990: Client DKWS closed its connection.
May 23 20:30:11 vmdev mosquitto[19547]: 1748025011: New connection from [REDACTED] on port 8883.
May 23 20:30:18 vmdev mosquitto[19547]: 1748025018: New client connected from [REDACTED] as DKWS (u'danielkluka').
May 23 20:30:21 vmdev mosquitto[19547]: 1748025021: Client DKWS closed its connection.
May 23 20:30:42 vmdev mosquitto[19547]: 1748025042: New connection from [REDACTED] on port 8883.
May 23 20:30:49 vmdev mosquitto[19547]: 1748025049: New client connected from [REDACTED] as DKWS (u'danielkluka').
May 23 20:30:52 vmdev mosquitto[19547]: 1748025052: Client DKWS closed its connection.
```

Fig. 2.29: Demonstration of a logger used to monitor the traffic of the proposed secure system.

Installation and Initial Configuration The following commands ensure the system is up-to-date and install both the broker and its client utilities:

Listing 2.8: Installing required Debian packages

<code>sudo apt-get update -y</code>	1
<code>sudo apt-get upgrade -y</code>	2
<code>sudo apt-get install mosquitto mosquitto-clients -y</code>	3

Once installed, the default configuration file is located at `/etc/mosquitto/mosquitto.conf`, where port 1883 is enabled by default for unsecured communication. To enforce encryption and authentication, the port should be changed to 8883 and TLS-related options configured accordingly. The broker is then activated as follows:

Listing 2.9: Starting and enabling the Mosquitto service

<code>sudo systemctl start mosquitto</code>	1
<code>sudo systemctl enable mosquitto</code>	2

Authentication via Username and Password To restrict access, Mosquitto supports authentication using a username and password file. Anonymous access must be explicitly disabled and the path to the credential file defined in the config file:

Listing 2.10: Authentication-related configuration options

```
allow_anonymous false 1
password_file /etc/mosquitto/passwd 2
```

TLS Encryption of MQTT Traffic To secure data transmission using TLS, certificates must be generated and integrated into Mosquitto's configuration. The OpenSSL package provides tools for generating all necessary keys and certificates:

Listing 2.11: Installing OpenSSL tools

```
sudo apt-get install openssl -y 1
```

Certificates are stored in a designated folder such as `/etc/mosquitto/certs/`. First, the certificate authority (CA) must be created:

Listing 2.12: Generating CA certificate

```
openssl genrsa -out ca.key 2048 1
openssl req -new -x509 -days 3650 -key ca.key -out ca.crt 2
```

It is critical to enter the correct values during certificate creation, particularly the Common Name (CN), which must match the identity of the CA. Server and client certificates are generated similarly:

Listing 2.13: Creating server certificates

```
openssl genrsa -out server.key 2048 1
openssl req -new -key server.key -out server.csr 2
openssl x509 -req -in server.csr -CA ca.crt -CAkey ca.key -CAcreateserial -out 3
    ↪ server.crt -days 3650
```

The certificate signing request (CSR) is signed by the CA key to issue the final certificate. The client certificate is generated using the same steps:

Listing 2.14: Creating client certificates

```
openssl genrsa -out client.key 2048 1
openssl req -new -key client.key -out client.csr 2
openssl x509 -req -in client.csr -CA ca.crt -CAkey ca.key -CAcreateserial -out 3
    ↪ client.crt -days 3650
```

Finally, Mosquitto must be explicitly instructed to use the specified certificates for establishing secure TLS connections on port 8883. The configuration file created for the Mosquitto broker defines the certificate authority (CA) root, the paths

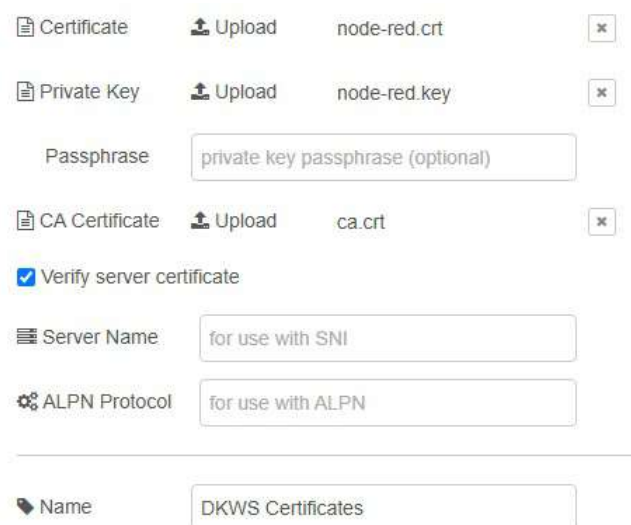
to the server certificate and private key, the authentication file for verifying clients, and the basic communication setup. This setup includes enabling the MQTT protocol and specifying the TLS 1.2 version for secure transport:

Listing 2.15: TLS-related broker configuration

```
password_file /etc/mosquitto/passwd 1
log_dest syslog 2
log_dest stdout 3
4
# TLS MQTT 5
listener 8883 6
protocol mqtt 7
tls_version tlsv1.2 8
cafile /etc/mosquitto/certs/ca.crt 9
certfile /etc/mosquitto/certs/server.crt 10
keyfile /etc/mosquitto/certs/server.key 11
require_certificate true 12
allow_anonymous false 13
```

Node-RED

The Node-RED server acts as a client in this connection, connecting to the broker. Client certificates generated for this server can be uploaded directly to the MQTT node to receive data or to send data to the broker.



The screenshot shows the configuration interface for an MQTT node in Node-RED. It includes fields for uploading a Certificate (node-red.crt), Private Key (node-red.key), and CA Certificate (ca.crt). There is a checkbox for "Verify server certificate" which is checked. Below this are input fields for "Server Name" (containing "for use with SNI") and "ALPN Protocol" (containing "for use with ALPN"). At the bottom, there is a "Name" field containing "DKWS Certificates".

Fig. 2.30: Used Node-RED certificates.

2.7.2 System Security Level Analysis

This section analyzes the security aspects of the IoT-based weather station system that transmits environmental data to a remote server over a network. The objective is to identify potential threats and vulnerabilities associated with individual system components and to assess how these may affect the overall security posture of the station.

The analysis places particular emphasis on:

- the resilience of the system to both physical and software-based attacks,
- and the specific security requirements posed by NB-IoT communication technology.

The security of the system is evaluated through the lens of five **core cybersecurity service categories**, which are typically enforced using cryptographic techniques:

- **Data confidentiality** – protection against unauthorized access and traffic analysis.
- **Data integrity** – ensuring that information remains unaltered during transmission.
- **Authentication** – verifying the identity of users and devices.
- **Access control** – regulating access to resources based on identity.
- **Non-repudiation / proof of message origin** – preventing denial of actions and validating source authenticity.

These categories form the foundation of secure IoT system design and are used as the basis for evaluating the weather station's defense mechanisms.

Security of Individual Components

A weather station consists of several components that may pose potential security risks. These include sensors, connectors, communication modules (such as the ESP32-S3 microcontroller and the BC660K-GL NB-IoT module), and remote servers responsible for processing the data. Each of these components plays a crucial role in ensuring the integrity, confidentiality, and availability of the data.

Equally important is the physical location of the weather station and the servers, which may either facilitate or prevent unauthorized access in the event of a targeted attack.

Sensors The sensors of the weather station are optimized for high measurement accuracy and are equipped with a connection monitoring mechanism. In the event

of a sensor disconnection, the system continues to operate without the affected sensor to ensure that other critical meteorological data are not lost.

The developed weather station is installed on the roof of the faculty building, and there was no need for this mechanism to be fully active during development. It was partially enabled, but for other purposes. During the development phase, most of the testing was conducted using a prototype board, with a careful approach taken to verify whether any sensor had become disconnected. In such cases, the weather station attempted to re-initialize the sensor.

Potential issues such as software bugs, sensor damage, or accidental disconnection were considered throughout the process. Later in the development, the connectors were replaced with versions that include mechanical fuses, in order to prevent unintentional disconnection and improve system reliability.

However, this mechanism also functions as a safety measure in the event of a complete sensor disconnection. If an attacker disconnects a sensor and inserts a malicious device between the sensor and the microcontroller, or connects directly to the sensor port to perform an attack, the microcontroller will not establish communication unless successful sensor initialization is achieved.

There are no additional built-in safety mechanisms within the sensors themselves, as they are simple devices intended for embedded systems. Instead, higher demands are placed on the physical enclosures to prevent unauthorized access, protect against tampering or damage, and to avoid disconnection of individual sensors.

The overall system design focuses primarily on mitigating the risk of data tampering during transmission and implements security measures at the communication protocol level.

Communication Module The NB-IoT module Quectel BC660K-GL communicates using the Mosquitto MQTT broker, which operates on a server located at the faculty. Communication is secured using TLS encryption, ensuring the integrity and authenticity of both meteorological and diagnostic data transmitted by the weather station. This standard provides mutual authentication between the device and the server, significantly reducing the risk of unauthorized access.

It is also essential to regularly update the firmware of the communication module to ensure the application of current security patches and to eliminate vulnerabilities that may exist in outdated versions.

Servers and Data Storage Servers hosted at the faculty are regularly updated and patched to minimize the risk of security breaches. Access to these servers

is strictly controlled, with users assigned specific permissions to prevent unauthorized actions such as data manipulation or system modifications. User access is managed through individual login credentials used for authenticated logins.

The servers enhance data security by encrypting stored data and using TLS encryption for all communication between clients and servers—in this case, between the weather station and the **Node-RED** server and the **Mosquitto** broker, both secured with TLS.

Data are collected from multiple sources, and the weather station itself is equipped with additional sensors to improve measurement accuracy. This setup supports data correlation and enables validation of individual sensor readings. Although no mechanism is currently implemented to detect anomalies or potential security threats from suspicious sensor data, it represents a valuable direction for future development.

Vulnerability Description

Despite the implemented security measures, a weather station remains exposed to various risks and potential attack vectors. Some of the most significant threats include physical access to the station, software vulnerabilities within the firmware or communication stack, and man-in-the-middle (MitM) attacks targeting data transmission between the station and remote servers.

Physical Access Risks External sensors can be disconnected, damaged, or tampered with by an attacker, potentially compromising the integrity of the measured data. It is therefore important to implement a robust physical barrier that internally shields the sensors and prevents unauthorized access, damage, or disconnection. Attention must also be paid to sensor connectors, which may be accessible to an attacker and should be concealed or physically protected.

The weather station is currently deployed on the roof of the faculty building and features a complex, modular design that was necessary during the development phase. Future plans involve creating a more compact weather station with minimized dimensions and concealed cabling, which will improve physical security and reduce the likelihood of unauthorized access or manipulation.

Software Vulnerabilities Outdated firmware versions introduce potential security vulnerabilities that are typically addressed through updates containing critical security patches. Operating modules with outdated firmware, or performing incorrect updates, significantly increases the risk of exploitation through known vulnerabilities.

To mitigate these risks, all modules and systems used by the weather station are regularly updated as part of routine maintenance procedures.

Man-in-the-Middle (MITM) Attacks Mistakes made during certificate exchange or misconfiguration of cryptographic protocols can significantly increase the risk of data breaches. If the communication between the server and the client is not fully encrypted, an attacker may intercept or manipulate the transmitted measurements. Furthermore, failure to verify the validity of certificates—particularly that of the certificate authority (CA)—increases the risk of certificate spoofing and man-in-the-middle attacks.

Additional threats include DNS spoofing, especially in the case of a compromised mobile operator or when DNS queries are transmitted without encryption. The weather station uses the Vodafone CZ operator for data transmission, and the operator maintains knowledge of the destination servers. The IP address of the faculty server is included on the operator's internal whitelist, which ensures that data can be routed only to trusted endpoints. This represents an additional layer of control that strengthens overall communication security and reinforces the trustworthiness of the received data.

Limited Resources in IoT Devices IoT devices with low computing power and limited energy face several constraints. If their memory, storage, processor, or transmission speed is limited, this affects the security and reliability of these devices.

In such a case, the use of conventional encryption algorithms is not possible, and the possibilities of updates, data collection and transmission of larger amounts of data are limited. The weather station has therefore been designed to provide maximum performance with minimum power consumption. It was also equipped with sufficient battery capacity and the power and data consumption was optimised. This allows the use of common encryption algorithms required for secure data transmission.

Assessing the resilience to security threats

NB-IoT is one of the most advanced and increasingly available technologies in the world. It uses authentication and encryption mechanisms that are considered strong and are based on LTE network standards. Each device using NB-IoT technology is accompanied by a SIM card that contains a unique identifier.

These devices are used, for example, for complex environmental monitoring, smart metering or automation in industry. This chapter describes resilience to selected security threats and also focuses on authentication mechanisms and protections against potential attacks.

Authentication and Encryption Application layer encryption is recommended, but devices can operate without these mechanisms. This increases their vulnerability and exposes them to the risk of eavesdropping or tampering. Therefore, it is important to have properly implemented authentication mechanisms and to have secured all modules and systems used by devices with this technology. Trust and security of communication in an NB-IoT environment is therefore key, but it is not a guarantee of immunity to other risks.

Prevention of Replay Attacks Message replay is a threat in untimed transmissions. Messages should contain some form of unique identifier. Timestamps are a common solution and protection against the threat of message replay in NB-IoT networks, and the same principle is implemented in the proposed weather station. This makes it possible to discern what messages have been sent and in what order.

Resilience to DDoS Attacks NB-IoT devices are less vulnerable to DDoS attacks than other traditional Internet devices because NB-IoT technology is isolated in a mobile network with limited reach to the Internet. Devices communicate through operators with a specific signalling structure preventing direct addressability. Server-side protection in the form of connection limits, rate limiting, or detection of strange behavior is recommended and useful in increasing the security and trustworthiness of the communication.

Signal Interference Signal interference is one of the common parasitic phenomena negatively affecting the quality of NB-IoT communication. This signal interference is common in urban areas with a high prevalence of devices using similar frequency bands. This degrades the signal and physical obstructions or electromagnetic noise have the same effect. When using this technology, it is important to have a good quality antenna and a properly designed antenna connection to the communication module, which was given high priority in the design of the weather station circuit board.

The target location of the weather station on the roof of the faculty outside the city increases the quality of the connection, but it is also important to reduce the amount of data consumption, which was also done within the weather station. The use of retransmissions or adaptive transmission control plays an important role. The choice of the operator, which should have good coverage of the technology, also contributes to the robustness of the weather station.

Conclusion

The main objective of the thesis was to design a secure data transmission system in NB-IoT environment. The system consists of a device, in this case a weather station, which measures data from selected sensors and sends it via the MQTT broker Mosquitto to the Node-RED server. The server stores the data in the time series database InfluxDB and all the visualized data are visualized in graphs on the Grafana platform.

This system is safe, energy-efficient and capable of transmitting meteorological and diagnostic data from the weather station. Extensive development has led to this goal, which explored parts of the thesis assignment. During the development process, a hardware architecture was designed to meet the requirements of professional stations, namely high robustness and accuracy. The device was developed to minimize the cost of the professional stations and the device fulfilled this purpose.

The hardware design prioritized cost-effectiveness, robustness, and expandability. The station integrates multiple sensors, including the DS18B20 temperature sensor, the VEML7700 light intensity sensor, the SDS011 air quality sensor, and the WXT536 weather transmitter. Components are mounted on a custom-designed PCB that incorporates low-power modules such as TP4056 for battery charging, a voltage regulator TPS63020, SX1308 for efficient voltage conversion, and MAX3232 for RS-232 communication. The power control circuitry is based on MOSFET transistors, which enable dynamic power management.

Compared to professional stations, the device emphasizes modularity, low power and data consumption and yet is still capable of operating in challenging meteorological conditions. The software architecture of the device takes care of the processing of the measurements, delivering secure data transmission ensuring data integrity and confidentiality. The operation of the device with these comprehensive services is ensured by the use of low-energy NB-IoT technology along with efficient battery usage.

The thesis also includes a comprehensive analysis of the security risks faced by devices in the NB-IoT environment and the risks faced by devices in the form of weather stations. Based on this analysis, security mechanisms are implemented and future recommendations are proposed that could further optimize the entire system in terms of security. By implementing security technologies, the credibility and reliability of the implemented system is enhanced.

The system is capable of long-term operation in harsh conditions and is resistant to physical and software attacks, it is also resistant to the natural adversities of nature, which it comprehensively measures. The device has applications in areas of the country where conventional infrastructure is not available. It will be deployed

primarily in the city of Brno, where it will measure meteorological variables and air quality at various locations. In addition, it is planned to extend the station with additional sensors for higher accuracy and expanded functionality. The equipment is suitable for automated real-time data processing.

The thesis highlights the capabilities of NB-IoT technology in the form of seamless and reliable transmission using modern encryption technologies. Protecting sensitive information is much more important nowadays than in the past due to the higher number of possible threats. It is also important to properly analyze security risks for a full system security evaluation.

An important objective was also to research the market, current solutions and available components that would contribute to the reliability and robustness of the overall system. Optimising energy consumption was also achieved thanks to the availability of electronic components designed for these purposes. This also aids in the high accuracy of the data acquired and proper analysis of the diagnostic data can help to detect a possible attack on the equipment.

Compared to professional stations, the device emphasizes modularity, low power and data consumption and yet is still capable of operating in challenging meteorological conditions. The software architecture of the device takes care of the processing of the measurements, delivering secure data transmission ensuring data integrity and confidentiality. The operation of the device with these comprehensive services is ensured by the use of low-energy NB-IoT technology along with efficient battery usage.

Professional weather stations can cost up to 2,000,000 CZK depending on the configuration used and their service can cost another 100,000 CZK. The proposed weather station reduces this price to around 7,500 CZK, making it a competitive device using advanced modern technology and high quality. The modularity of the device with the possibility to extend it with additional functions makes it a device with great potential in the market, especially due to its proven functionality.

This project has reaffirmed that the seamless integration of robust security mechanisms, energy-efficient designs, and advanced technologies is essential for the successful implementation of IoT applications. As IoT technologies continue to evolve, the findings from this thesis provide a pathway for future innovations that emphasize security, efficiency, and adaptability, ensuring that IoT systems are well-equipped to meet the diverse challenges and opportunities of tomorrow.

All necessary electronic attachments of the **thesis project** of the developed system are available in the GitHub repository¹. In the appendices of the diploma thesis there is **Technical Documentation of Weather Station Components** contain-

¹<https://github.com/danielkluka/Diploma-Thesis>

ing a summary of important HW parameters of the weather station, description of individual components of the developed boards and technical specifications of the used sensors. The appendices are further supplemented by a comprehensive **flowchart** of the weather station measurement algorithm and automatic documentation created using the **Doxygen** tool describing the created **sensor library**. A professional visualization of the **radiation shield** is also available in the appendices, as well as a detailed schematic wiring diagram of the **DKWS board**.

Bibliography

- [1] Portal www.beliana.sk, SLOVENSKÁ AKADÉMIA VIED. *Atmosférické zrážky* [online]. 1999, [cited 2024-10-12]. Available at: <https://beliana.sav.sk/heslo/atmosfericke-zrazky>.
- [2] LUGANO, Gaia. *Types of Atmospheric Precipitation* [online]. 2024, [cited 2024-10-15]. Available at: <https://app.biorender.com/biorender-templates/t-642b28c6df53c422dd036a7f>.
- [3] REPA, Pavol, Bc. *Kompenzace teplotní nestálosti přijímané úrovně signálu mikrovlnných spojů* [online]. Bachelors thesis. Thesis supervisor Ing. BUBNIAK Milan. Brno: Vysoké učení technické v Brně, Fakulta elektrotechniky a komunikačních technologií, Ústav telekomunikací, 120 s. 2023, [cited 2024-10-12]. Available at: https://www.vut.cz/studenti/zav-prace?zp_id=151072.
- [4] SKOUMAL, Vladimír, Bc. *Výzkum metod pro kvantifikacie útlumu efektem vlhké antény* [online]. Bachelors thesis. Thesis supervisor Ing. BUBNIAK Milan. Brno: Vysoké učení technické v Brně, Fakulta elektrotechniky a komunikačních technologií, Ústav telekomunikací, 71 s. 2023, [cited 2024-10-12]. Available at: https://www.vut.cz/studenti/zav-prace?zp_id=151075.
- [5] Portal BioClio, Vzdelávací portál o problematike bioklimatológie a hydrológie krajiny, www.bioclio.wordpress.com. *Princípy a prístroje na meranie zrážok* [online]. 2024, [cited 2024-10-15]. Available at: <https://bioclio.wordpress.com/principy-a-pristroje-na-meranie-zrazok/>.
- [6] Portal Civil Engineering Home, www.cementconcrete.org. *Rain Gauge: Uses, Types, diagram, rainfall measurement, Data Adjustment and site Selection* [online]. 2020, [cited 2024-10-15]. Available at: <https://cementconcrete.org/water-resources/hydrology/rain-gauge/2637/>.
- [7] PAVELKOVÁ CHMELOVÁ Renata, FRAJER Jindřich. *Základy fyzické geografie 1 - hydrologie, pracovní verze určena k ověření ve výuce* [online]. CZ.1.07/2.2.00/18.0014, Olomouc: Univerzita Palackého v Olomouci, Katedra geografie. 2013, [cited 2024-10-15]. Available at: <http://distgeo.upol.cz/uploads/vyuka/skripta-pavelkova-frajer.pdf>.
- [8] Portal MeteoRadar.cz, INMETEO, s.r.o. *Co je to meteoradar* [online]. 2023, [cited 2024-10-15]. Available at: <https://www.meteoradar.cz/o-radaru.php>.

- [9] Portal MeteoRadar.cz, INMETEO, s.r.o. *Meteoradar v Česku* [online]. 2023, [cited 2024-10-15]. Available at: <https://www.meteoradar.cz/meteoradar-cesko.php>.
- [10] Portal meteocentrum.cz. *Satelitní snímky z družice Meteosat* [online]. 2024, [cited 2024-10-16]. Available at: <https://www.meteocentrum.cz/satelitni-snimky>.
- [11] CHWALA Christian, KUNSTMANN Harald. *Commercial microwave link networks for rainfall observation: Assessment of the current status and future challenges* [online]. Advanced Review. German Research Foundation. 2019-2-16, [cited 2024-10-16]. Available at: <https://doi.org/10.1002/wat2.1337>.
- [12] Portal Slovakia Topoľčany, Mravenisko, Automatická meteorologická stanica, www.meteoto.sk. *Meteorologické pojmy* [online]. 2011, [cited 2024-10-19]. Available at: <https://www.meteoto.sk/meteopojmy.php>.
- [13] Portal BioClio, Vzdelávací portál o problematike bioklimatológie a hydrológie krajiny, www.bioclio.wordpress.com. *Meranie teploty vzduchu* [online]. 2024, [cited 2024-10-19]. Available at: <https://bioclio.wordpress.com/meranie-teploty-vzduchu/>.
- [14] Portal meteoblue, weather close to you, www.meteoblue.com. *Temperature* [online]. 2024, [cited 2024-10-19]. Available at: <https://content.meteoblue.com/en/research-education/specifications/data-sources/measurements/temperature>.
- [15] Portal Electrical Technology, www.electricaltechnology.com. *PTermocouple - Types, Construction, Working and Applications* [online]. 2024, [cited 2024-10-19]. Available at: <https://www.electricaltechnology.org/2022/04/thermocouple-types-construction-working-applications.html>.
- [16] Portal Krokus, internetový obchod, www.krokus.sk. *Ako funguje barometer: Vedecké vysvetlenia atmosférického tlaku* [online]. 2024, [cited 2024-10-19]. Available at: <https://shorturl.at/kXW5u>.
- [17] Portal InstTools, Instrumentation Tools, www.instrumentationtools.com. *What is a barometer?* [online]. 2024, [cited 2024-10-19]. Available at: <https://instrumentationtools.com/what-is-a-barometer/>.
- [18] Portal mensor, www.blog.mensor.com. *From Mercury to Digital: Various Types of Barometers for Measurement* [online]. 2023, [cited 2024-10-19]. Available at: <https://shorturl.at/NKa8B>.

- [19] Portal ATO, www.pressuresensors.net. *Capacitive Pressure Sensor Working Principle* [online]. 2022, [cited 2024-10-19]. Available at: <https://www.pressuresensors.net/capacitive-pressure-sensor-working-principle>.
- [20] KLUKA, Daniel, Bc. *Modulární streamovací systém s cloudovým úložištěm* [online]. Bachelors thesis. Thesis supervisor Ing. Lukáš Kratochvíla. Brno: Vysoké učení technické v Brně, Fakulta elektrotechniky a komunikačních technologií, Ústav automatizace a měřicí techniky, 87 s. 2023, [cited 2024-10-19]. Available at: <https://www.vut.cz/studenti/zav-prace/detail/151858>.
- [21] Portal Azure, www.azure.microsoft.com. *IoT technologies and protocols* [online]. 2024, [cited 2024-10-18]. Available at: <https://azure.microsoft.com/en-us/solutions/iot/iot-technology-protocols>.
- [22] JÍLEK, Jiří, Bc. *Návrh přesného srážkoměru s možností real-time odečtu* [online]. Bachelors thesis. Thesis supervisor Ing. Radek Možný. Brno: Vysoké učení technické v Brně, Fakulta elektrotechniky a komunikačních technologií, Ústav telekomunikací, 62 s. 2023, [cited 2024-10-19]. Available at: https://www.vut.cz/studenti/zav-prace?zp_id=151055.
- [23] Portal PROMWAD, Electronics design, www.promwad.com. *Low Power Wireless Technologies for Your Future Device: Selection Guide* [online]. 2024-04-15, [cited 2024-10-20]. Available at: <https://promwad.com/news/low-power-wireless-technologies>.
- [24] Portal VelosIOT, www.blog.velosiot.com. *Different LPWAN Technologies Explained* [online]. 2023-06-12, [cited 2024-10-20]. Available at: <https://blog.velosiot.com/different-lpwan-technologies-explained>.
- [25] Portal A1 Digital, www.a1.digital. *IoT Protocols: A comprehensive guide for enterprises* [online]. 2024, [cited 2024-10-21]. Available at: <https://www.a1.digital/news/iot-protocols-a-comprehensive-guide/>.
- [26] Portal Geeks for Geeks, www.geeksforgeeks.org. *Difference between AMQP and HTTP Protocols* [online]. 2024-07-29, [cited 2024-10-21]. Available at: <https://www.geeksforgeeks.org/difference-between-amqp-and-http-protocols/>.
- [27] Portal Geeks for Geeks, www.geeksforgeeks.org. *Protokol CoAP (Constrained Application Protocol)* [online]. 2024-07-26, [cited 2024-10-21]. Available at: <https://www.geeksforgeeks.org/constrained-application-protocol-coap/>.

- [28] Portal Geeks for Geeks, www.geeksforgeeks.org. *Distributed Database System* [online]. 2023-09-19, [cited 2024-10-21]. Available at: <https://www.geeksforgeeks.org/distributed-database-system/>.
- [29] Portal Geeks for Geeks, www.geeksforgeeks.org. *Introduction of Message Queue Telemetry Transport Protocol (MQTT)* [online]. 2024-02-26, [cited 2024-10-21]. Available at: <https://www.geeksforgeeks.org/introduction-of-message-queue-telemetry-transport-protocol-mqtt/>.
- [30] Portal Geeks for Geeks, www.geeksforgeeks.org. *Differences between TCP and UDP* [online]. 2024-12-09, [cited 2024-12-09]. Available at: <https://www.geeksforgeeks.org/differences-between-tcp-and-udp/>.
- [31] ESP-IDF Programming Guide, docs.espressif.com. *ESP32-S3-DevKitC-1* [online]. 2022, [cited 2024-12-09]. Available at: <https://docs.espressif.com/projects/esp-idf/en/v4.4.3/esp32s3/hw-reference/esp32s3/user-guide-devkitc-1.html>.
- [32] Distributor Amazon, www.amazon.com. *ESP32-S3-DevKitC-1-N16R8 ESP32 S3 Development Board WiFi + Bluetooth MCU Module, Dual Type-C ESP32-S3-WROOM-1 Cores Microcontroller Processor Integrates Complete Wi-Fi and BLE Functions* [online]. 2024, [cited 2024-12-09]. Available at: <https://shorturl.at/eVWKh>.
- [33] Quectel, www.quectel.com. *LPWA BC660K-GL NB2* [online]. 2024, [cited 2024-12-09]. Available at: <https://www.quectel.com/product/lpwa-bc660k-gl-nb2/>.
- [34] Distributor SOS electronic, www.soselectronic.com. *Multi-band LTE Cat NB2 module - BC660K-GL* [online]. 2021-08-31, [cited 2024-12-09]. Available at: <https://www.soselectronic.com/en-cz/articles/quectel/multi-band-lte-cat-nb2-module-bc660k-gl-2593>.
- [35] Distributor empastore, www.empastore.com. *BC660K-GL-TE-B KIT NB-IoT Module Series* [online]. 2024, [cited 2024-12-09]. Available at: <https://www.empastore.com/bc660k-gl-te-b-kit>.
- [36] Distributor laskakit, www.laskakit.cz. *DS18B20 Digital waterproof temperature sensor 1m* [online]. 2024, [cited 2024-12-09]. Available at: https://www.laskakit.cz/user/related_files/umw_ds18b20_en.pdf.
- [37] Distributor laskakit, www.laskakit.cz. *DS18B20 Digital waterproof temperature sensor 1m* [online]. 2024, [cited

- 2024-12-09]. Available at: <https://www.laskakit.cz/en/dallas-digitalni-vodotesne-cidlo-teploty-ds18b20-1m/>.
- [38] Distributor laskakit, www.laskakit.cz. *Dallas DS18B20 orig. digital waterproof temperature sensor 1m* [online]. 2024, [cited 2024-12-09]. Available at: <https://www.laskakit.cz/en/dallas-ds18b20-orig--digitalni-vodotesne-cidlo-teploty-1m/>.
- [39] Distributor laskakit, www.laskakit.cz. *Dallas DS18B20 digital temperature sensor, module* [online]. 2024, [cited 2024-12-09]. Available at: <https://www.laskakit.cz/en/digitalni-cidlo-teploty-dallas-ds18b20--modul/>.
- [40] Distributor laskakit, www.laskakit.cz. *Light intensity sensor VEML7700, I2C* [online]. 2024, [cited 2024-12-09]. Available at: https://www.laskakit.cz/user/related_files/veml7700.pdf.
- [41] Distributor laskakit, www.laskakit.cz. *Light intensity sensor VEML7700, I2C* [online]. 2024, [cited 2024-12-09]. Available at: <https://www.laskakit.cz/en/snimac-intenzity-osvetleni-veml7700--i2c/>.
- [42] Distributor laskakit, www.laskakit.cz. *Nova PM SDS011 Optical air quality sensor PM2.5 PM10* [online]. 2024, [cited 2024-12-09]. Available at: https://www.laskakit.cz/user/related_files/sds011_laser_pm2-5-v1-3.pdf.
- [43] World Health Organization, www.who.int. *WHO global air quality guidelines: particulate matter (PM2.5 and PM10), ozone, nitrogen dioxide, sulfur dioxide and carbon monoxide* [online]. 2021-09-22, [cited 2024-12-09]. Available at: <https://www.who.int/publications/i/item/9789240034228>.
- [44] Portal ATMO, atmotube.com. *What is PM?* [online]. 2024, [cited 2024-12-09]. Available at: <https://atmotube.com/air-quality-essentials/what-are-the-pms>.
- [45] Distributor laskakit, www.laskakit.cz. *Nova PM SDS011 Optical air quality sensor PM2.5 PM10* [online]. 2024, [cited 2024-12-09]. Available at: <https://www.laskakit.cz/en/nova-pm-sds011-opticky-senzor-kvality-ovzdusi-pm2-5-pm10/>.
- [46] Vaisala, www.vaisala.com. *WXT530 Series User Guide* [online]. 2024, [cited 2024-12-09]. Available at: <https://docs.vaisala.com/r/M211840EN-G/en-US>.

- [47] Distributor Specto Technology, www.spectotechnology.com. *Vaisala WXT536 Weather Sensor* [online]. 2024, [cited 2024-12-09]. Available at: <https://www.spectotechnology.com/product/vaisala-wxt536-weather-sensor/>.
- [48] Distributor laskakit, www.laskakit.cz. *Solar panel 6V 1W* [online]. 2024, [cited 2024-12-09]. Available at: <https://www.laskakit.cz/en/solarni-panel-6v-1w/>.
- [49] Distributor laskakit, www.laskakit.cz. *Li-ion cell charger TP4056 with microUSB protection* [online]. 2024, [cited 2024-12-09]. Available at: <https://www.laskakit.cz/en/nabijacka-li-ion-clanku-tp4056-s-ochranou-microusb/>.
- [50] Distributor laskakit, www.laskakit.cz. *Micro voltage stabilizer module AMS1117 3.3V* [online]. 2024, [cited 2024-12-09]. Available at: <https://www.laskakit.cz/en/micro-modul-stabilizatoru-napeti-ams1117-3-3v/>.
- [51] Distributor laskakit, www.laskakit.cz. *Automatic Buck-Boost TPS63020 power converter 1.8-5.5V 2A* [online]. 2024, [cited 2024-12-09]. Available at: <https://www.laskakit.cz/en/automaticky-buck-boost-tps63020-napajeci-menic-1-8-5-5v-2a/?variantId=16136>.
- [52] Distributor laskakit, www.laskakit.cz. *Step-up boost converter with SX1308 2A* [online]. 2024, [cited 2024-12-09]. Available at: <https://www.laskakit.cz/en/step-up-boost-menic-s-sx1308-2a/>.
- [53] Distributor laskakit, www.laskakit.cz. *TTL to RS232, MAX3232 converter* [online]. 2024, [cited 2024-12-09]. Available at: https://www.laskakit.cz/user/related_files/max3232.pdf.
- [54] Distributor laskakit, www.laskakit.cz. *TTL to RS232, MAX3232 converter* [online]. 2024, [cited 2024-12-09]. Available at: <https://www.laskakit.cz/en/prevodnik-ttl-na-rs232--max3232/>.
- [55] Distributor GMelectronic, www.gme.cz. *STMicroelectronic TIP132 darlingtonův tranzistor* [online]. 2024, [cited 2024-12-09]. Available at: <https://www.gme.cz/v/1488498/stmicroelectronic-tip132-darlingtonuv-tranzistor>.
- [56] Distributor laskakit, www.laskakit.cz. *LaskaKit CH9102 Programmer USB-C, microUSB, UART* [online]. 2024, [cited

2024-12-09]. Available at: <https://www.laskakit.cz/en/laskakit-ch9102-programmer-usb-c--microusb--uart/>.

- [57] Distributor laskakit, www.laskakit.cz. *GeB LiPol Battery 503035 500mAh 3.7V JST-PH 2.0* [online]. 2024, [cited 2024-12-09]. Available at: <https://www.laskakit.cz/en/baterie-li-po-3-7v-500mah-lipo/>.

Symbols and Abbreviations

°C	degrees Celsius
ADC	analog to digital converter
CA	certificate authority
CSR	certificate signing request
dBm	decibel-milliwatts
DKWS	Daniel Kluka Weather Station
ESP	Espressif Systems
g/m³	grams per cubic meter
hPa	hectopascal
HTTP	hypertext transfer protocol
HTTPS	hypertext transfer protocol secure
IoT	internet of things
KB	kilobyte
kHz	kilohertz
LED	light emitting diode
Li-Ion	lithium-ion battery
LiPol	lithium-polymer battery
LoRaWAN	long range wide area network
LPWAN	low power wide area network
LTE	long-term evolution
lx	lux
mA	milliampere
MAC	media access control
MB	megabyte

MHz	megahertz
mm	millimeter
mm/h	millimeters per hour
MOSFET	metal–oxide–semiconductor field-effect transistor
MQTT	message queuing telemetry transport
mV	millivolt
nA	nanoampere
NB-IoT	narrowband internet of things
NFC	near field communication
openssl	open-source secure sockets layer
OS	operating system
PCB	printed circuit board
PEM	privacy-enhanced mail
PSRAM	pseudo static RAM
PWM	pulse width modulation
RH	relative humidity
RTC	real-time clock
SDI-12	serial data interface at 1200 baud
SIGFOX	proprietary LPWAN technology
SIM	subscriber identity module
SNTP	simple network time protocol
SRAM	static random access memory
SSH	secure shell
SSL	secure sockets layer
TCP	transmission control protocol

TLS	transport layer security
UART	universal asynchronous receiver-transmitter
UDP	user datagram protocol
USB	universal serial bus
USB-C	universal serial bus type-C
V	volt
VCC	voltage at the common collector
W	watt
Wi-Fi	wireless fidelity

List of Appendices

A	Technical Documentation of Weather Station Components	113
A.1	ESP32-S3-WROOM-1 N16R8	114
A.2	Quectel BC660K-GL	115
A.3	Sensors	116
A.3.1	Temperature Sensor UMW DS18B20	116
A.3.2	Light Intensity Sensor Vishay VEML7700	117
A.3.3	Air Quality Sensor Nova PM SDS011	118
A.3.4	Weather Transmitter Vaisala WXT536	119
B	Main Algorithm Flow Chart	123
C	Doxygen Documentation	125
D	Radiation Shield Visualisation	127
E	DKWS PCB Schematic Documentation	131

A Technical Documentation of Weather Station Components

Table A.1: Overview of main DKWS hardware components

Component	Key Parameters	Interfaces	Typical Power Consumption	Datasheet
ESP32-S3-WROOM-1 N16R8	Dual-core Xtensa LX7, 240 MHz, 512 kB SRAM, 8 MB PSRAM, 16 MB Flash, Wi-Fi 2.4 GHz, BT 5 LE	UART0/1/2, SPI, I ² C, ADC, PWM, GPIO	7–8 μ A (deep sleep), \sim 80 mA (Wi-Fi TX)	Espressif ESP32-S3 Datasheet [31]
Quectel BC660K-GL	LTE Cat NB2, eDRX/PSM support, 23–33 dBm TX, SMT 35.0 \times 32.0 \times 2.25 mm	UART (AT commands), GPIO, ADC	800 nA (PSM), 35 mA (idle), \leq 220 mA (TX)	Quectel BC660K-GL HW Design V1.1 [33]
UMW DS18B20	−55 to +125 $^{\circ}$ C, \pm 0.5 $^{\circ}$ C, 9–12-bit resolution	1-Wire (parasitic power support)	Stand-by 1 μ A	Maxim DS18B20 Datasheet; UMW variant [36]
Vishay VEML7700	0–120,000 lx, 16-bit ADC, \leq 0.0036 lx LSB	I ² C (400 kHz)	170 μ A (active), 0.5 μ A (shutdown)	VEML7700 Datasheet Rev. 1.6 [40]
Nova PM SDS011	PM _{2.5} /PM ₁₀ : 0–999.9 μ g/m ³ , laser 0.3 μ m	UART 9600 Bd, PWM output	<4 mA (sleep), 70 mA (active)	Nova PM SDS011 Specification [42]
Vaisala WXT536	T, RH, p, wind (ultrasonic), rain/hail (acoustic), IP65	SDI-12, RS-232/422/485, analog IN/OUT	0.2 mA (standby), 3.5 mA (typ.), 1.2 A (heater)	Vaisala WXT530 Series Manual M211973 [46]
TP4056	Li-Ion CC/CV charging, 4.2 V, 1 A, DW01A + FS8205A protection	USB 5 V / VIN 4.5–6 V	Typ. 500–1000 mA (charging)	TopPower TP4056 Datasheet [49]
TPS63020	Buck-boost 1.8–5.5 V IN, up to 3 A OUT, fixed 3.3 V	I ² C (mode switching)	90–95 % efficiency, 35 μ A IQ	TI TPS63020 Datasheet SLVS819 [51]
SX1308	Step-up DC/DC, 2–24 V IN, 3–28 V OUT, 2 A	Adjustable via trimmer	Max. 98 % efficiency	SUNROM SX1308 Datasheet [52]
IRLZ44N	N-MOSFET, $R_{DS(on)} = 22$ m Ω (@ $V_{GS} = 4$ V), $I_D = 47$ A	Logic-level gate (2–4 V)	Low switching losses	IR IRLZ44N Datasheet
Solar Panel	6 V / 4.5 W, poly-Si, max. 750 mA	–	Depends on irradiance	Manufacturer datasheet
Batteries	2 \times 18650 Li-Ion, 3.7 V, 3500 mAh, parallel	–	7 Ah total capacity	Manufacturer datasheet

High demands are placed on the components used in the weather station in Table A.1. These include high computing performance, low power consumption, mechanical and electrical robustness, support for advanced cybersecurity mechanisms, modularity, and long-term availability.

For these reasons, the components selected for the device meet the strictest

requirements for NB-IoT systems and guarantee both reliability and security — not only under current conditions, but also over a long-term horizon of up to 10 years. Additional components on the PCB include:

- MAX3232 (RS-232 \leftrightarrow UART converter, voltage range 3–5.5 V)
- Debug/power pins, jumpers and buttons for ESP32-S3 and BC660K-GL
- Protection elements (TVS, fuses, ESD)

Schematics and layer layout of the PCB are provided in Appendices A–C. Datasheets for each component are referenced in the bibliography.

A.1 ESP32-S3-WROOM-1 N16R8

The ESP32-S3-DevKitC-1 in Figure A.1 is a development motherboard developed by Espressif that features Wi-Fi 2.4 GHz, 802.11 b/g/n and Bluetooth 5 (BLE) connectivity. It was used in the development of the prototype board, and eventually the microcontroller ESP32-S3-WROOM-1 is implemented on the PCB circuit board created for this work. Its most important feature is the integration of complete Wi-Fi and Bluetooth functions in low power consumption mode. In sleep mode, the module consumes extremely low amounts of current, making it an ideal microcontroller for use within a prototype weather station. The board itself offers an ample amount of I/O pins and is powered by a 3.3 V supply. A wide range of peripherals are suitable and compatible with many sensors, displays, or other components to expand the possibilities within the project. It is suitable for ambient operating temperatures from -40 to 65 °C.[31]

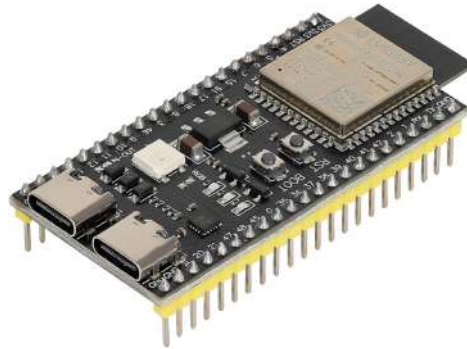


Fig. A.1: Microcontroller ESP32-S3 DevKitC-1 WROOM-1 N16R8.[32]

The N16R8 configuration includes a dual-core 32-bit Xtensa LX7 processor with a 240 MHz operating frequency, 512 kB SRAM, 8 MB PSRAM and 16 MB Flash memory. The combination of these components provides increased performance, increased memory, and improved power efficiency suitable for IoT development.

The dual-core processor provides smooth multitasking and performs multiple tasks simultaneously without performance loss. Support for instruction vectoring is suitable for signal processing and speeding up neural network computations. In sleep mode, it consumes only 7 or 8 μA . [31]

A.2 Quectel BC660K-GL

The BC660K-GL-TE-B KIT development motherboard in Figure A.2 was used in the development of the prototype board, and eventually the module BC660K-GL was implemented on the PCB circuit board created for this work. Narrowband-Internet of Things is a cellular wireless technology based on Low Power Wide Area (LPWA) standards and significantly improves the power consumption of user devices and increases battery life, which can exceed more than 10 years when using this technology. [33][34]



Fig. A.2: NB-IoT module Quectel BC660K-GL-TE-B KIT. [35]

The Quectel BC660K-GL is a high-performance LTE Cat NB2 module that supports multiple frequency bands and has extremely low power consumption. It is suitable for IoT, smart metering, bike sharing, smart parking, smart city, security, and agricultural and environmental monitoring applications. It provides services for Short Message Service (SMS) and data transmission. It is suitable for ambient operating temperatures from -40 to 85 $^{\circ}\text{C}$. [33][34]

Supported frequency bands:

- B1–B5 / B8 / B12–B14 / B17–B20 / B25 / B28 / B66 / B70 / B85

Supported communication protocols:

- UDP, TCP, PING, LwM2M, SNMP, COAP, COAPS, HTTP, HTTPS, MQTT, MQTTS, SSL, TLS

It sends SMS messages in text mode and, like the ESP32-S3 microcontroller, it also has a wide range of usable peripherals. During sleep, it consumes only 800 nA of current.[33][34]

A.3 Sensors

Since the weather station measures air quality and uses the **Vaisala WXT536** multi-parametric sensor, this makes it a device that outperforms the competition in terms of parameters and offers a wide range of measured meteorological variables not found in other common weather stations. Ultrasonic sensors or acoustic sensors are also not common in the measurement of these quantities and give the weather station high accuracy, robustness and value.

A.3.1 Temperature Sensor UMW DS18B20

The DS18B20 digital temperature sensor in Figure A.3 from **UMW Youtai Semiconductor** in a waterproof design is a replica of the popular and accurate DS18B20 sensor from **Maxim Integrated**. The main noticeable difference between the two sensors is the price, with UMW's sensor being only 1/4 the price of Maxim Integrated's sensor. The original intention was to work with the original sensor in this project, but it was only later discovered what sensor was actually being used when studying the documentation. The original sensor tends to sell out very often and vendors tend to push the UMW vendor variant on their site rather than the original variant, and the same thing happened when ordering components for this project.[36][37][38]

The DS18B20 measures temperature in degrees Celsius with a resolution of 9 to 12 bits. It is powered by a **One Wire** bus, which has the advantage of being powered by only one data wire. The operating temperature is from -55 to $+125$ °C with an accuracy of ± 0.4 °C (range -10 to $+70$ °C). Unlike the manufacturer's sensor, **Maxim Integrated** does not support parasitic wiring (drawing power only from the data bus with no external power supply) and requires a 2.5 or 5.5 V input voltage for functionality. It is also necessary to connect a $4.7\text{ k}\Omega$ pull-up resistor between the data and plus wires of the power supply. Due to its waterproof property, it can be used in environments with excessive humidity or in tanks with liquids;



Fig. A.3: Temperature sensor UMW DS18B20.[37]

furthermore, for example, for HVAC environmental control, temperature monitoring in buildings and equipment, machines, and in process monitoring and control systems.[36][37][38]

For the prototype board, a variant of the sensor in Figure A.4 was also used for a short period of time, which was mounted directly on the board and installed inside the weather station to monitor the internal temperature of the protective box. This monitoring would allow monitoring of the working conditions of the weather station components. The aim is to design a robust device that can withstand harsh conditions, and the monitoring of this temperature is also part of the subsequent monitoring and development of the weather station. This time, the sensor, labelled Dallas, was also from the manufacturer UMW Youtai Semiconductor.



Fig. A.4: Temperature sensor UMW Dallas DS18B20.[39]

A.3.2 Light Intensity Sensor Vishay VEML7700

The VEML7700 in Figure A.5 is a high-precision digital light intensity sensor from Vishay. It is manufactured and sold in several versions, for example in a small

transparent housing or in a small transparent housing mounted directly on the circuit board. For this project, the latter version was chosen, which includes a high-sensitivity photodiode, a low-noise amplifier and a 16-bit A/D converter. Pull-up resistors are also used.[40]

The sensor is powered at 3.3 or 5 V and communicates with devices using an I2C bus whose logic levels can be converted by an integrated 16-bit A/D logic level converter to 3.3 and 5 V. The VEML7700 provides a measurement range from 0 to 120,000 lux with a resolution of 0.0036 lux ([lx] – lumen per square meter [lm/m^2]).[40]

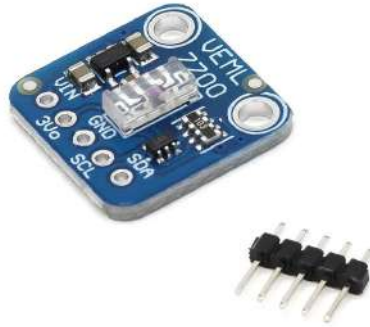


Fig. A.5: Light intensity sensor Vishay VEML7700.[41]

For comparison, a bright sunny day can range from 32,000 to 100,000 lux, a cloudy day 1,000 to 25,000 lux, etc. The sensor can also measure the amount of white light given without the unit. The sensor is also suitable for operating temperatures from -25 to $+85$ °C.[40]

A.3.3 Air Quality Sensor Nova PM SDS011

The SDS011 laser dust sensor in Figure A.6 is designed to monitor dust particles in the air with a diameter greater than 0.3 micrometers [μm]. These are microscopic solid or liquid particles in the air that are a significant indicator of air pollution. The sensor measures PM2.5 and PM10, which are 2.5 and 10 μm in diameter. This value is given in micrograms per cubic metre [$\mu\text{g}/\text{m}^3$].[42]

PM2.5 particles are fine particles 30 times smaller than the diameter of a human hair. They come from industrial processes, cars, power stations, smoke, or chemical reactions in the air. They enter the lungs and blood and pose a greater health risk to humans in the form of respiratory or cardiovascular diseases, for example.[43]

PM10 particles are larger in diameter and are produced, for example, by grinding, demolition, dust whirling, transport, etc. They get trapped in the upper respiratory tract (nose and throat), and prolonged exposure to these particles can cause, for example, breathing problems or irritation.[43]



Fig. A.6: Air quality sensor Nova PM SDS011.[45]

The SDS011 is powered by an input voltage of 4.7 to 5.3 V and has a low power consumption of less than 4 mA in sleep mode. It can measure dust particles with an accuracy of $0.3 \mu\text{m}$, and the measurement range is from 0 to $999.9 \mu\text{g}/\text{m}^3$. The operating temperature of the sensor is from -10 to $+50$ °C, and the atmospheric pressure from 86 to 110 kPa. It uses a UART bus or PWM for its communication.[42]

It is important that the sensor is installed in the correct position, as it contains a fan that draws air into the measuring chamber, in which the amount of particles measured by the laser sensor is measured. Incorrect positioning may cause the fan to fail to draw in sufficient air for the measurement, and the measurement will therefore not be reliable. Among other things, wear of the fan bearing is also increased. It is advised to clean the measuring chamber of dust build-up over a period of months and keep the inlet tube as short as possible. It is also important that the inlet tube is anti-static and does not trap dust particles. The measuring chamber must not be illuminated with light to avoid damaging the sensor, and the measurement of the amount of particles in it takes approximately 30 seconds or 1 minute.[42]

A.3.4 Weather Transmitter Vaisala WXT536

The WXT536 in Figure A.7 is one of the professional and high-end multi-parameter sensors that can simultaneously measure air temperature, humidity, pressure, precipitation, and wind. The low current consumption makes the sensor suitable for projects using solar pan-

els. **Vaisala**'s sensor series exceeds the IEC60945 marine standard.[46]

Ultrasonic sensors are used to measure the wind, which can also be used to measure its direction. Barometric pressure, temperature, and humidity are capacitively measured using a PTU module. The measurement of precipitation is carried out by an acoustic sensor that does not flood, clog, damp, or resist in measuring even moderate precipitation with high sensitivity.[46]



Fig. A.7: Multiparameter weather sensor **Vaisala** WXT536.[47]

Barometric pressure is monitored from 500 to 1100 hPa with an accuracy of ± 0.5 hPa at temperatures from 0 to $+30$ °C and ± 1 hPa at temperatures from -52 to $+60$ °C. The output resolution of this measurement is 0.1 hPa, while values can also be displayed in **bar** or **inHg** units.[46]

Another measured parameter is the air temperature, which is recorded from -52 to $+60$ °C with an accuracy of ± 0.3 °C from 0 to $+30$ °C and ± 0.6 °C over the entire temperature range. The output resolution of the measurement is 0.1 °C. Relative humidity is measured from 0 to 100 %RH, with an accuracy of ± 3 %RH for humidity from 0 to 90 %RH and ± 5 %RH for humidity from 90 to 100 %RH. Output resolution is 0.1 %RH.[46]

Wind speed measurement is made in the range of 0 to 60 m/s with an accuracy of $\pm 3\%$ or 0.1 m/s. The time response is 0.25 seconds and the output resolution is 0.1 m/s, while the values can also be displayed in units of km/h, mph, or knots. Wind direction is monitored from 0 to 360 degrees with an accuracy of ± 3 degrees at a wind speed of 10 m/s. The output resolution is 1 degree.[46]

The device also allows the measurement of precipitation using a collection area of 60 cm². The output resolution of the rainfall measurement is 0.01 mm and the accuracy of the rainfall accumulation is better than $\pm 5\%$, this value depending on the weather conditions. The rainfall intensity is measured from 0 to 200 mm/h with a resolution of 0.1 mm/h. The device can also monitor hail with a resolution of 0.1 hits/cm²/h, allowing accurate monitoring of its intensity.[46]

In terms of inputs and outputs, the device supports a power supply range of 6 to 24 V with a tolerance of -10 to $+30\%$. The average power consumption is a minimum of 0.2 mA at 12 V in standby mode, with a typical consumption of 3.5 mA at 12 V. The heating voltage can be connected in the 12 V AC/DC or 24 VDC range, with a typical heating current of 1.2 A at 24 VDC. The device provides digital outputs compatible with SDI-12, RS-232, RS-485 and RS-422 protocols, allowing easy integration into a variety of systems.[46]

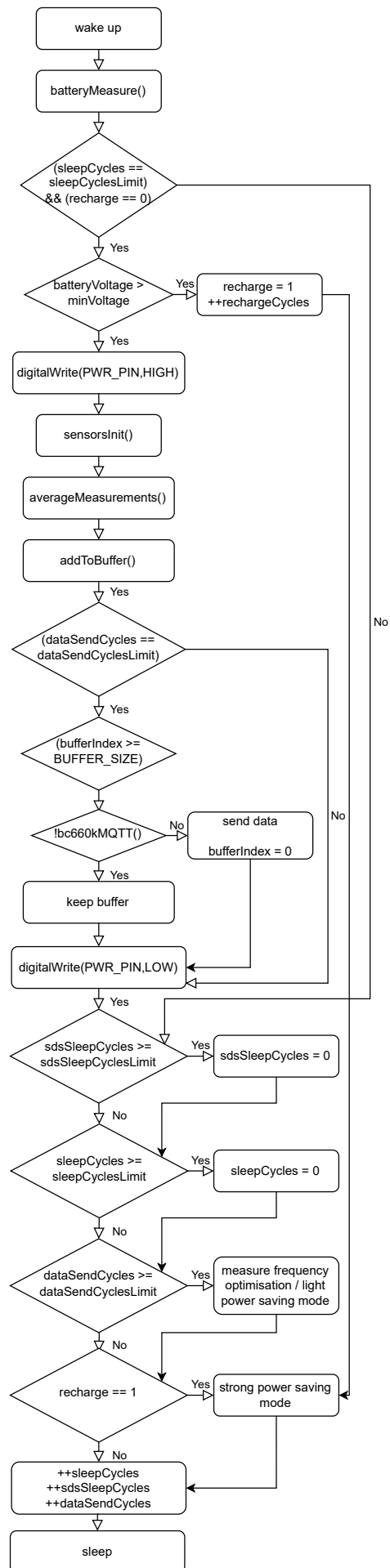
Mechanical specifications of the device include IP65 protection, which guarantees protection against dust and water, and a weight of 0.7 kg. The device is designed to operate in harsh environments with a temperature range of -52 to $+60$ °C and relative humidity from 0 to 100 %RH. The pressure conditions for its operation range from 500 to 1100 hPa and the wind speed that the device can withstand is up to 60 m/s.[46]

In addition, the device supports analog inputs and outputs. In the case of the WXT536, analog inputs can be connected for voltages ranging from 0 to 2.5 V, 5 V and 10 V or resistive sensors ranging from 800 to 1330 Ohms.[46]

This comprehensive range of functions and parameters makes the WXT536 a versatile device suitable for monitoring multiple environmental variables with high accuracy. Its rugged design and wide compatibility allow it to be used in a variety of applications including meteorology, industry, and research.[46]

B Main Algorithm Flow Chart

Flowchart describing the main algorithm of the weather station can be found on the next page.



C Doxygen Documentation

This documentation is automatically generated and can be found in the *index.html* file.

FEKT ÚSTAV TELEKOMUNIKACÍ

Design of a secure data transmission system in NB-IoT environment

Main Page Related Pages Classes Files Search

Functions

bool	dsInitialize (bool &dsInit, DallasTemperature &sensor)	Air temperature sensor DS18B20 initialization function.
bool	vemlInitialize (bool &vemlInit, Adafruit_VEML7700 &veml)	Light intensity sensor VEML7700 initialization function.
bool	sdsInitialize (bool &sdsInit, int &SDS_RX, int &SDS_TX, HardwareSerial &SDS011Serial, SdsDustSensor &sds)	Air quality sensor SDS011 initialization function.
bool	wxtInitialize (bool &wxtInit, int &WXT_RX, int &WXT_TX, HardwareSerial &WXT536Serial)	Multiparametric weather transmitter WXT536 initialization function.
bool	checkI2CConnection (uint8_t address)	I2C connection check function.
bool	dsMeasure (float &tempC, DallasTemperature &sensor)	Air temperature sensor DS18B20 measurement function.
bool	vemlMeasure (float &lux, float &white, Adafruit_VEML7700 &veml)	Light intensity sensor VEML7700 measurement function.
bool	sdsMeasure (float &pm25, float &pm10, SdsDustSensor &sds)	Air quality sensor SDS011 measurement function.
bool	wxtMeasure (HardwareSerial &WXT536Serial, String &receivedData, String &completeMessage, float &windDir, float &windSp, float &temp, float &humi, float &pres, float &rain, float &heaterT, float &heaterV)	Multiparametric weather transmitter WXT536 measurement function.
void	parseWXT536Data (String data, float &windDirData, float &windSpData, float &tempData, float &humiData, float &presData, float &rainData, float &heaterTData, float &heaterVData)	Multiparametric weather transmitter WXT536 data parsing function.
String	extractValue (String data, String key, String delimiter)	Multiparametric weather transmitter WXT536 data extraction function.

Variables

int	retries = 0
int	max_retries = 5

Fig. C.1: Automatically generated Doxygen documentation for the file `Sensors.cpp`.

D Radiation Shield Visualisation

The proposed radiation shield is modified and reinforced with aluminium profiles strengthening critical parts. A steel cable is also used to connect the parts together and prevent them from falling off the roof in the event of plastic failure. The solar panel holder is fitted with a larger, more powerful solar panel. A strong construction adhesive resistant to UV, wind, frost, and rain is used, to which the shield itself is resistant. Strong plastic tapes are also used. The shield also partially protects the wiring of the sensors used.

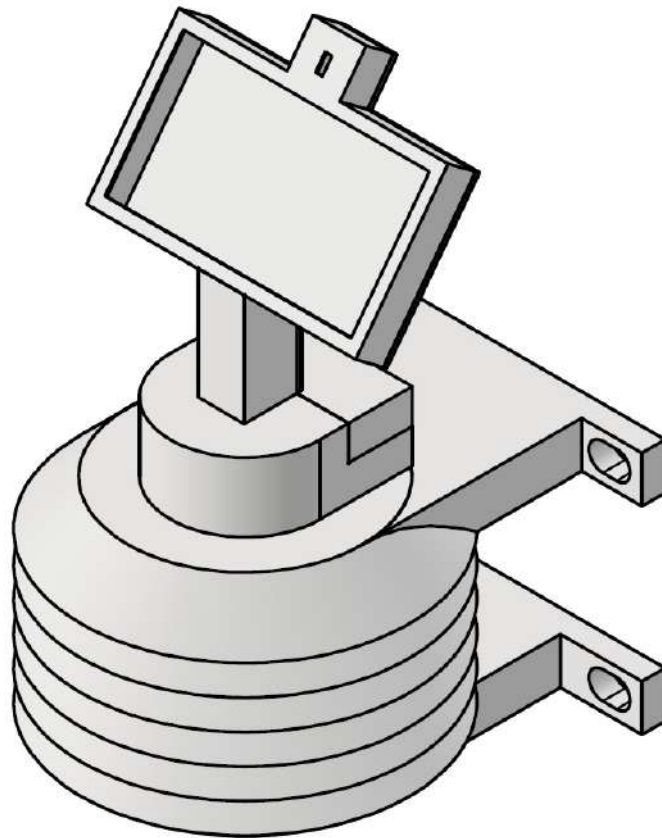


Fig. D.1: Front side of the proposed radiation shield.

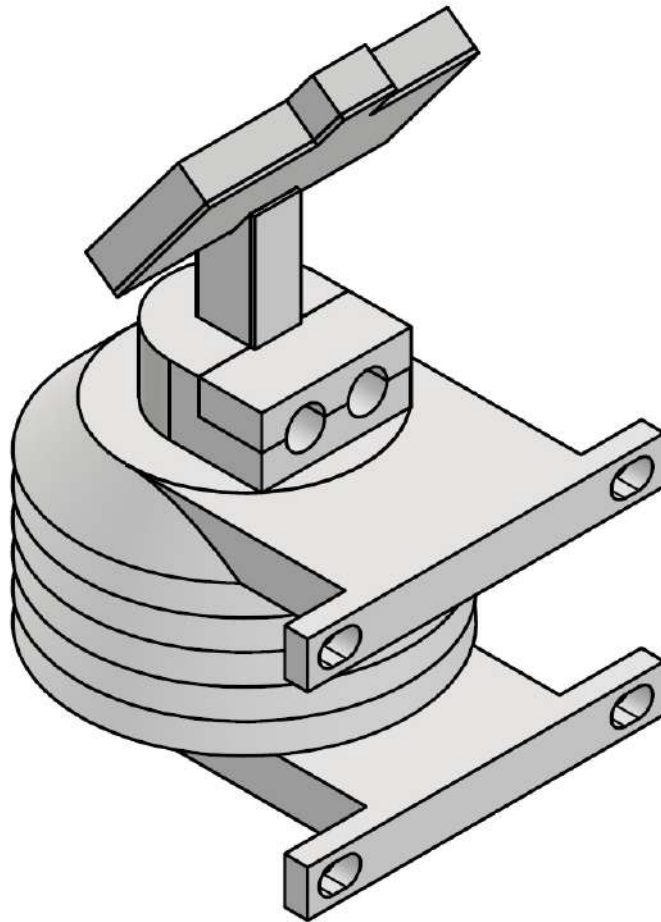


Fig. D.2: Back side of the proposed radiation shield.

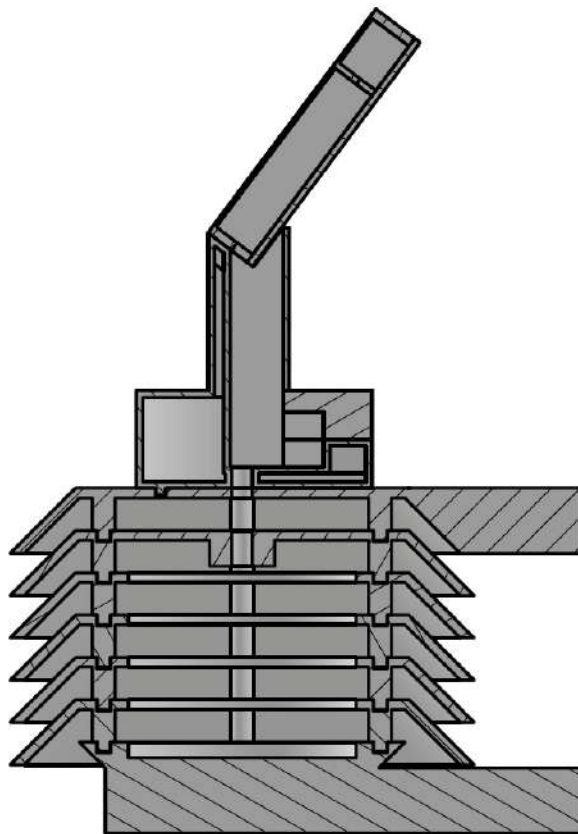
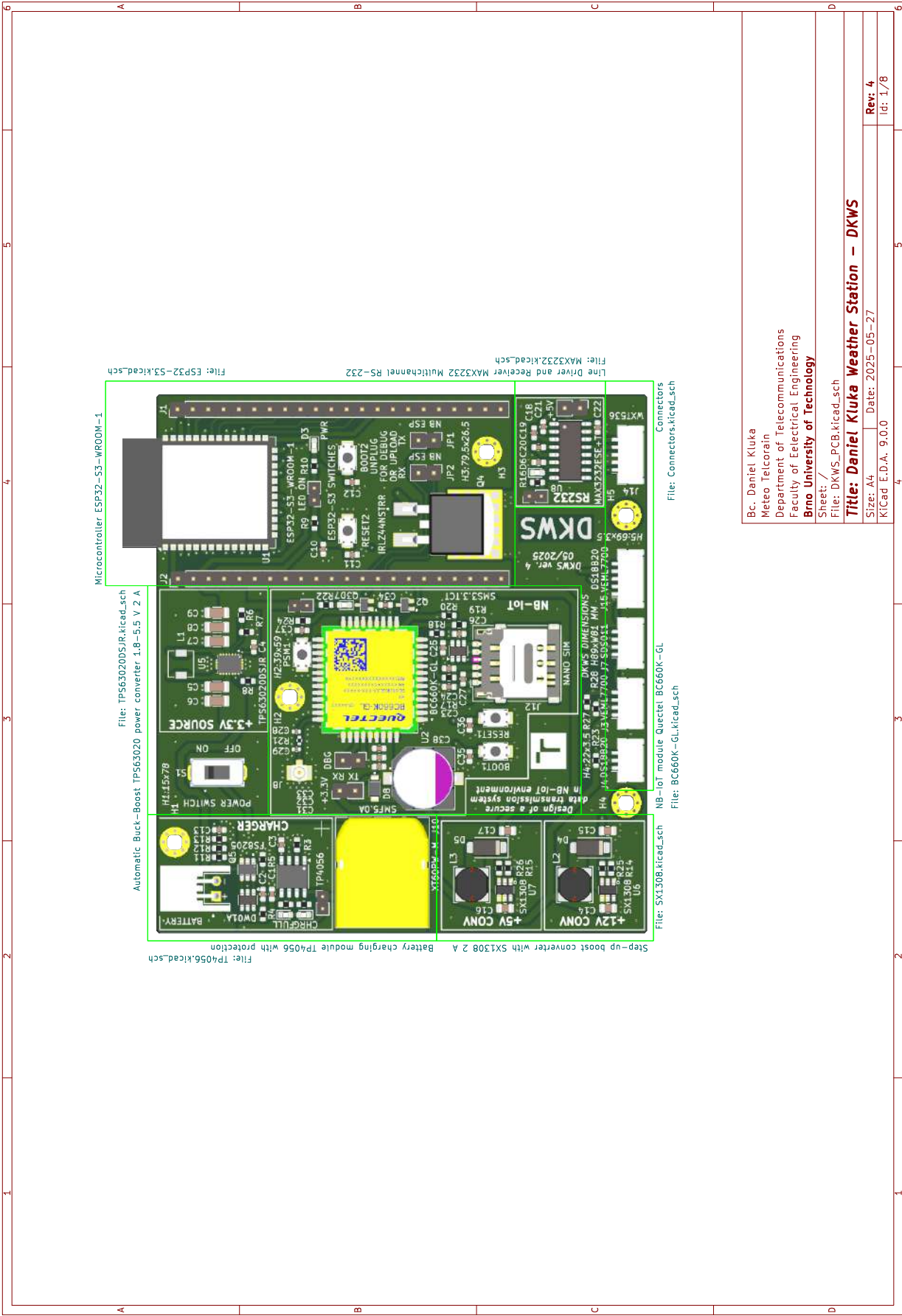


Fig. D.3: Cross section side of the proposed radiation shield.

E DKWS PCB Schematic Documentation

The following pages contain complete schematic documentation of the proposed DKWS PCB, for which the prototype board serves as a template. For each area of the board, a detailed schematic is created that describes the wiring of the individual electronic components. These areas represent the modules that are introduced during the development of the prototype board.



Bc. Daniel Kluka
Meteo Telcorain
Department of Telecommunications
Faculty of Electrical Engineering
Brno University of Technology

Title: Daniel Kluka Weather Station – DKWS

Sheet: /
File: DKWS_PCB.kicad_sch

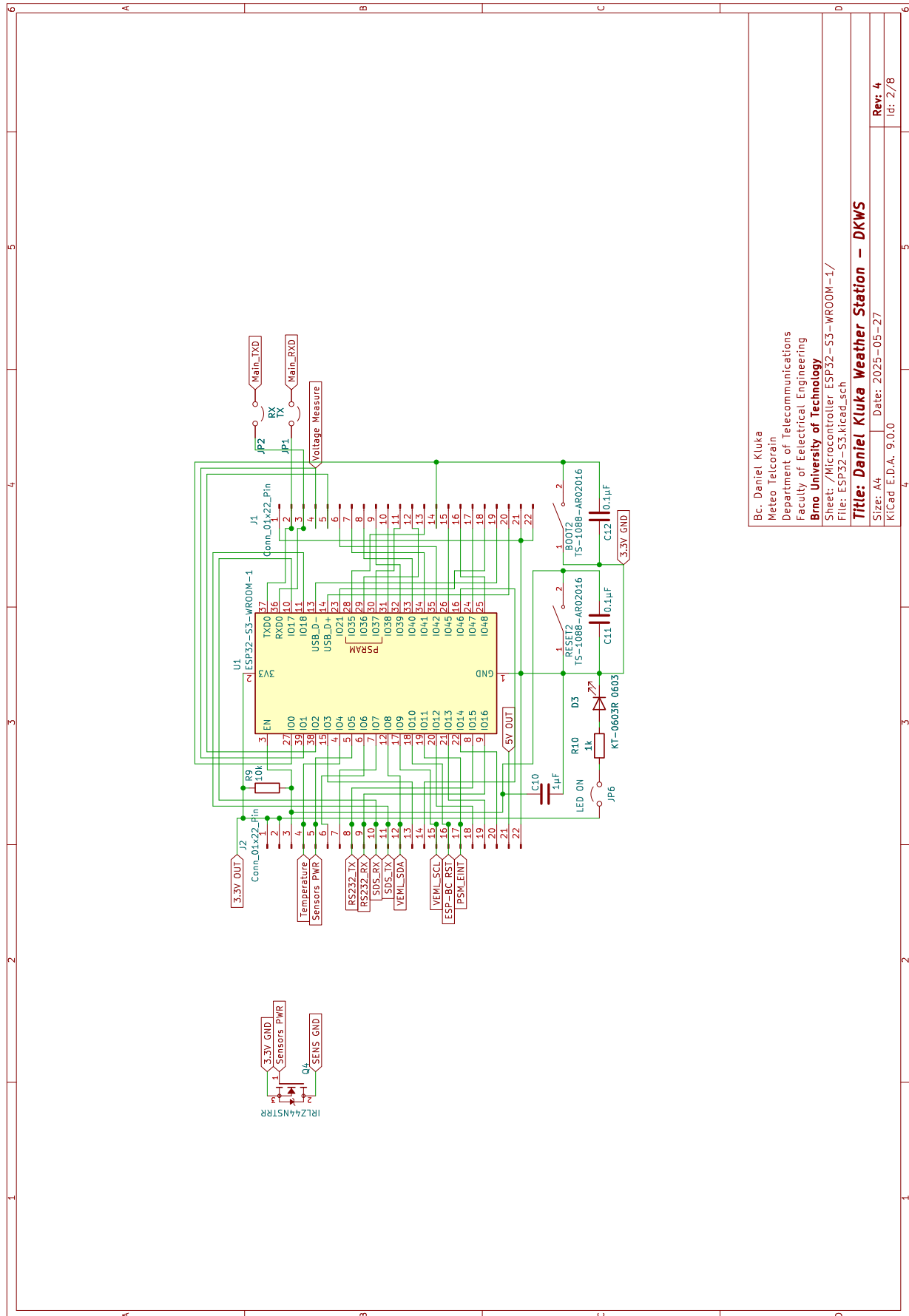
Size: A4

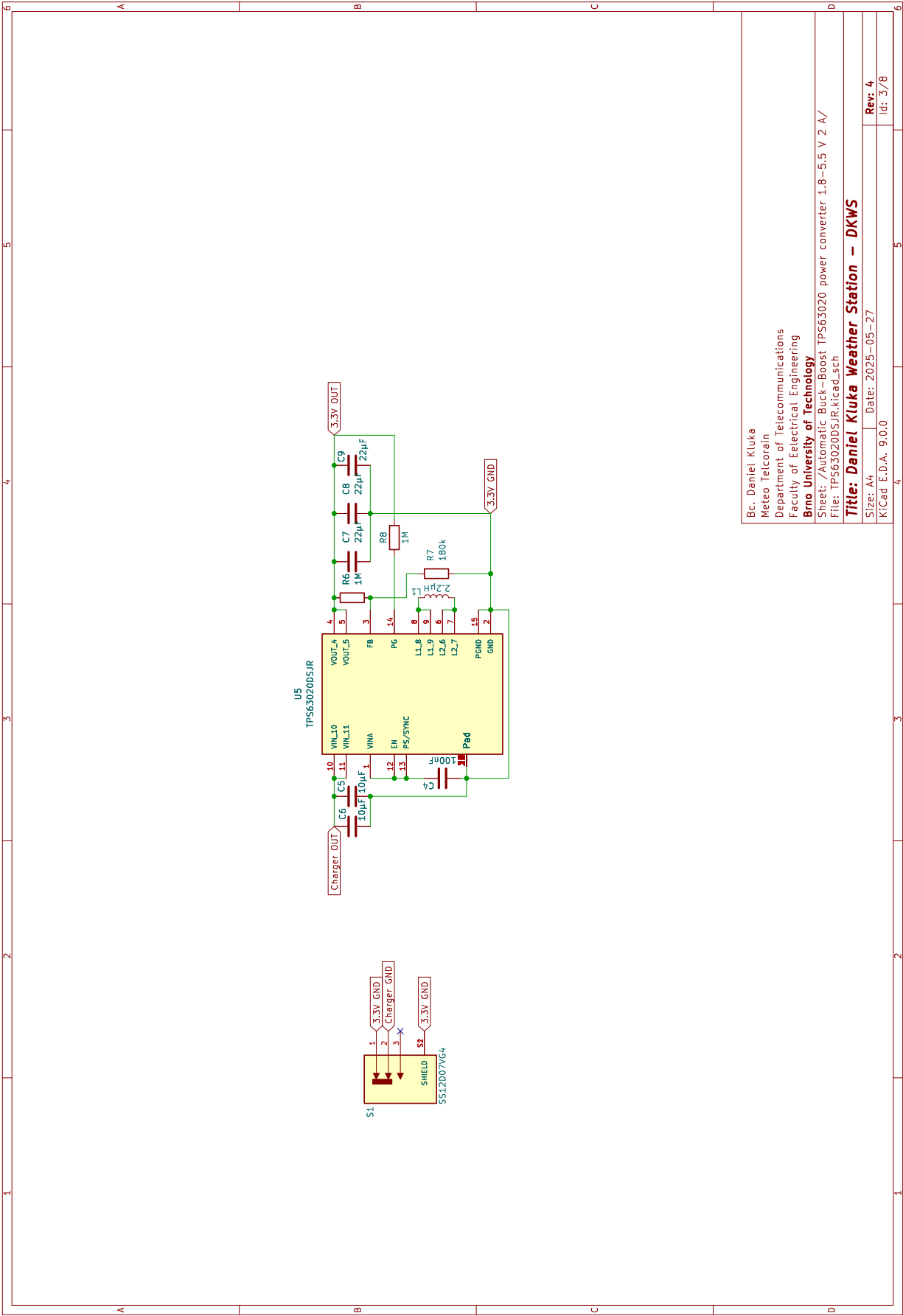
Rev: 4

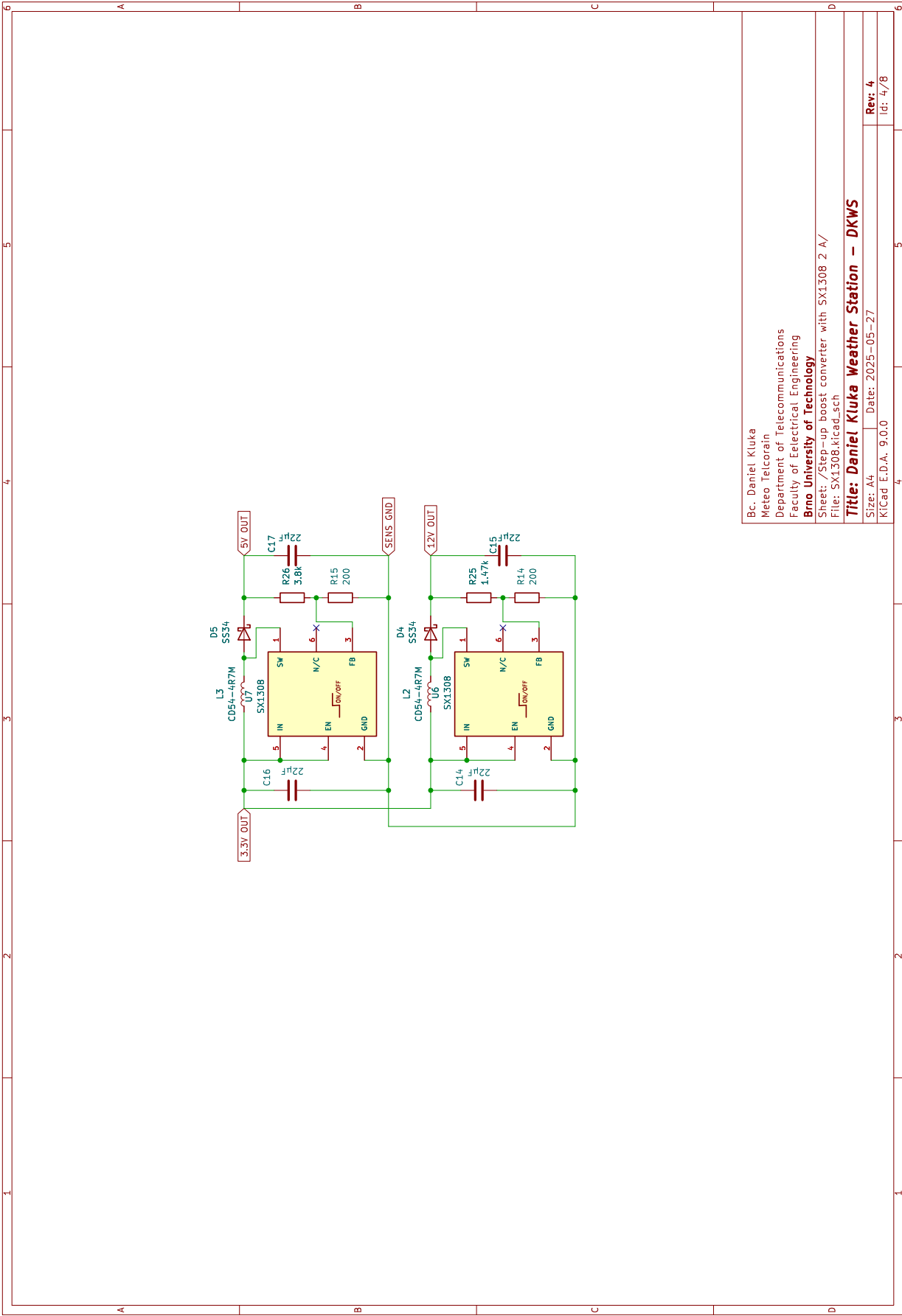
Date: 2025-05-27

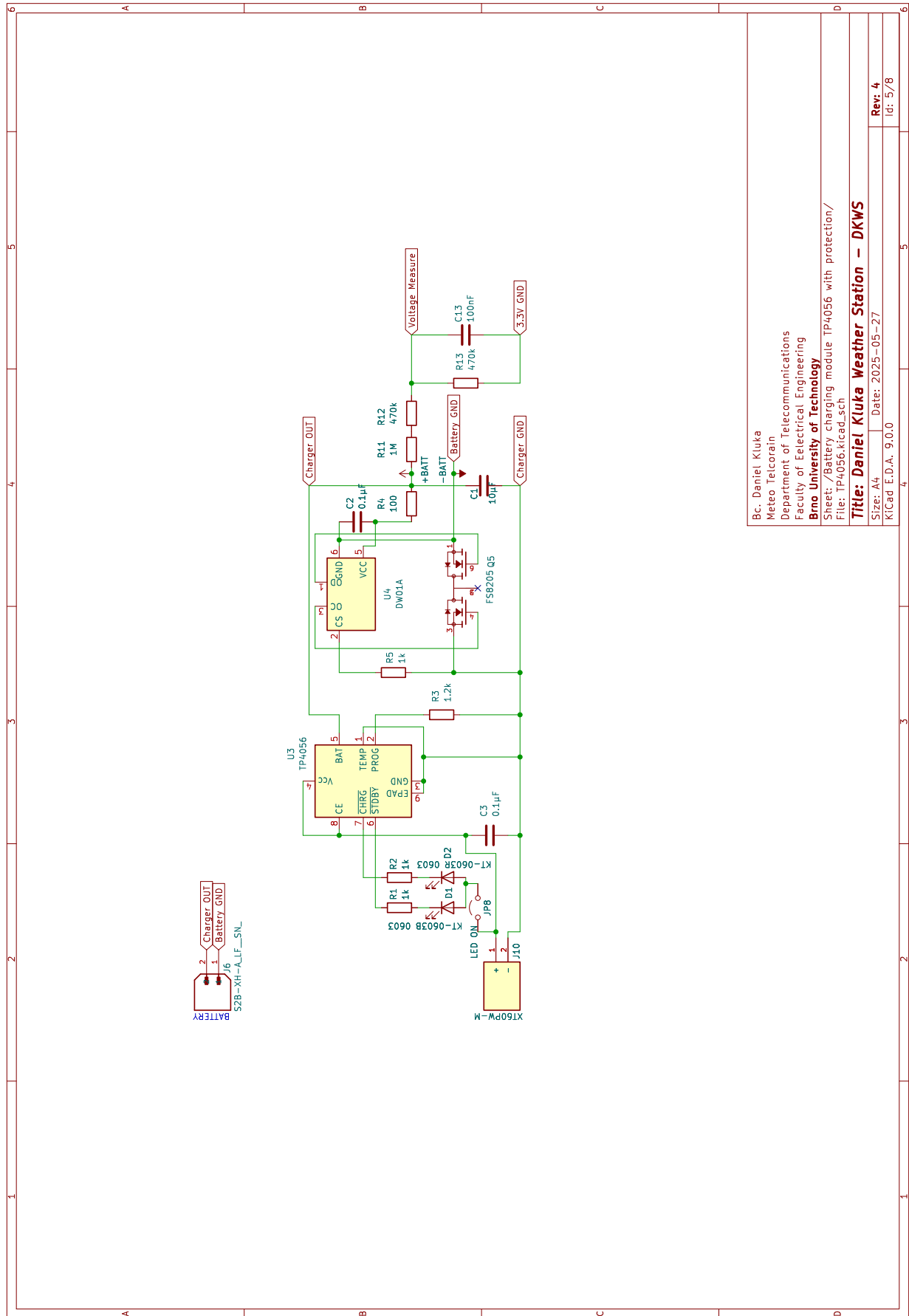
Id: 1/8

KiCad E.D.A. 9.0.0





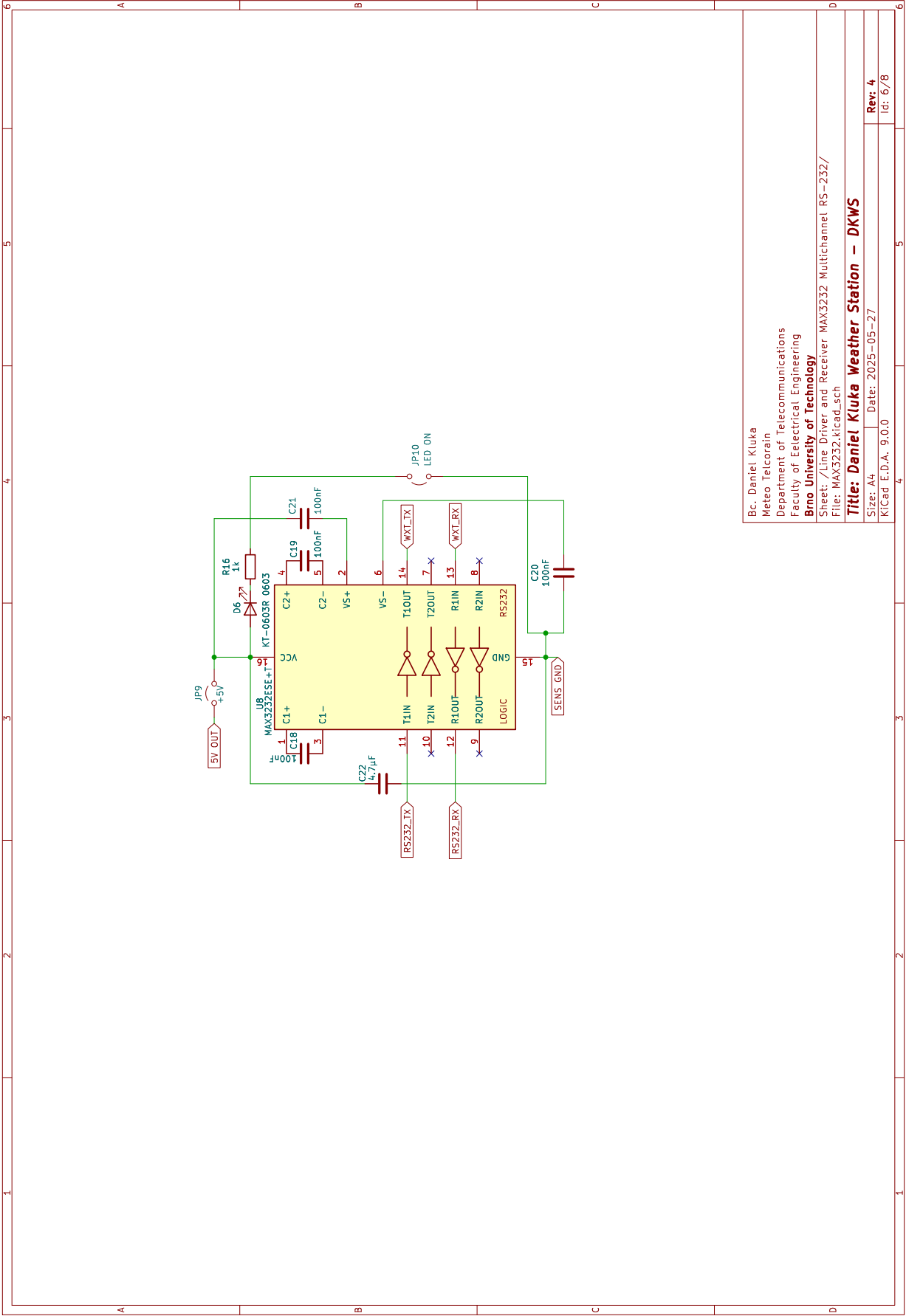


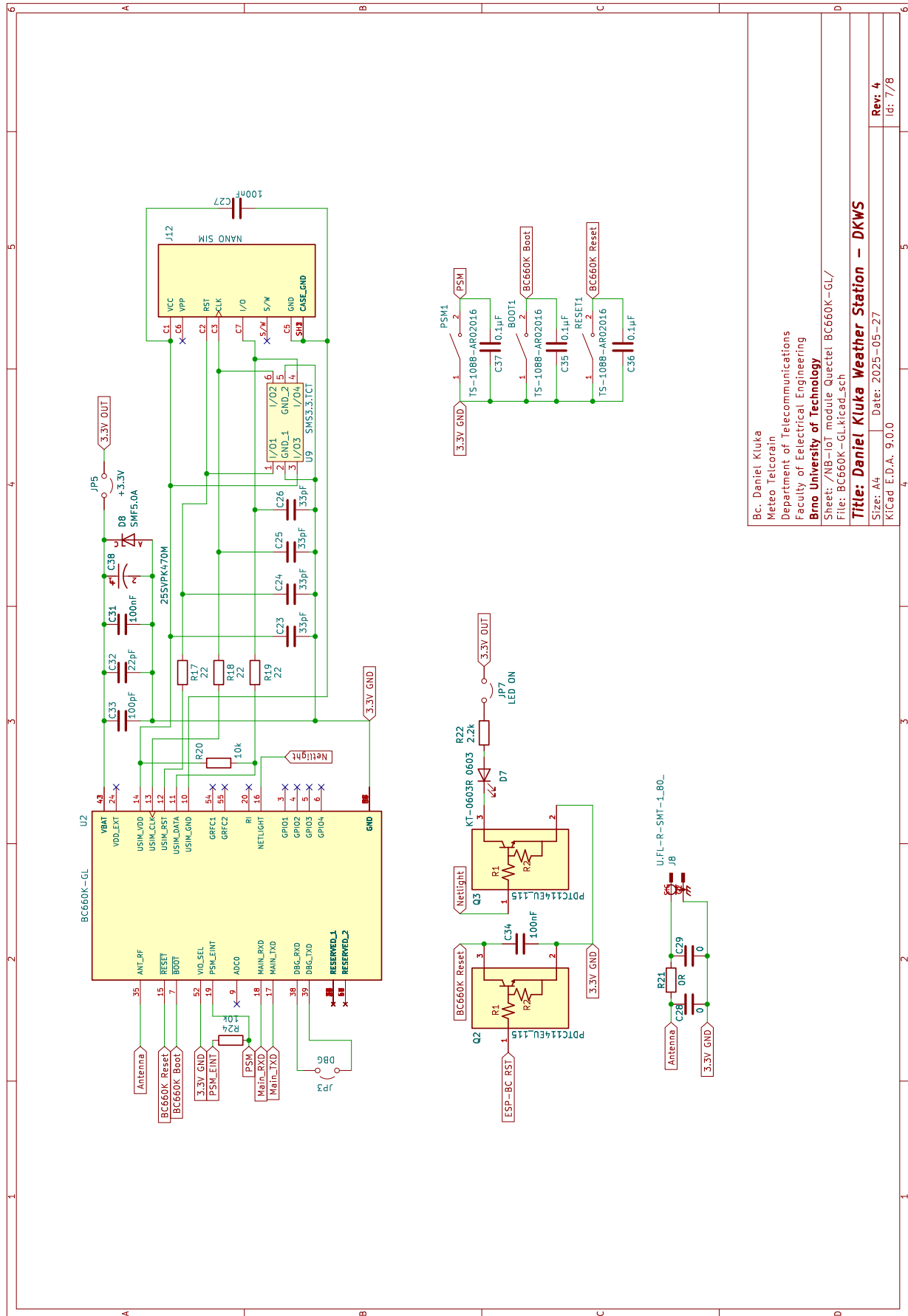


Bc. Daniel Kluka
Meteo Telcorain
Department of Telecommunications
Faculty of Electrical Engineering
Brno University of Technology
Sheet: /Battery charging module TP4056 with protection/
File: TP4056.kicad.sch

Title: Daniel Kluka Weather Station – DKWS

Size: A4	Date: 2025-05-27	Rev: 4
KiCad E.D.A. 9.0.0		Id: 5/8





Bc. Daniel Kluka
 Meteo Telcorain
 Department of Telecommunications
 Faculty of Electrical Engineering
Brno University of Technology
 Sheet: /NB-IoT module Quectel BC660K-GL/
 File: BC660K-GL.kicad_sch

Title: Daniel Kluka Weather Station – DKWS

Size: A4
 KiCad E.D.A. 9.0.0
 Date: 2025-05-27
 Rev: 4
 Id: 7/8

